Nitrogen-enriched Ionic Coordination Polymers: Design, Syntheses and Functional Studies

A Thesis

Submitted in Partial Fulfillment of the Requirements

for the Degree of

Doctor of Philosophy

by

Biplab Manna

ID: 20103067

Indian Institute of Science Education and Research (IISER), Pune

2016

Dedicated

to my parents

Certificate

Certified that the work described in this thesis entitled "*Nitrogen-enriched Ionic Coordination Polymers: Design, Syntheses and Functional Studies*" submitted by *Mr. Biplab Manna* was carried out by the candidate, under my supervision. The work presented here or any part of it has not been included in any other thesis submitted previously for the award of any degree or diploma from any other university or institution.

Date: 29th April 2016

Dr. Sujit K. Ghosh
Research Supervisor

Email: sghosh@iiserpune.ac.in | Contact no: +91 (20) 25908076

Declaration

I declare that this written submission represents my ideas in my own words and wherever other's ideas have been included; I have adequately cited and referenced the original sources. I also declare that I have adhered to all principles of academic honesty and integrity and have not misrepresented or fabricated or falsified any idea/data/fact/source in this submission. I understand that violation of the above will result in disciplinary actions by the Institute and can also evoke penal action from the sources, which have thus not been properly cited or from whom appropriate permission has not been taken when needed.

Date: 29th April 2016

Biplab manna

ID: 20103067

Acknowledgement

First of all, I would like to convey my special appreciation and thanks to my research supervisor **Dr. Sujit K. Ghosh**, who guided me and continuously motivated me in the last five years. His inspiring supervision helped me to execute my research projects in a systematic way. I cannot forget his stimulating research tips which assisted me a lot to think about new research ideas. Thank you very much sir for being such a wonderful mentor for me and I truly believe that this will be helpful in my future also.

I sincerely acknowledge Indian Institute of Science Education and Research (IISER), Pune and its director Prof. K. N. Ganesh for providing start-of-the-art research facilities and an outstanding research ambiance.

I am also thankful to the CSIR, India for providing my research fellowship during the period of five years.

I am very grateful to the Research Advisory Committee (RAC) members Dr. Sujit K. Ghosh, Dr. Nirmalya Ballav and Dr. Rajesh G. Gonnade (National Chemical Laboratory, Pune) for their invaluable advices provided during RAC meetings.

I am also very thankful to the entire chemistry department at IISER Pune and all faculty members especially to Dr. Angshuman Nag, Dr. R. Bhoomishankar, Dr. M. Jayakannan, Dr. H. N. Gopi, Dr. Pinaki Talukdar, Dr. Partha Hazra, Dr. Arnab Mukherjee, Dr. Aloke Das, Dr V. G. Anand for their valuable suggestions during my research period.

I would like to express my sincere thanks to Ma'am (Dr. Sudarshana Mukherjee) for her invaluable research tips.

My Best wishes to Suvan for a wonderful life ahead.

I feel extremely lucky to have such wonderful lab members Dr. Sanjog Nagarkar, Dr. Biplab Joarder, Dr. Tarak Nath Mandal, Abhijeet, Partha da,

Soumya, Avishek, Aamod, Partha, Arif, Amitosh, Amrit, Yogesh, Samraj, Prateek, Shivani, Kriti, Arunava, Kingshuk, Naveen, Govind, Priyangshu, Shweta Singh, Shweta. Thank you all for providing a friendly environment in the lab.

My special thanks go to my immediate lab senior and my dear friends Dr. Sanjog Nagarkar and Dr. Biplab Joarder for their valuable inputs during stay at IISER Pune. Thank you very much for being such a incredibly sportive lab mates.

I would also like to thank Remiya Ma'am (Dr. Remiya Korah) and Dr. Surjeet Singh for being so supportive to me during their short term stay at IISER Pune.

I am very thankful to Mr. Alok Panwar for helping me in my research during his stay at IISER Pune.

I also thank Dr. V. S. Rao, former registrar at IISER-Pune for his precious support and timely help.

I very thankful to Archana for her help during single crystal X-ray studies and Neeraj, Swati, Nilesh Dumre, Anil, Yatish for their help during various instrumental analyses.

I would also like to thank Mr. Mayuresh, Mr. Tushar, Mr. Mahesh, Mr. Nitin, Mr. Prabhas for their administrative and official support during my research period at IISER, Pune.

I would like to thank all my IISER friends specially Arindam, Sunil, Bapu, Koushik, Partha, Sudeb, Avik, Supratik, Barun, Sushil, Arivind, Anupam da, Abhigyan da, Tanmoy, Sagar, Gopal, Shyama, Rajkumar, Maidul, Rahi, Sayan da, Bijoy da, Amit, Rejaul, Chandra, Soumendra, Debanjan, Rajarshi, Shanku, Ravikiran, Kiran.

I am also thankful to my teachers Dr. Suman Das and Dr. Chandan Adhikary, Dr. Indranil Bhattacharya, Dr. Koushik Ghosh, and Susanta Hazra, (during

graduation, Masters and school period) for their invaluable teaching and constant support.

I thank Dr. Umeshareddy Kacherki (deputy librarian) and Anuradha for library support .

I would like to thank my seniors and dear friends Arijit da and Suman da from NCL Pune.

I am indebted to my parents (my father; Mr. Nirmal Manna and mother; Mrs. Kajol Manna) and my sister (Mrs. Smritikana Manna) for their unconditional love, encouragement, endless patience, sacrifice, and blind support.

I would also like to thank American Chemical Society (ACS), Royal Society of Chemistry (RSC), John Wiley & Sons, and Springer for publishing several research articles produced during my research at IISER Pune.

Biplab Manna

Contents

Synopsis

The primary focus of my thesis is based on the syntheses and systematic studies of ionic coordination polymers/ metal-organic frameworks by utilizing neutral nitrogen rich linkers, consequently highlighting the structure-property based rationale, operative behind their diverse functional aspects. Ecologically toxic anions' trapping being an exigent aspect in today's world, new-generation porous sorbent materials serving such green, energy-economic phenomena need to be astutely designed. Such ionic frameworks have also posed as seemingly intriguing compounds from the standpoint of targeted ion conductor materials, for their potential use in hydrogen fuel cell membranes relevant to clean energy applications. Therefore, keeping in mind these two functional facets, I seek to develop efficient anion-trapping and ion conductor coordination polymer materials based on the aforementioned design principles.

During my PhD tenure, a considerable effort has been devoted behind the design, synthesis and functional investigation of ionic coordination polymers (CPs)/ metal-organic frameworks (MOFs). By judicious choice of organic linkers and metal salts, a number of ionic CPs has been synthesized. Mainly, nitrogen rich organic linkers have been extensively used for the construction of such ionic CPs. In case of cationic CPs, free anions present in the network can be exchanged with other incursive anions; thus providing an efficient route to encapsulate unwanted anions. Utilizing protonated amine as a counter cation, anionic CPs might induce proton conducting behavior which is potentially useful in fuel cell applications. Hence, depending on the nature of frameworks and extra framework ions, desired functions can be aimed by opting for such ionic CPs.

Chapter 1. *General Introduction to Ionic Coordination Polymers*

In this chapter, first of all, I have briefly discussed regarding porous coordination polymers/ metal-organic frameworks and their potential applications based on the fascinating host-guest interactions and tunable surface area. Secondly, the basic protocol behind the development of ionic coordination polymers possessing extra framework ion(s) providing additional network functionalities have been presented. In these occasions, the necessity of using neutral nitrogen enriched ligands for the rational syntheses of cationic CPs has been described. The usefulness of anion exchange by using such cationic CPs has been covered here. The framework's dynamism aspects in such cationic CPs have also been discussed. The role of introducing a particular type of extra framework cation in anionic CPs aimed at achieving desired feature has been shown. Here, the importance of protonated cationic species in the anionic CPs for rational construction of proton conducting material has been comprehensively discussed. Finally, the importance of using nitrogen enriched ligands has been also discussed to make functional materials.

Chapter 2. *Guest Driven Dynamic Behavior of A Cationic Coordination Polymer*

In this chapter, a three dimensional (3D) cationic CP/ MOF has been synthesized from a neutral N-donor ligand and $Cd(ClO_4)_2$.The cationic CP shows guest triggered inherent

dynamic behaviour at room temperature (**Figure 1**). A single-crystal-to-single-crystal (SCSC) transformation experiment enabled the guest dependent structural dynamism to be well understood. The framework also displays facile anion exchange behaviour and anion dependent structural dynamism (***CrystEngcomm***. **2015**, *17*, 8796-8800).

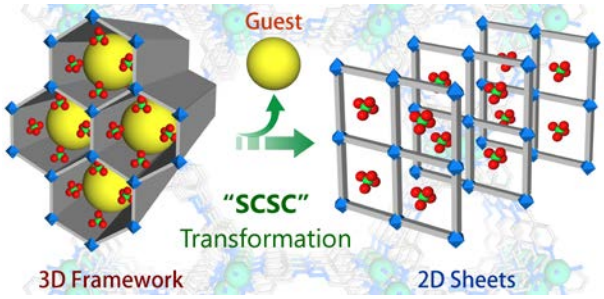

Figure 1: Guest driven dynamic behaviour of a 3D cationic CP.

Chapter 3. *Anion Responsive Tunable Luminescence and Structural Dynamism of A Flexible Cationic Coordination Polymer*

In this chapter, I report a porous cationic CP, made of one dimensional (1D) chains of Zn(II) and a newly designed neutral N-donor organic ligand (L) with extra-framework nitrate anions, which shows interesting guest- and anion-dependent structural dynamism. Dynamic structural behavior has been demonstrated by single-crystal-to-single crystal (SCSC) structural transformation (**Figure 2**). The compound shows slow opening of the framework upon guest inclusion, and size-selective sorption of a number of hydrophobic guest molecules. Anions of the framework are easily exchangeable, and the compound shows interesting anion-responsive tunable luminescent behaviour (***Angew. Chem. Int. Ed.*** **2013**, *52***,** 998-1002).

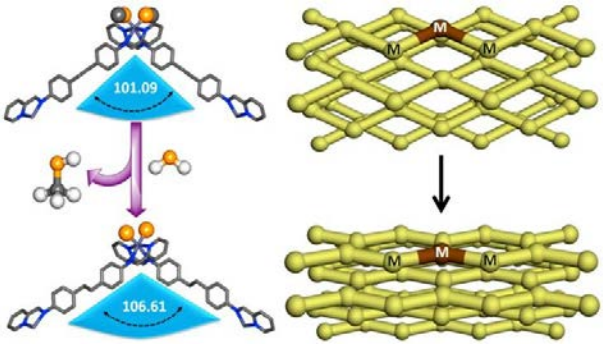

Figure 2: Guest dependent dynamic structural changes in a cationic framework.

Chapter 4. *Anion Triggered Tunable Bulk Phase Homochirality and Luminescence of A Cationic Coordination Polymer*

In this chapter, reaction of a linear bi-chelating N-donor achiral ligand with Zn(II)afforded a homochiral cationic framework with six-fold one-dimensional helical chains. The compound showed selective anion exchange behavior with interesting anion-responsive tunable bulk-phase homochirality (**Figure 3**). The cationic framework also presented anion-driven variable luminescence and sorption behavior (***Chem.Eur.J***. **2014**, *20*,12399-12404).

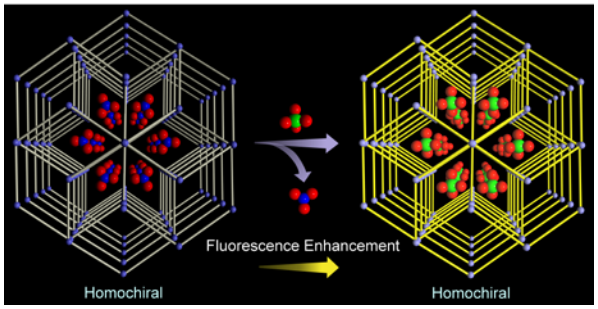

Figure 3: Anion responsive fluorescence enhancement with retention of framework homochirality.

Chapter 5. *Rational Integration of Water Array and Protonated Amine in An Anionic Coordination Polymer for Proton Conduction*

Moving next, a new function of metal-sulfate-based coordination polymer (CP) for proton conduction was investigated through the rational integration of a continuous water array and protonated amines in the coordination space of the CP. The H-bonded arrays of water molecules along with nitrogen-rich aromatic cation (protonated melamine) facilitate proton conduction in the compound under humid conditions (**Figure 4**). Although several reports of metal-oxalate/phosphate-based CPs showing proton conduction are known, this is the first designed synthesis of a metal-sulfate-based CP bearing water arrays functioning as a solid-state proton conductor (***Inorg.Chem***. **2015**, *54*, 5366-5371).

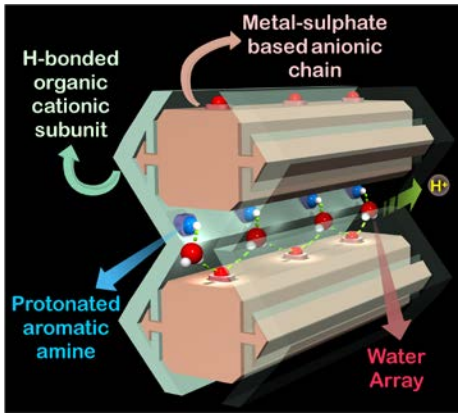

Figure 4: Water assisted proton conduction in a metal-sulfate based anionic CP.

Chapter 6. *Conclusions and Future Outlook*

In summary, the aforementioned four chapters (chapter 2-chapter 5) encompass an ample discussion on four ionic cationic coordination polymers: three cationic and one anionic in nature, along with their unique open framework structure-driven respective application facets, as elaborately described in each of the last four chapters of this thesis. Keeping in mind the coherent deign principle based approach adopted in each of these works, it seems appropriate to judiciously leave the focus on these discussed works, and their articulate integration as anticipated from a focussed thesis work. In fact, while it is quite evident that there a number of other publications (achieved over the PhD tenure)not being purposefully included in this thesis discussion, it is rather comprehensible from recognizing the streamlined and tailored course of actions adopted behind the four included works, leading to a converging approach of discussion.

Abbreviations

Anal.	Analysis
Calc	Calculated
CCDC	Cambridge Crystallographic Data Centre
CCD	Charge-coupled device
CD	Circular-dichroism
CPE	Constant phase element
DMF	N, N-Dimethyl formamide
DEF	N, N-Diethyl formamide
EtOH	Ethanol
EIS	Electro chemical impedance spectroscopy
FT-IR	Fourier transform infra red-spectra
gm	Gram
MeOH	Methanol
Mg	Milligram
MHz	Megahertz
min	Minutes
mL	Milliliter
mM	Micro molar
mmol	Milli moles
MOF	Metal organic framework
NLO	Non-linear optics
N-donor	Nitrogen donor
PCP	Porous coordination polymer
PXRD	Powder X-Ray Diffraction
RT	Room Temperature
RH	Relative humidity
SCXRD	Single Crystal X-Ray Diffraction
TGA	Thermogravimetric Analysis
THF	Tetrahydrofuran
UV	Ultraviolet

Research Publications

Included in thesis

1. Dynamic Structural Behaviour and Anion-Responsive Tunable Luminescence of a Flexible Cationic Metal–Organic Framework.
   Biplab Manna, Abhijeet K. Chaudhari, Biplab Joarder, Avishek Karmakar, and Sujit K. Ghosh.
   Angew. Chem. Int. Ed. **2013**, *52*, 998-1002.

2. Anion-Responsive Tunable Bulk Phase Homochirality and Luminescence of a Cationic Framework.
   Biplab Manna, Biplab Joarder, Aamod V. Desai, Avishek Karmakar and Sujit K. Ghosh.
   Chem. Eur.J. **2014***, 20*,12399-12404*.*

3. Single-Crystal to Single-Crystal Transformation of an Anion Exchangeable Dynamic Metal-Organic Framework.
   Biplab Manna, Aamod V.Desai,Naveen Kumar, Avishek Karmakar and Sujit K.Ghosh.
   CrystEngComm . **2015***, 17,* 8796-8800*.*

4. Neutral N-donor Ligand Based Flexible Metal-Organic Frameworks.
   Biplab Manna, Aamod V. Desai and Sujit K. Ghosh.
   Dalton Trans., *10.1039/C5DT03443D* (Perspective).

5. Coherent Fusion of Water Array and Protonated Amine in a Metal-Sulfate based Coordination Polymer for Proton Conduction.
   Biplab Manna, Bihag Anothumakkool, Aamod V. Desai, Partha Samanta,Sreekumar Kurungot and Sujit K. Ghosh.
   *Inorg.Chem.***2015**, *54*, 5366-5371.

Not included in thesis

6. Guest Driven Structural Transformation Studies of a Luminescent Metal-Organic Framework.
   Biplab Manna, Shweta Singh and Sujit K. Ghosh.
   J.Chem. Sci. **2014***, 126,* 1417–1422*.*

7. Selective Anion Exchange and Tunable Luminescent Behaviours of MOF based Supramolecular Isomers.
   Biplab Manna, Shweta Singh, Avishek Karmakar, Aamod V. Desai and Sujit K.Ghosh.
   Inorg.Chem. **2015**, *54*, 110-116.

8. A π-electron Deficient Diaminotriazine Functionalized MOF for Selective Sorption of Benzene over Cyclohexane.
   Biplab Manna, Soumya Mukherjee, Aamod V. Desai, Shivani Sharma, Rajamani Krishna and Sujit K. Ghosh.
   Chem.Commun . **2015**, *51,* 15386-15389.

9. A Water Stable Cationic Metal-Organic Framework as Dual Adsorbent of Oxo-Anion Pollutants.
   Aamod V. Desai, **Biplab Manna**, Avishek Karmakar, Amit Sahoo, and Sujit K. Ghosh.

Angew. Chem. Int. Ed. **2016,** 10.1002/anie.201600185 (Just accepted)

10. Dynamic Metal-Organic Framework with Anion Triggered Luminescence Modulation Behaviors.
Avishek Karmakar, **Biplab Manna**, Aamod V. Desai, Biplab Joarder and Sujit K.Ghosh.
Inorg.Chem. **2014**, *53*, 12225-12227.

11. An Amide Functionalized Dynamic Metal-Organic Framework Exhibiting Visual Colorimetric Anion Exchange and Selective Uptake of Benzene over Cyclohexane.
Avishek Karmakar, Aamod V.Desai, **Biplab Manna**, Biplab Joarder and Sujit K. Ghosh.
*Chem. Eur.J.***2015***, 21*, 7071-7076*.*

12. An Aqueous Phase Nitric Oxide Detection by an Amine Decorated Metal-Organic Framework.
Aamod V. Desai, Partha Samanta, **Biplab Manna** and Sujit K. Ghosh.
Chem.Commun .**2015**, *51*, 6111-6114.

13. Amino Acid based Dynamic Metal-Biomolecule Frameworks.
Biplab Joarde , Abhijeet K.Chaudhari, Sanjog S. Nagarjkar, **Biplab Manna** and Sujit K. Ghosh.
Chem. Eur. J. **2013***, 19,* 11178-11183*.*

14. Framework-Flexibility Driven Selective Sorption of *p*-Xylene over Other Isomers by a Dynamic Metal-Organic Framework.
Soumya Mukherjee ,Biplab Joarder, **Biplab Manna,** Aamod V. Desai and Sujit K. Ghosh.
Sci. Rep. **2014***, 4,* 5761*.*

15. Exploiting of Guest Accessible Aliphatic Amine Functionality of a Metal-Organic Framework for Selective Detection of 2,4,6-Trinitrophenol (TNP) in Water..
Soumya Mukherjee , Aamod V. Desai, **Biplab Manna,** Arif I. Inamdar and Sujit K. Ghosh.
Cryst. Growth Des. **2015***, 15,* 4627–4634*.*

Chapter 1

General Introduction to Ionic Coordination Polymers

1. Introduction

1.1. Porous coordination polymers or metal-organic frameworks:

Porous coordination polymers (PCPs) or metal-organic frameworks (MOFs) are extended crystalline solid materials which are built from the self-assembly of metal ion or metal ion cluster and organic bridging ligands (**Figure 1.1**).[1] A wide range of organic struts such as formates, polycarboxylates, phosphonates, sulphonates, pyridyl, imidazolate, triazolate, tetrazolate etc. are often found to anchor with metal nodes to generate PCPs.

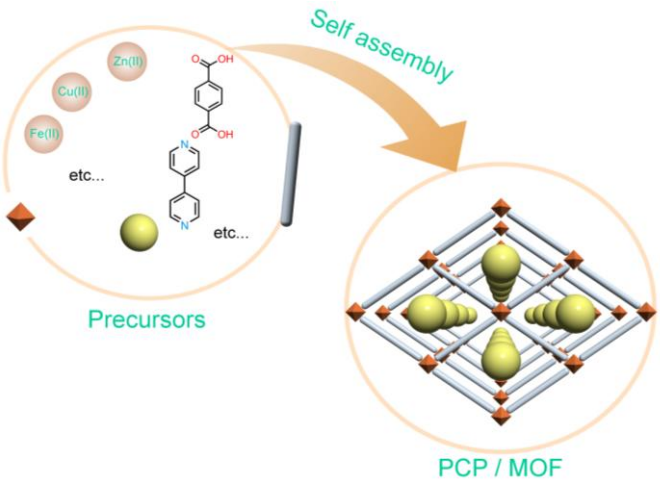

Figure 1.1: *Schematic representation showing formation of PCP from metal ions and organic linkers.*

The key advantages of such materials over other classical porous materials (e.g. zeolites, porous carbons etc.) stem from their superior host-guest interactions, designable architecture, tunable pore structure and functionality.[2] Moreover, structural flexibility in PCPs enables them to take up selective adsorbate from a mixture of species.[3] Owing to the above mentioned unique features, PCPs/MOFs (**Figure 1.2**) are considered to be promising materials and exhibit wide range of potential functions such as storage, separation, sensing, catalysis, magnetism, NLO, drug delivery, polymerisation, clean energy application (proton conduction) etc.[4] (**Figure 1.3**). Additionally, PCPs with homochiral nature are often found to show asymmetric catalysis,

enantioselective separation.[5] A few of the applications related to the thesis will be discussed briefly in the following sections.

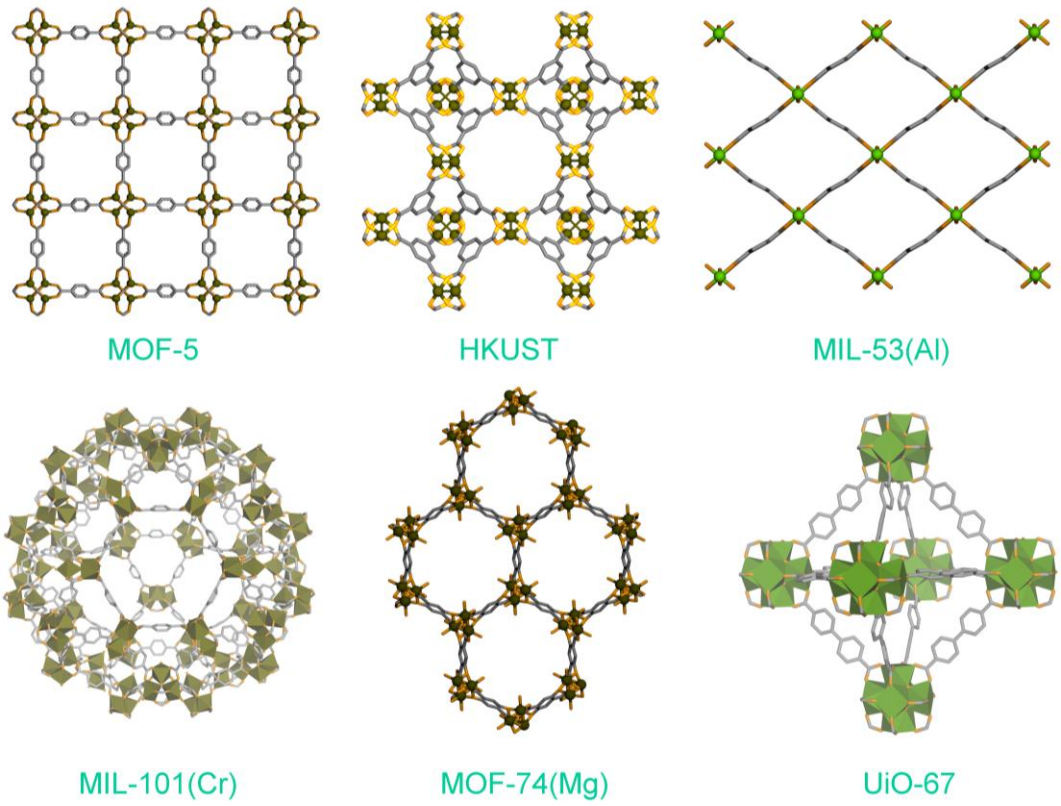

Figure 1.2: *Structures of various well known MOFs in the literature (MOF-5,* [6] *HKUST,* [7] *MIL-53,* [8] *MIL-101,* [9] *MOF-74,* [10] *and UiO-67*[11]*).*

1.2. Few applications of porous coordination polymers:

1.2.1. Separation:

From industrial prospects, it is very crucial to separate a particular gas from a mixture. Among all other separation techniques, adsorption based separation is one of the well recognized tools for this purpose.[12] Though a number of adsorbent host materials have been widely exploited, MOFs have gained much attention in recent years for this separation purpose.[13] Tailor-made synthesis, adjustable porosity and selective host–guest interactions are the main driving forces which boost up MOFs towards this function. Pore dimensions and adsorbate-adsorbent

interactions dictate how efficient a MOF will be for achieving gas separation. For example, size selective adsorption is achieved for O_2 over N_2 with MOF based adsorbent having pore size 3.5Å x3.5 Å.[14] Free amine functionality, alkali metal nodes or open metal sites (OMS) in MOFs are often exploited for selective CO_2 adsorption.[15] Apart from gases, adsorptive separation of liquids is also important from industrial point of view. In this context, separation of liquids with similar boiling points such as benzene/cyclohexane and C_8 aromatic hydrocarbons (o-xylene/*p*-xylene/*m*-xylene) are very crucial and challenging too. MOFs with prefunctionalized linkers and structural flexibility are well utilized for such selective separation.[16]

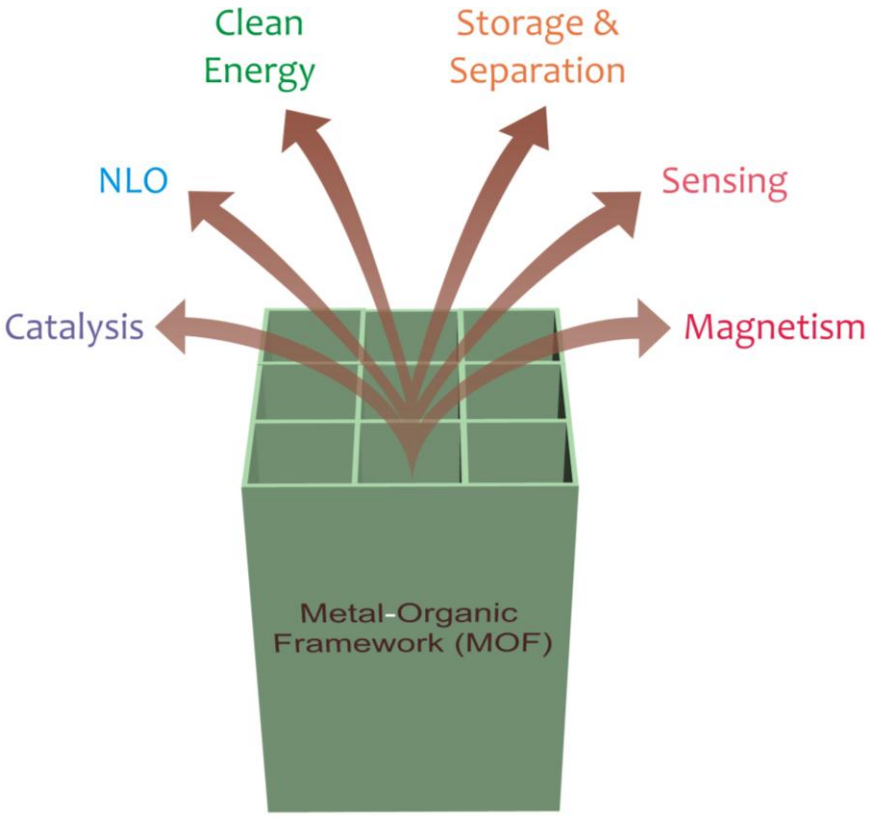

Figure 1.3: *Various potential applications of PCPs / MOFs.*

1.2.2. Chemical sensing:

Very recently, PCPs have been found to be used as sensory materials.[17] Luminescent PCPs could do the job in both ways: "turn on" and "turn off" manners. Guest accessible pores, structural tenability, high crystallinity and tunable band gap put them one step ahead as sensory materials. Selective host-guest interactions between host species (PCPs) and analytes (guest) provide the probable optical signal. Pre-concentration effects of analytes are considered to be sensitive detection technique. In the last few years, detection of life-threatening nitro explosives has been well achieved by using luminescent PCPs in laboratory scale.[18] However, clear cut mechanisms of sensing of molecules by PCPs are yet to be studied thoroughly which means there is potential room for finding new detection mechanisms, with efficient new generation PCPs.

1.2.3. Clean energy application (Proton Conduction):

Globally utilisation of energy is increasing day by day because of fast modernization, population growth and other factors.[19] Moreover, at the same time, so called fossil fuel amount is getting reduced. Hence, in order to address the high energy demand, various auxiliary energy technologies have been suggested. Fuel cell technology is considered one of the most important and promising energy sources which can fulfil not only the energy demand criteria but also it is environmental friendly.[20] Hydrogen fuel cell utilises a solid state proton exchange membrane material, hydrogen as fuel and oxygen as an oxidant to produce electrical energy and water (as a bi-product).[21] For better performance of hydrogen fuel cell, the membrane material should be high proton conducting and durable over a wider temperature range (30-300^{o}C). Very recently, PCPs / MOFs have been found one of the alternative solid state proton conducting material, because of their tunable chemical structure, adjustable porosity and high thermal stability.[22] Also their highly crystalline nature helps to trace the conduction mechanism. By two ways, PCPs have been observed to conduct proton: i) intrinsic root; in this manner protonic source and carrier both are present in the framework structure, ii) extrinsic root; this case involves introduction of protonic source or carrier molecules into pores of PCP structure. Till date, several reports came up with water assisted or anhydrous proton conducting PCPs; [23] but still there are scopes for the improvement of conductivity values, actual device fabrication etc.

1.3. Ionic coordination polymers:

Most of the classical carboxylate based PCPs are electrically neutral owing to the presence of equal number of positive charge from metal ions and negative charge from anionic ligands

which means such frameworks possess zero residual charge. But there are examples of charged frameworks which possess positive or negative charges on it, and presence of such extra-framework ions make them globally neutral. Such framework species with residual charges are termed as ionic CPs.[24] On account of the presence of such extra-framework ions as additional functionality, ionic CPs are gaining much attention and have been found to exhibit several potential functions such as ion exchange, ion sensing, adsorptive separation, catalysis, proton conduction etc.[25] Ionic CPs are classified into two sub categories: i) Cationic CPs; where the network contains positively charges and presence of extra-framework anions in the lattice make them neutral, ii) Anionic CPs; these include negatively charged frameworks and positively charged extra framework ions (**Figure 1.4**).

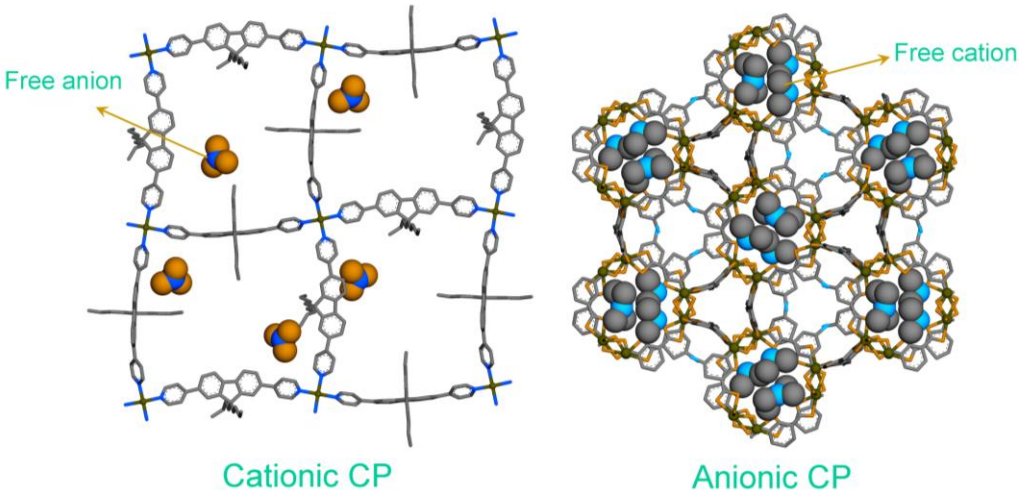

Figure 1.4: *Structures of representative cationic CP showing free anions in the lattice (left)* [26] *and anionic CP (right) depicting free cation.*[27]

1.3.1. Cationic coordination polymers:

These are composed of positively charged network and extra framework anions (**Figure 1.5**). The anions often reside in the porous channels of the framework and or weakly coordinated to the metal nodes.[28] Such anions are found to be exchanged with other incursive anions which leads to anion exchange based various important applications.[29]

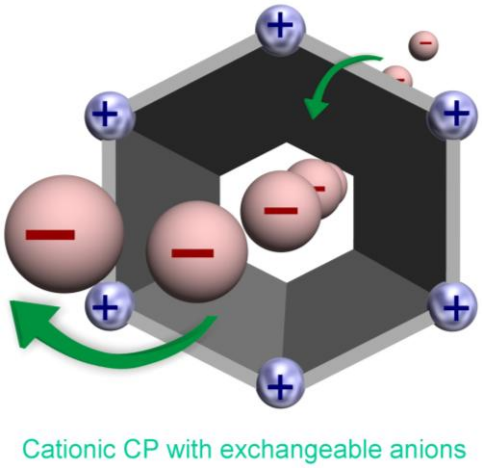

Figure 1.5: Schematic representation of cationic CP with exchangeable free anions.

1.3.1.1. Design strategies of cationic coordination polymers:

Widely accepted routes involve the reactions of neutral nitrogen donor ligands with metal salts in presence of solvent or guest molecules to produce cationic CPs (**Figure 1.6**).[25b]

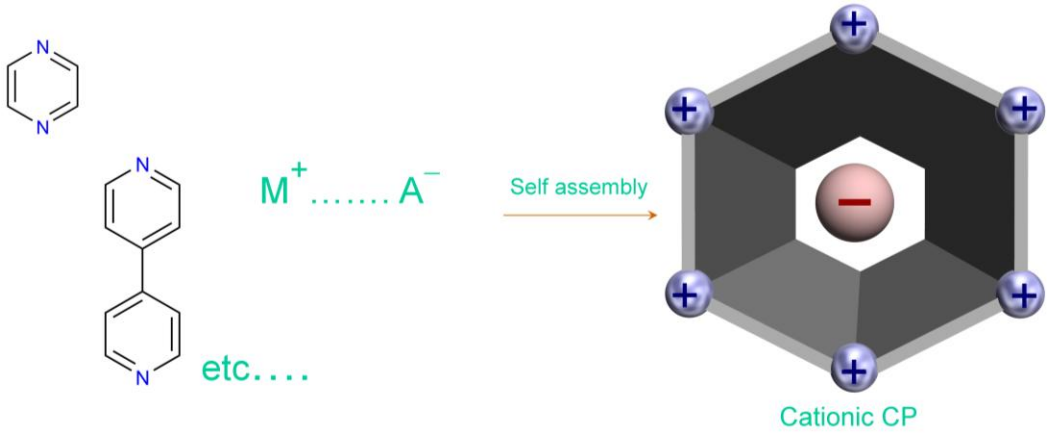

Figure 1.6: *Schematic representation showing design synthesis of cationic CP.*

Over the years, 4,4′-bipyridine has been extensively used for constructing such cationic CPs with free anions in the porous channels.[30] Hence, people came up with pyridyl functionalized various kinds of organic linkers enriched in neutral nitrogen to build up such frameworks. A very

common synthetic route involves the slow diffusion of nitrogen-enriched organic linkers and metal salts in long glass tube to produce crystals of cationic CPs (**Figure 1.7**).[31]

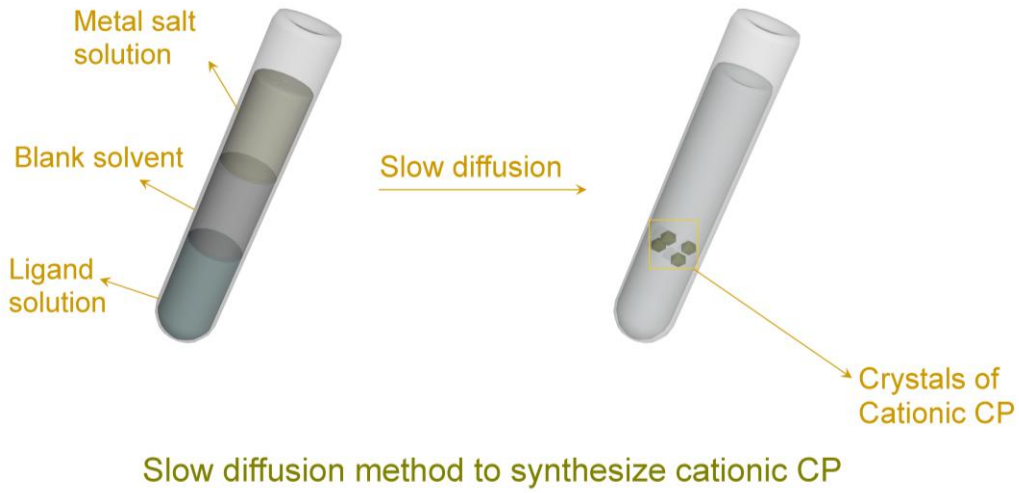

Figure 1.7: *Schematic representation showing slow diffusion method for constructing crystals of cationic CP.*

1.3.1.2. Anion exchange:

This has been well documented in the literature that free or weakly coordinated anions in the cationic CPs could be exchanged with other variety of anions leading to the exchanged solids.[32] This exchange process is found to be dependent on the size, shape and coordinating tendencies of incoming anions. The exchanged products are often observed to exhibit different chemical and physical properties compared to the original compound, which might be useful for desired applications of interests.[29b, 33] In general, crystals or crystalline powder of cationic CP is stirred very slowly in a solution of excess of incursive anion of interest, to get exchanged product (**Figure 1.8**). Experimental methods such as FT-IR, UV-Vis and elemental analysis are often used to check the extent of exchange. Few of important anion exchange based applications will be discussed briefly in the following sections.

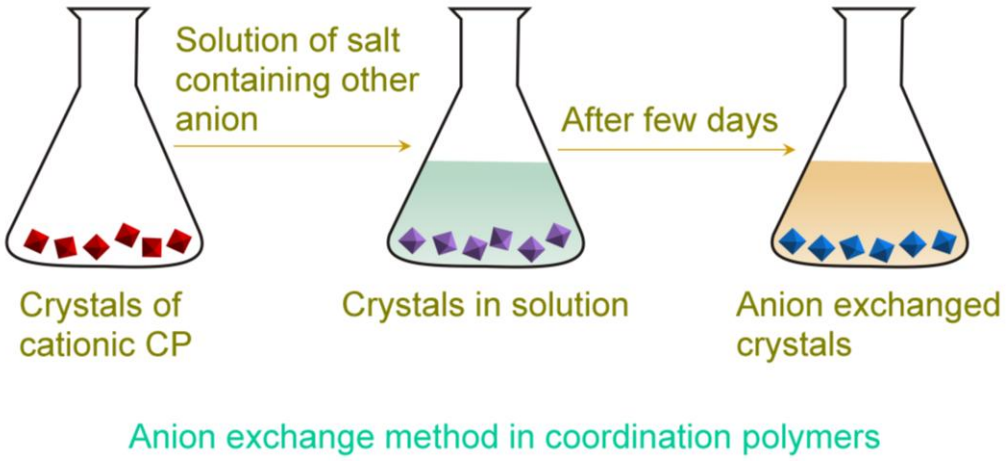

Figure 1.8: *Schematic representation showing anion exchange method at room temperature.*

1.3.1.2.1. Applications of anion exchange:

1.3.1.2.1. a. Removal of unwanted anions:

Various industrial wastes contain oxo-anions like ClO_4^-, CrO_4^{2-}, $Cr_2O_7^{2-}$, PO_4^{3-}, AsO_4^{3-}, MnO_4^-, ReO_4^-, TcO_4^- which are known to cause serious health problems.[34] Moreover, these anions dissolve in water and are responsible for water pollution too.[35] Apart from those oxo-anions, other anions, like SCN^-, N_3^- and $N(CN)_2^-$ are also known as hazardous. To address this problem, various anion exchangeable materials such as resins, inorganic materials have been used for the exchange and trapping of such unwanted anions. But poor selectivity, slow rate of exchange and their high cost confine their further use. Hence, it is primarily important to develop efficient materials for trapping and exchanging of those hazardous anions. Cationic CP with exchangeable free anions is one of the important classes of materials which might be fruitful for this purpose. Recently, various cationic CPs have been exploited for the effective encapsulation and exchange of such anions.[36] Further improvements in this context are urgently necessary towards the real time applications.

1.3.1.2.1. b. Anion sensing:

Conjugated N-donor ligands when combine with d^{10} metal nodes, they are generally found to form luminescent cationic CPs. Such luminescent cationic CPs are very useful in sensing applications. Free anions present in such networks could be exchanged with other anions of

different electronic properties which lead to physical changes in the host systems. Luminescence nature of the host (parent) framework considerably changes upon the exchange phenomena to provide a detectable optical signal for the anion. Few cationic CPs have been proposed to exhibit as solid state anion sensor materials. In a recent report, Wang *et al*. showed the detection of $Cr_2O_7^{2-}$ (heavy oxo-anion) by a Ag(I)-based cationic CP.[37] Dong and co-workers found a Cd(II) based cationic CP which behaved as switchable luminescent materials in response to various anions.[38] Our group came up with a Zn(II) based cationic CP which showed differences in emission profiles with changes in anions.[33a] Though such strategies are very effective for developing a anion sensory materials but this is still in nascent stage, and require much more inputs to find out precise detailed mechanisms behind luminescence changes upon exchange phenomena with various anions. Apart from this luminescence read out, visual colour changes are considered to be the most effective and simple tool for detecting a species. In this respect, cationic CPs composed of colored transition metal ions and/or photochemically active conjugated organic linkers provide a platform for naked eye anion recognition. Substitution of free anions with other anions in such host matrices leads to various exchanged adducts which are easily differentiable in ambient conditions through visual color changes. Recently, a number of cationic CPs has been shown to display such naked eye colorimetric anion sensing behavior.[26,29b,39]

1.3.1.3. Dynamic behavior of cationic CP:

Cationic CPs are very often found to show structural dynamism. Such frameworks generally respond to different kinds of chemical and physical stimuli to bring out structural changes.[3a] A list of stimuli such as anions, guests (free or coordinated) and light as physical stimuli are known to render such flexibility. To understand such dynamic materials in depth, it is very important to know each phase in molecular level. Single-crystal-to-single-crystal (SCSC) transformation technique has been extensively used to elucidate such minute changes.[40] Such systems show supreme host-guest interactions, and manifest very important functions, like chemical separation, magnetism, sensing etc.[41] Over the years, several cationic CPs have been reported which depicted such structural flexibility. Very recently in a review article, a comprehensive discussion about various exogenous stimuli has been made, which causes structural changes in similar systems (**Figure 1.9**).[42]

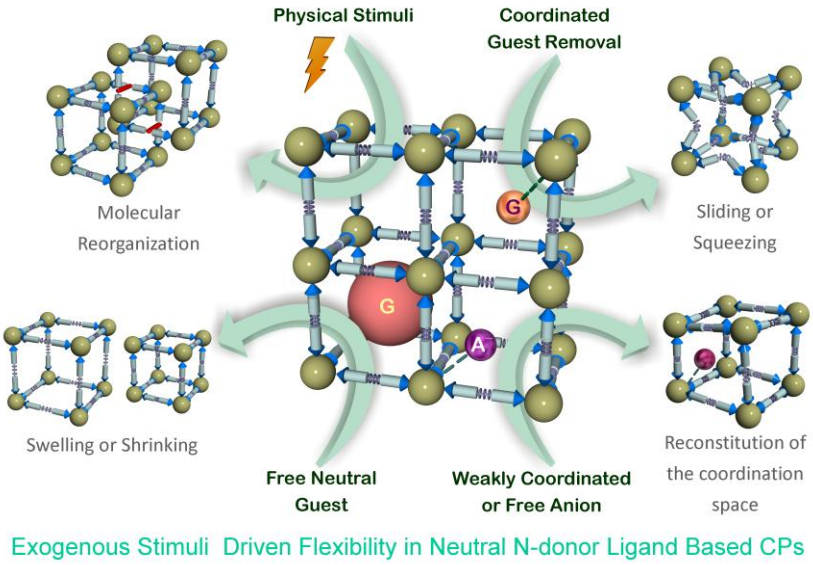

Figure 1.9: *Schematic representation of structural dynamism for cationic CP.*[42]

1.3.2. Anionic coordination polymers:

Such species have negatively charged network and positively charged extra-framework cations in the lattice (Figure 1.9.1).

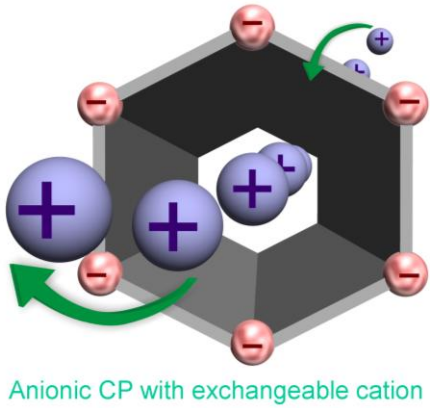

Scheme 1.9.1: *Schematic representation of anionic CP with exchangeable free cations.*

Such extra-framework cations are often found to provide additional functionality to the overall CP. Due to this supplementary framework functionality, anionic CPs have been observed to serve several potential applications like separations of gases, drug delivery, catalysis, NLO,

chemical sensing, proton conduction etc.[43,4c] Among them, proton conducting aspect related to the thesis will be further discussed separately in the following section. Moreover, exchanging of these cations with other cations leads to chemical and physical perturbation of the host systems.

1.3.2.1. Design strategies of anionic coordination polymers:

Metal ions like Cd(II), Zn(II) and In(III), when react with multidentate bridging organic ligands such as oxalate, formate etc. in presence of DMF or DEF under solvothermal conditions, generally they produce anionic CPs. Hydrolysis of solvents DMF or DEF provides dimethyl amine (DMA) or DEA (diethyl amine), which are generally occluded in the anionic CPs for the purpose of network charge balance.[44] Moreover, anions like sulphate, phosphate, and carbonate are used to form anionic CPs during the combination with metal salts (**Figure 1.9.2**).[45]

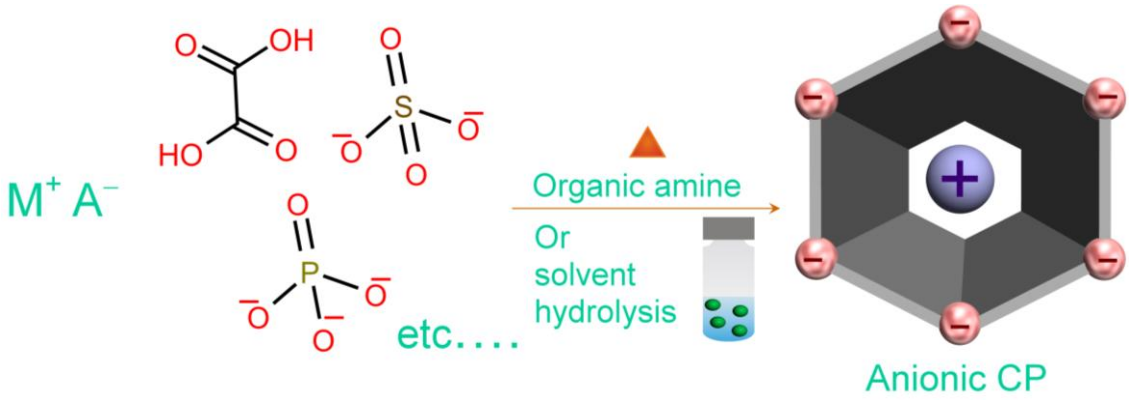

Figure 1.9.2: *Schematic representation showing design synthesis of anionic CP.*

Polar organic cations, other inorganic cations, and or DMA / DEA from solvent hydrolysis do get involved as extra-framework cations. It is not very straightforward to construct such anionic CPs and largely depends on the reaction conditions.

1.3.2.2. Proton conducting applications:

Solid state proton conducting materials are generally used in hydrogen fuel cells.[21] Nafion, a fluorinated sulfonic acid based organic polymer material is being extensively utilized as proton conducting membrane.[46] Sulfonic acid part of this membrane provides the proton source and requires humid conditions for conducting the proton. This means that Nafion works at only low temperatures and at high temperatures, it is ineffective. Apart from this, its lack of long range

order does not allow to understand the molecular level conduction mechanisms. PCPs are considered one of the best materials which can easily overcome the drawbacks of Nafion. It has been well documented in the literature that anionic CPs with protonated amine cations (extra - framework cation), and carrier molecules (such as water) are very effective in conducting proton (**Figure 1.9.3**). Here, protonated amine cations (e.g. ammonium, imidazolium, benzimidazole cation) act as proton sources, and are usually hydrogen bonded with the carrier molecules to conduct proton. [45c, 47]

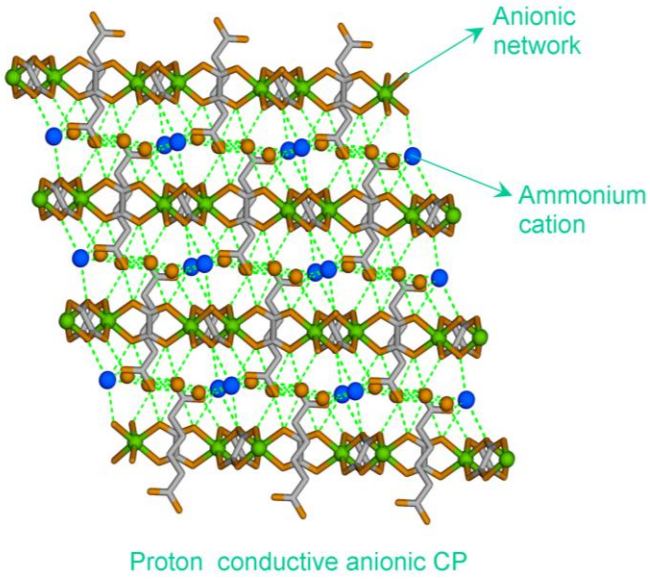

Figure 1.9.3: *Proton conducting anionic CP showing ammonium cation, hydrogen bonded with water molecules.*[47b]

Recently, our group came up with a Zn-oxalate based anionic CP, which conducts proton in both hydrous as well anhydrous conditions.[48] The CP contains dimethyl ammonium cations which are strongly hydrogen bonded with sulphate anions to provide a conductive pathway. In another report, S. Kitagawa *et al*. showed the use of a Zn-phosphate based anionic CP bearing benzimidazolium cation as a solid state proton conductor.[45c] H. Kitagawa and co-workers have shown several oxalate based anionic CPs, which behave as proton conducting solids.[43e, 47b, 49] Hence, designing an anionic CP with rational choice of extra-framework cation is very crucial, and simultaneously important towards the fabrication of solid state proton conductors.

1.4. Overview of the thesis:

In chapter 2, a simple Schiff based ligand with metal binding pyridyl functionality have been utilized for constructing cationic CP, and its anion exchange behavior along with structural dynamism have been further investigated.

In the next (3rd) chapter, I have used a newly designed N-donor ligand with bichelating sites to fabricate a cationic CP with free anions in it. Modulation in luminescence properties of the framework in presence of varied anions has been extensively studied. SCSC technique has been used for the understanding of dynamic behaviour of the cationic framework.

In 4th chapter, homochiral nature of a cationic CP has been studied. Moreover, effects of extra - framework anions on framework homochirality have been investigated with the help of solid state CD spectra.

In chapter 5, an anionic CP has been designed based on a metal-sulfate chain, bearing charge balancing protonated melamine cations. Rational integration of these protonated melamine cations and array of water molecules in the anionic CP do conduct proton under humid condition.

In Chapter 6, conclusions and future outlook of the thesis has been briefly discussed.

1.5. References:

(1) (a) Yaghi, O. M.; O'Keeffe, M.; Ockwig, N. W.; Chae, H. K.; Eddaoudi, M.; Kim, J. *Nature* **2003**, *423*, 705-714. (b) Eddaoudi, M.; Moler, D. B.; LI, H.; Chen, B.; Reineke, T. M.; O'Keeffe, M.; Yaghi, O. M. *Acc. Chem. Res.* **2001**, *34*, 319-330. (c) Kim, K. *Chem. Soc. Rev.* **2002**, *31*, 96-107.(d) Zhou, H.-C.; Long, J. R.; Yaghi, O. M. *Chem. Rev.* **2012**, *112*, 673 – 674. (e) Ferey, G. *Chem.Soc.Rev.* **2008,** *37*, 191-214. (f) Kim, K. *Chem. Soc. Rev.* **2002**, *31*, 96-107. (g) Moulton, B.; Zaworotko, M. J. *Chem. Rev.* **2001**, *101*, 1629-1658.(h) Robson, R. *J. Chem. Soc., Dalton Trans.* **2000**, 3735-3744.

(2) (a) Horcajada, P.; Gref, R.; Baati, T.; Allan, P. K.; Maurin, G.; Couvreur, P.; Ferey, G.; Morris, R. E.; Serre, C. *Chem. Rev.* **2012**, *112*, 1232-1268. (b) Ferey, G.; Serre, C. *Chem. Soc. Rev.* **2009**, *38*, 1380-1399.

(3) (a) Horike, S.; Shimomura, S.; Kitagawa, S. Nat. Chem. **2009**, *1*, 695-704.

(4) (a) Special issue on MOF *Chem. Soc. Rev*. **2009**, *38*, 1201–1508. (b) An, J.; Geib, S. J.; Rosi, N. L. *J. Am. Chem. Soc*. **2009**, *131*, 8376 – 8377. (c) Ma, L.; Falkowski, J. M.; Abney, C.; Lin, W. *Nat.Chem*. **2010**, *2*, 838 – 846. (d) Guo, Z.; Cao, R.; Wang, X.; Li, H.; Yuan, W.;Wang, G.; Wu, H.; Li, J. *J. Am. Chem. Soc.* **2009**, *131*, 6894 –6895 (e) Coronado, E.; Espallargas, G.M. *Chem. Soc. Rev*. **2013**, *42*, 1525-1539. (f) Uemura, T.; Yanaia, N.; Kitagawa, S. *Chem. Soc. Rev*., **2009**, *38*, 1228–1236. (g) Yu, J.; Cui, Y.; Xu , H.; Yang , Y.; Wang , Z.; Chen, B.; Qian, G. *Nat. Commun*. **2013**, *4*, 10.1038/ncomms3719. (h) Li, S.-L.; Xu, Q. *Energy Environ. Sci*. **2013**, *6*, 1656−1683.

(5) (a) Seo, J. S.; Whang, D.; Lee, H.; Jun, S. I.; Oh, J.; Jeon, Y. J.; Kim, K. *Nature*. **2000**, *404*, 982– 986. (b) Li, G.; Yu, W.; Cui, Y. *J. Am. Chem. Soc*. **2008**, *130*, 4582 –4583.

(6) Li, H.; Eddaoudi, M.; O'Keeffe, M.; Yaghi, O. M. *Nature*. **1999**, *402*, 276– 279.

(7) Chui, S.S.; Lo, S.M.; Charmant, J.P.; Orpen, A.G.; Williams, I.D. *Science.* **1999**, *283*, 1148-1150.

(8) Loiseau, T.; Serre, C.; Huguenard, C.; Fink, G.; Taulelle, F.; Henry, M.; Bataille, T.; Ferey, G.; *Chem. Eur. J.* **2004**, *10*, 1373-1382.

(9) Ferey, G.; Mellot-Draznieks, C.; Serre, C.; Millange, F.; Dutour, J.; Surble, S.; Margiolaki, I. *Science.* **2005**, *309*, 2040-2042.

(10)Rosi, N. L.; Kim, J.; Eddaoudi, M.; Chen, B.; O'Keeffe, M.; Yaghi, O. M. *J. Am. Chem. Soc*. **2005**, *127*, 1504-1518.

(11) Cavka, J. H.; Jakobsen, S.; Olsbye, U.; Guillou, N.; Lamberti, C.; Bordiga, S.; Lillerud, K. P. *J. Am. Chem. Soc*. **2008**, *130*, 13850–13851.

(12) Rouquerol, F.; Rouquerol, I.; Sing, K. *Adsorption by Powders and Porous Solids-rinciples Methodology and Applications*, Academic Press, London, **1999**.

(13) Li, J.-R.; Kuppler, R. J.; Zhou,H.-C. *Chem. Soc. Rev*., **2009**, *38*, 1477–1504.

(14) Ma, S.Q.; Wang, X. S.; Collier, C.D.; Manias, E.S.; Zhou, H.-C. *Inorg. Chem*., **2007**, *46*, 8499-8501.

(15) (a) Sumida, K.; Rogow, D.L.; Mason, J.A.; Mcdonald, T.M.; Bloch, E.D.; Herm, Z.R.; Bae, T.-H.; Long, J.R. *Chem. Rev*., **2012**, *112*, 724-781. (b) Queen, W. L.; Hudson, M. R.; Bloch, E. D.; Mason, J. A.; Gonzalez, M. I.; Lee, J. S.; Gygi, D.; Howe, J. D.; Lee, K.; Darwish, T. A.; James, M.; Peterson, V. K.; Teat, S. J.; Smit, B.; Neaton, J. B.;

Long, J. R.; Brown, C. M. *Chem. Sci.* **2014**, *5*, 4569-458.

(16) (a) Shimomura, S.; Horike, S.; Matsuda, R.; Kitagawa, S. *J. Am. Chem. Soc*. **2007**, *129*, 10990-10991. (b) Joarder, B.; Mukherjee, S.; Chaudhari, A. K.; Desai, A. V.; Manna, B.; Ghosh, S. K. *Chem. Eur. J.* **2014**, *20*, 15303-15308. (c) Mukherjee, S.; Joarder, B.;Manna, B.; Desai, A. V.; Chaudhari, A. K.; Ghosh, S. K. *Sci.Rep*., **2014**, *4*, *DOI: 10.1038/srep05761*.

(17) Allendrof, M.D.; Bauer, C. A.; Bhakta, R. K.; Houka, R. J.T. *Chem. Soc. Rev*. **2009**, *38*, 1330-1352.

(18) Nagarkar, S. S.; Joarder, B.; Chaudhari, A. K.; Mukherjee, S.; Ghosh, S. K. *Angew. Chem. Int. Ed*. **2013**, 52, 2881-1885.

(19) U.S. Department of Energy, U.S. Energy Information Administration: International Energy Outlook 2013 (Report: DOE/EIA-0484(2013)), **2013**.

(20) Winter, M.; Brodd, R. J.; *Chem. Rev.*, **2004**, *104*, 4245-4269.

(21) Hamrock, S.; Yandrasits, M.; *Polym. Rev*., **2006**, *46*, 219–244.

(22) Horike, S.; Umeyama, D.; Kitagawa, S. *Acc. Chem. Res*. **2013**, *46*, 2376-2384.

(23) Ramaswamy, P.; Wong, N.E.; Shimizu, G.K.H. *Chem. Soc. Rev*. **2014**, *43*, 5913-5932.

(24) Custelcean, R.; Moyer,B. A. *Eur. J. Inorg. Chem*. **2007**, 1321–1340.

(25) (a) Procopio, E.Q.; Fukushima, T.; Barea, E.; Navarro, J.A.R.; Horike, S.; Kitagawa, S. *Chem. Eur. J.* **2012**, 18, 13117–13125. (b) Karmakar, A.; Desai, A.V.; Ghosh, S. K. *Coord. Chem. Rev.* **2015**, *DOI: 10.1016/j.ccr.2015.08.007.*

(26) Ma, J.-P.; Yu, Y.; Dong, Y.-B. *Chem. Commun*. **2012**, *48*, 2946 – 2948.

(27) Zheng, S.-T.; Zuo, F.; Wu, T.; Irfanoglu, B.; Chou, C.; Nieto, R. A.; Feng, P.; Bu, X. *Angew. Chem. Int. Ed*. **2011**, *50*, 1849 –1852.

(28) (a) Min, K. S.; Suh, M. P. *J. Am. Chem. Soc*. **2000**, *122*, 6834 – 6840. (b) Yang, Q.-Y.; Li, K.; Luo, J.; Pana, M.; Su, C.-Y. *Chem. Commun*. **2011**, *47*, 4234 – 4236.

(29) (a)Maji, T. K.; Matsuda, R.; Kitagawa, S. *Nat. Mater*. **2007**, *6*, 142 –148. (b) Chen, Y.-Q.; Li, G.-R.; Chang, Z.; Qu, Y.-K.; Zhang, Y.-H.; Bu, X.-H. *Chem. Sci*. **2013**, *4*, 3678 –3682.

(30) (a) Noro, S.; Kitagawa, S.; Kondo, M.; Seki, K. *Angew. Chem., Int. Ed*. **2000**, 39, 2082–2084. (b) Li, D.; Kaneko, K. *Chem. Phys. Lett*. **2001**, 335, 50–56. (c)

Biradha, K.; Domasevitch, K. V.; Moulton, B.; Seward, C.; Zaworotko, M. J. *Chem. Commun*., **1999**, 1327-1328.

(31) (a) Biradha, K.; Fujita, M. *Angew. Chem. Int. Ed*. **2002,** *41*, 3392-3395. (b) Inokuma, Y.; Yoshioka, S.; Ariyoshi, J.; Arai, T.; Fujita, M. *Nature Protocols.*, **2014**, *9*, 246–252.

(32) (a) Fei, H.; Rogow, D.L.; Oliver, S.R.J. *J. Am. Chem. Soc*. **2010**, *132*, 7202–7209. (b) Tzeng, B.-C.; Chiu, T.-H.; Chen, B.-S.; Lee, G.-H.; *Chem. Eur. J*. **2008**, *14*, 5237 – 5245.

(33) (a) Karmakar, A.; Manna, B.; Desai, A.V.; Joarder, B.; Ghosh, S.K. *Inorg. Chem.* **2014**, *53*, 12225–12227. (b) Wang, J.-C.; Liu, Q.-K.; Ma, J.-P.; Huang, F.; Dong, Y.-B. *Inorg. Chem*. **2014**, *53*, 10791–10793.

(34) Izak, P.; Hrma, P.; Arey, B.W.; Plaisted, T.J.; *J. Non-Cryst. Solids.*, **2001**, *289*, 17.

(35) (a) Perchlorate environmental contamination: toxicological review and risk characterization; Second external review draft, NCEA-1-0503; U.S. EPA, Office of Research and Development, National Center for Environmental Assessment, U.S. Government Printing Office: Washington, DC, **2002**. (b) Howarth, A. J.; Liu, Y.; Hupp, J. T.; Farha, O. K. *CrystEngComm*, **2015**, *17*, 7245–7253.

(36) (a) Fu, H.-R.; Xu, Z.-X.; Zhang, J. *Chem. Mater*. **2015** , *27*, 205–210. (b) Fei, H.; Bresler, M. R.; Oliver, S. R. J. *J. Am. Chem. Soc*. **2011**, *133*, 11110–11113.

(37) Li, X.; Xu, H.; Kong, F.; Wang, R. *Angew. Chem. Int. Ed*. **2013**, *52*, 13769 –13773.

(38) Hou, S.; Liu, Q.-K.; Ma, J.-P.; Dong, Y.-B. *Inorg. Chem.*, **2013**, *52* , 3225–3235.

(39) (a) Sun, J.-K.; Wang, P.; Yao, Q.-X.; Chen, Y.-J.; Li, Z.-H.; Zhang, Y.-F.; Wu, L.-M.; Zhang, J. *J. Mater. Chem*. **2012**, *22*, 12212–12219. (b) Karmakar, A.; Desai, A.V.; Manna, B.; Joarder, B.; Ghosh, S. K. *Chem. Eur. J*. **2015**, *21*, 7071–7076.

(40) Zhang, J.-P.; Liao, P.-Q.; Zhou, H.-L.; Lin, R.-B.; Chen, X.-M. *Chem. Soc. Rev.*, **2014**, *43*, 5789—5814.

(41) Kitagawa, S.; Kitaura, R.; Noro, S.-i. *Angew. Chem. Int. Ed*. **2004**, *43*, 2334 –2375.

(42) Manna, B.; Desai, A.V.; Ghosh, S. K. *Dalton. Trans*., **2015**, *10.1039/c5dt03443d*.

(43) (a) An, J.; Rosi, N.L. *J. Am. Chem. Soc*. **2010**, *132*, 5578–5579. (b) Alkordi, M.H.; Liu, Y.; Larsen, R.W.; Eubank, J.F.; Eddaoudi, M. *J. Am. Chem. Soc*. **2008**,

130, 12639–12641. (c) Liu,Y.; Li, G.; Li, X.; Cui, Y. *Angew. Chem. Int. Ed*. **2007**, *46* , 6301–6304. (d) An, J.; Shade, C.M.; Chengelis-Czegan, D.A.; Petoud, S.; Rosi, N.L. *J. Am. Chem. Soc*. **2011**, *133*, 1220–1223. (e) Sadakiyo, M.; Okawa, H.; Shigematsu, A.; Ohba, M.; Yamada, T.; Kitagawa, H. *J. Am. Chem. Soc*. **2012**, *134*, 5472–5475.

(44) (a) Medina, M. E.; Dumont, Y.; Grenechec, J.-M.; Millange, F. *Chem. Commun*. **2010**, *46*, 7987–7989. (b) Chen, W.; Wang, J.Y.; Chen, C.; Yue, Q.; Yuan, H. M.; Chen, J. S.; Wang, S. N. *Inorg. Chem*. **2003**, *42*, 944–946.

(45)(a) Zhang, D.; Lu, Y.; Zhu, D.; Xu, Y. *Inorg. Chem*. **2013**, *52*, 3253−3258. (b) Yotnoi, B.; Rujiwatra, A.; Reddy, M. L. P.; Sarma, D.; Natarajan, S. *Cryst. Growth Des*. **2011**, *11*, 1347−1356. (c) Inukai, M.; Horike, S.; Chen, W.; Umeyama, D.; Itakurad, T.; Kitagawa, S. *J. Mater. Chem. A*, **2014**, *2*, 10404–10409. (d) Abrahams, B. F.; Haywood, M. G.; Robson, R.; Slizys, D. A. *Angew. Chem. Int. Ed*. **2003**, *42*, 1111-1115.

(46) Kreuer, A. K. D.; Paddison, S. J.; Spohr, E.; Schuster, M. *Chem. Rev.*, **2004**, *104*, 4637−4678.

(47) (a) Horike, S.; Chen, W.; Itakura, T.; Inukai, M.; Umeyama, D.; Asakurae, H.; Kitagawa, S. *Chem. Commun.*, **2014**, *50*, 10241—10243. (b) Sadakiyo, M.; Yamada, T.; Kitagawa, H. *J. Am. Chem. Soc.* **2009**, *131*, 9906–9907.

(48) Nagarkar, S.S.; Unni, S. M., Sharma, A.; Kurungot, S.; Ghosh, S.K. *Angew. Chem. Int. Ed*. **2014**, *53* , 2638–2642.

(49) (a) Sadakiyo, M.; Yamada, T.; Kitagawa, H. *J. Am. Chem. Soc*. **2014**, *136*, 13166−13169. (b) Sadakiyo, M.; Yamada, T.; Honda, K.; Matsui, H.; Kitagawa, H. *J. Am. Chem. Soc*. **2014**, *136*, 7701−7707.

Chapter 2

Guest Driven Dynamic Behavior of A Cationic Coordination Polymer

2.1. Introduction:

Guest molecules in the coordination space have found a profound role in directing the structures of metal-organic frameworks (MOFs) / porous coordination polymers (PCPs).[1] Especially in the domain of dynamic CPs, the guest molecules residing in the porous aperture can regulate structures to impart flexibility to the framework.[2] Soft porous CPs are well known to exhibit such guest dependent structural dynamism.[2a,3] Moreover, the framework flexibility may depend upon the nature of guest molecules. CPs entrapping high boiling solvent often show extrinsic dynamic nature, as an external stimuli like high temperature is required for conveying these molecules out of the framework.[4] On the other hand, presence of low boiling guests in a framework may generate inherent framework flexibility which forbids the necessity of an external stimuli, except air-drying conditions.[5] Particularly, manifestation of structural dynamism/flexibility by cationic CPs is very easy compared to other CPs.[5d,6] By employing appropriate low-boiling solvent systems for synthesis, the combination of a neutral N-donor ligand with metal ions yields cationic CPs which usually are occluded with low boiling solvents and extra framework anions.[7] On keeping such CPs away from mother liquor, the confined guests may easily leave the framework and create the possibility of structural changes in the system. Such structural modulations upon guest removal at room temperature renders inherent dynamism to the cationic CPs.[5c,5d] Recently, we have demonstrated the guest dependent dynamic behaviour of few cationic CPs.[5d,8] Such structural modifications can be well understood from their single-crystal-to-single-crystal (SCSC) transformation studies.[2a,9] In addition to these guest induced effects, extra framework anions of such cationic CPs can also be exchanged with foreign anions of varying size, shape and coordinating tendencies.[7c,7d,10] Substitution of such anions with other anions may also lead to structural and physical changes of the host systems.[5d,7e,11]

Here, in this chapter, a three dimensional (3D) cationic CP has been reported which is built from a neutral N-donor ligand (L) and Cd (II), ClO_4^- anions and free guests. The framework displays inherent structural dynamism through the loss of guest solvent molecules upon air-drying. The guest dependent structural changes have been well understood from the SCSC transformation studies (**Scheme 2.1**). The extra framework anions in the compound can be easily exchanged with other anions of different sizes and coordinating tendencies. The compound also shows anion dependent structural dynamism.

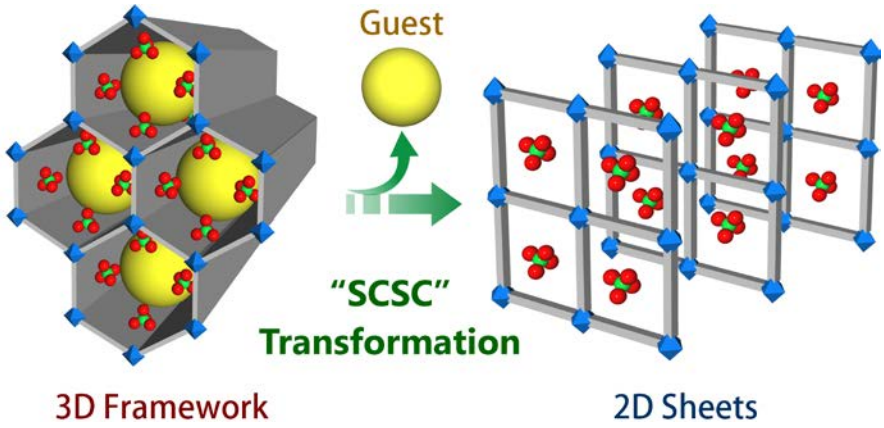

Scheme 2.1. *Schematic representation of guest driven dynamic structural transformation from a 3D framework to a 2D sheet.*

2.2. Experimental Section:

2.2.1. General remarks:

2.2.1.1. Materials: All the reagents and solvents were commercially available and used without further purification.

2.2.1.2. Physical measurements: Powder X-ray diffraction (PXRD) patterns were measured on Bruker D8 Advanced X-Ray diffractometer at room temperature using Cu-Kα radiation (λ= 1.5406 Å) with a scan speed of 0.5° min^{-1} and a step size of 0.01° in 2 *theta*. Thermogravimetric analysis was recorded on Perkin-Elmer STA 6000, TGA analyser under N_2 atmosphere with heating rate of 10° C/min. FT-IR spectra were recorded on NICOLET 6700 FT-IR Spectrophotometer using KBr Pellets.

2.2.1.3. X-ray Structural Studies: Single-crystal X-ray data of compound **1** and compound **2** were collected at 100 K on a Bruker KAPPA APEX II CCD Duo diffractometer (operated at 1500 W power: 50 kV, 30 mA) using graphite-monochromated Mo Kα radiation (λ = 0.71073 Å). Crystal was on nylon CryoLoops (Hampton Research) with Paraton-N (Hampton Research) oil. The data integration and reduction were processed with SAINT[12] software. A multi-scan absorption correction was applied to the collected reflections. The structure was solved by the direct method using SHELXTL[13] and was refined on F^2 by full-matrix least-squares technique

using the SHELXL-97[14] program package within the WINGX[15] programme. All non-hydrogen atoms were refined anisotropically. All hydrogen atoms were located in successive difference Fourier maps and they were treated as riding atoms using SHELXL default parameters. The structures were examined using the *Adsym* subroutine of PLATON[16] to assure that no additional symmetry could be applied to the models. **Appendix 2.1-2.2** indicate crystallographic data of compound **1** (CCDC-1044688) and **2** (CCDC-1044689), which can be obtained free of charge from The Cambridge Crystallographic Data Centre (via www.ccdc.cam.ac.uk/data_request/cif.).

2.2.2. Synthesis:

2.2.2.a Synthesis of Compound 1: DCM solution of the ligand (21 mg, 1mL) was taken into a glass tube onto which was poured tetrahydrofuran (THF) (1 ml) above which was layered methanolic solution of $Cd(ClO_4)_2.xH_2O$ (31 mg, 1mL). Rod Shaped yellow crystals suitable for X-ray studies were obtained after 15 days in 70 % yield. SQUEEZE routine of PLATON has been used to remove highly disordered guest molecules in compound **1**.

2.2.2. b Synthesis of Compound 2 : When parent crystals are being taken out from the mother liquor and kept in open air for about 2 hrs; it gives rise to another type of crystal (confirmed by single x-ray studies).

Elemental analysis (%) calcd for C_{28} H_{32} N_8 Cd_1 Cl_2 O_{11}: C 40.00, H 3.84, N 13.52. Found: C 40.92, H 3.98, N 13.86.

2.2.3 Anion exchange study: Single crystals of compound **1** were separately dipped in aqueous solutions (1 mmol/10 mL H_2O) of NaN_3 and KSCN for about 7 days at RT which yielded the anion exchanged product. The products were characterized by FT-IR, PXRD.

2.2.4 Anion selectivity study (Separation of N_3^- and SCN^-): Single crystals of compound **1** were separately dipped in aqueous solutions (10 mL) of equimolar NaN_3 (1 mmol) and KSCN (1mmol) for about 7 days at RT, giving rise to the anion exchange products, characterized by FT-IR spectra.

2.3. Result and discussions:

Reaction of ligand[17] (1, 4-bis (4-pyridyl)-2, 3-diaza-1, 3-butadiene) with $Cd(ClO_4)_2.xH_2O$ in a solvent combination of CH_2Cl_2/ tetrahydrofuran /methanol gave yellow colored rod shaped crystals of compound **1** $[\{Cd(L)_3.(ClO_4)_2\}\cdot xG]_n$ (where G are disordered low boiling solvent molecules) (**Figure 2.1**).

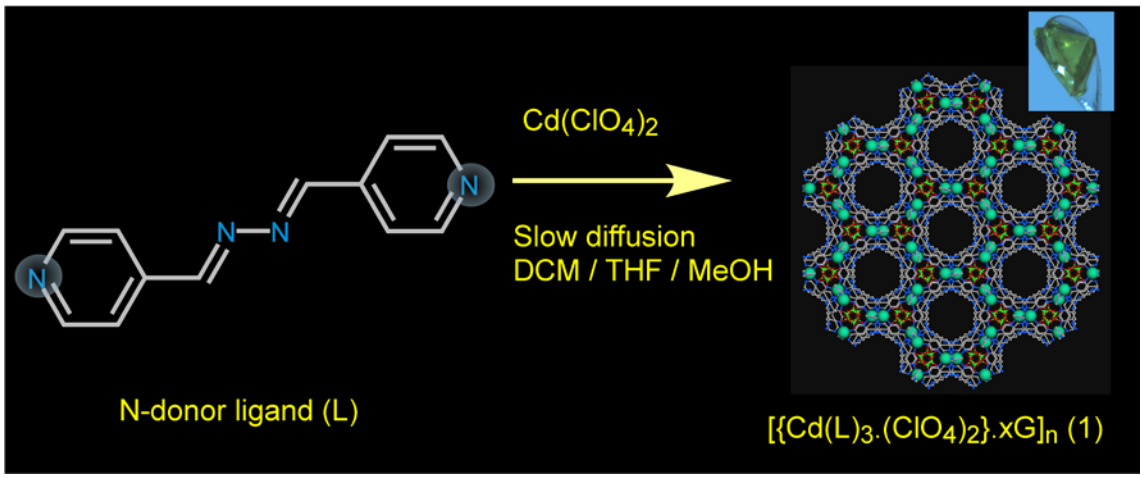

Figure 2.1. *Synthetic scheme of the cationic CP **1** .*

The compound **1** formed 3D kagome like structure with 1D porous channel as revealed from the single-crystal structural analysis. A very interesting aspect of compound **1** is that crystals of **1** undergo drastic structural transformation upon air drying without losing their single-crystalline nature. Single-crystal analysis of the new phase showed a remarkable one step dimensionality reduction to form a two-dimensional (2D) sheets like structure **2**$[\{Cd(L)_2(OH_2)_2.(ClO_4)_2\}.(THF)]_n$. A drastic lowering in unit cell volume also supports the formation of non porous structure (**2**) from the porous (**1**) parent framework. It is very interesting to note that low boiling guests easily come out from the framework (**1**) without any external stimuli like temperature, pressure and lead to the guest driven inherent dynamic nature of the cationic framework (**1**) (**Figure 2.2).** A single-crystal X-ray diffraction study (SC-XRD) revealed that compound **1** crystallizes in trigonal crystal system with space group R-3c (**Appendix 2.1**). An asymmetric unit of compound **1** contains half Cd(II), one and half ligands (L) , one ClO_4^- anion and disordered solvent molecules (**Figure 2.3**). SQUEEZE routine of PLATON has been used to remove highly disordered guest molecules in compound **1**.Each

Cd(II) shows connections with six N-pyridyl moieties of six different ligands forming a six coordinated distorted octahedral geometry. Each ligand connects two metal centres via its terminal N-pyridyl functionality to form an extended 3D cationic structure. Single net packing of the compound results in a kagome like structure with 1D pore channel along *c* axis (**Figure 2.4a**).

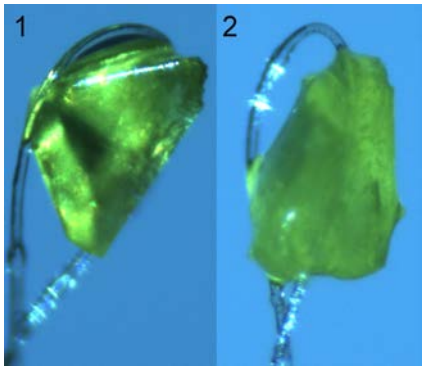

Figure 2.2. *Crystals image of compound **1** and **2** respectively (crystals have taken from the same batch reaction).*

Out of six ligands in a complete set of coordination of a metal centre, two shows trans geometry and four of them exhibit distorted cis geometry. Thus the overall packing of **1** shows the presence of free ClO_4^- anions in the interstitial voids of the cationic framework (**Figure 2.4b**).

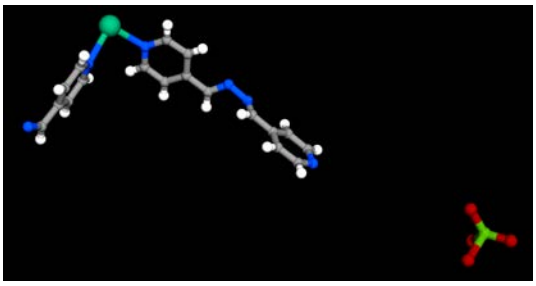

Figure 2.3. *Asymmetric unit of compound **1**(color code: Carbon; light grey, nitrogen;blue,oxygen;red,chlorine;green,cadmium;light green).*

SCSC structural transformation revealed abrupt changes in crystal system (monoclinic) in compound **2** from **1** (**Appendix 2.2**). Complete single -crystal structural analysis of **2** shows formation of 2D cationic sheets with free ClO_4^- anions in the framework lattice (**Figure 2.5 &**

Appendix 2.3). It is very worth noting that two coordinated ligands in **1** are being replaced by two water molecules in **2** leading to reduction of dimensionality by one step (3D→2D) resulting the formation of 2D sheets like structure (**Figure 2.6**). In order to obtain the stable phase of compound **1**, solvent exchange experiments were carried out with other non-coordinating solvents. But, it has been found that, **1** remains stable in solvents / mother liquor only and irreversibly transformed to 2nd phase upon removal from the solvent.

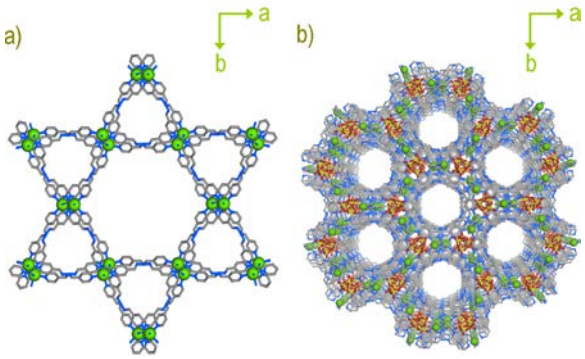

Figure 2.4. *a) Single net packing of compound **1** along c axis. b) Perspective view of overall packing of compound (**1**) along c axis (free solvent molecules are hidden).*

Close examination of structure of **2** shows that two ligands orient in cis form and rest two are intrans form around each Cd(II) centre. Moreover, oxygen atom of ClO_4^- anion forms H-bonds

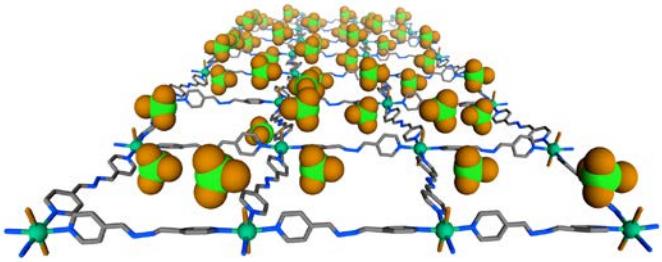

Figure 2.5. *2D cationic net with free ClO_4^- anions in compound **2** (color code: Carbon; light grey, nitrogen;blue,oxygen;orange,chlorine;green,cadmium;light green).*

with coordinated water molecules. In addition, Guest THF molecules in the structure are found to form various non-covalent interactions with C-H, ClO_4^- anions and coordinated water molecules.

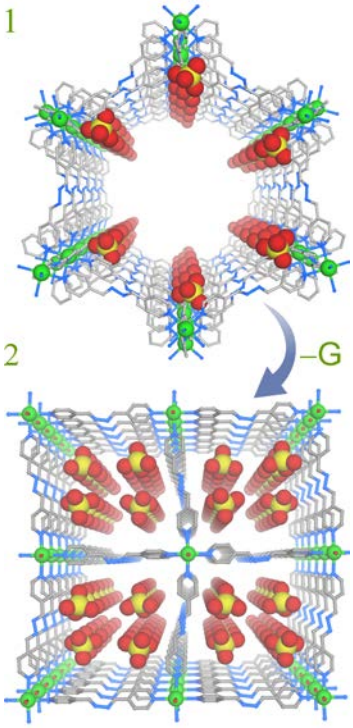

Figure 2.6. *Guest driven structural transformation upon air drying from **1** (3D) to **2**(2D) (Free solvent molecules are hidden) (color code; Carbon: grey, oxygen: red, nitrogen: blue, chlorine: yellow, cadmium: green).*

Powder X-ray diffraction (PXRD) patterns of **2** show that it is stable at room temperature as evident from variable time PXRD (**Figure 2.7**).

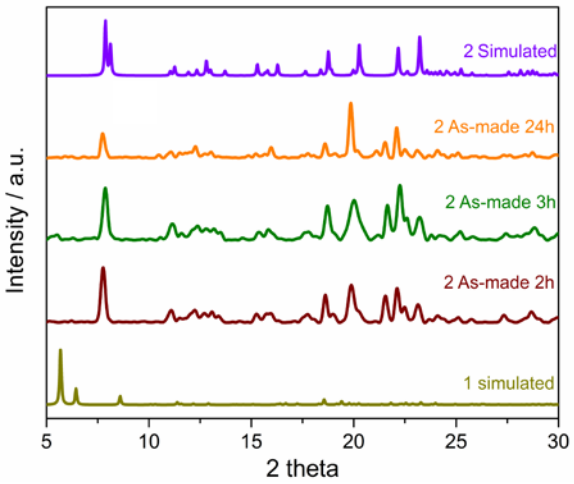

Figure 2.7. *Time dependent powder X-ray diffraction (PXRD) patterns of compound **2**.*

It is very important to note that **1** upon air drying changed to **2** by partial loss of guest molecules. Due to presence of such above mentioned non-covalent interactions between THF and framework, compound **2** is stable and does not lose any further guests on standing at room temperature (**Figure 2.8**).

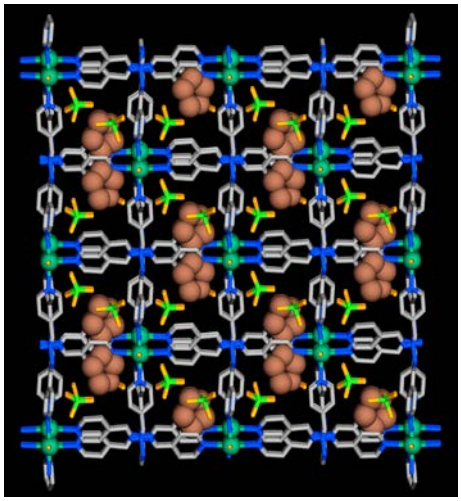

Figure 2.8. *Overall packing of compound 2 along c axis with free tetrahydrofuran as guests shown in CPK model (color code; Carbon: grey, oxygen: orange, nitrogen: blue, chlorine: green, cadmium: dark green).*

Thermogravimetric analysis (TGA) of **2** shows ~ 8% wt loss around 100^{o}C and does not show any further wt loss up to 290^{o}C (**Figure 2.9**).

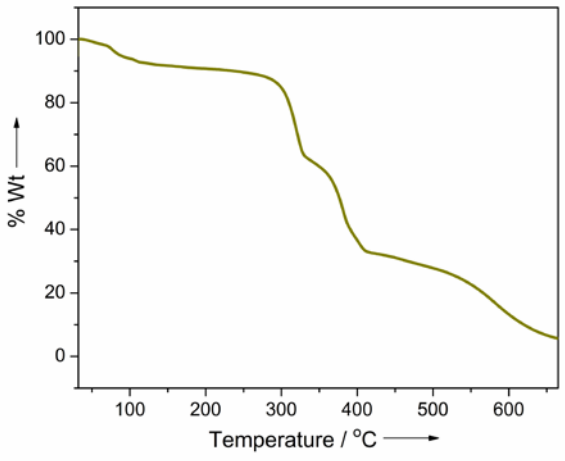

Figure 2.9. *TGA plot of compound **2**.*

Framework dynamic behaviour was also observed during the replacement of host anions by some incursive anions of different sizes, shapes and coordinating tendencies. From the above structural description it is evident that compound **2** contain free ClO_4^- anions in its lattice. To inspect the anion-driven framework's dynamic behaviour anion exchange experiments were performed. Strongly coordinating anions (viz. N_3^- and SCN^-) of different sizes and shapes have been chosen. In a typical experiment, crystals of compound **2** were separately dipped in aqueous solution of NaN_3 and KSCN for about ~7 days. FTIR spectroscopic tool was utilized to monitor the anion–exchange studies. It showed complete replacement of anions by incursive anions took place in ~ 7 days. Strong bands related to ClO_4^- (~1100 cm^{-1}) in compound **2** almost completely vanished and in place new bands appeared at ~2050 cm^{-1} for **2**⊃N_3^- and at ~ 2080 cm^{-1} for **2**⊃SCN^- respectively (**Figure 2.9.1**).

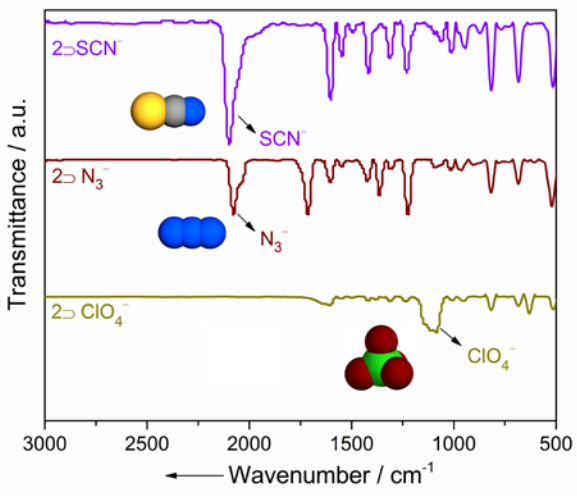

Figure 2.9.1. *FTIR spectra of compound **2** and its various anion exchanged products with highlighted bands of corresponding anions.*

The exchanged compounds (**2**⊃N_3^- and **2**⊃SCN^-) showed differences in PXRD patterns compared to compound **2** (**Figure 2.9.2**) Such differential PXRD patterns emerge owing to the different coordinating tendencies, size and shapes of foreign anions suggesting dynamic nature of the framework (**Appendix 2.4**). During the course of anion exchange I made several attempts to get X-ray quality single crystals of exchanged compounds, but unfortunately I was unable to

obtain the same (**Appendix 2.5**). During the course of anion exchange, I observed that the supernatant solution of

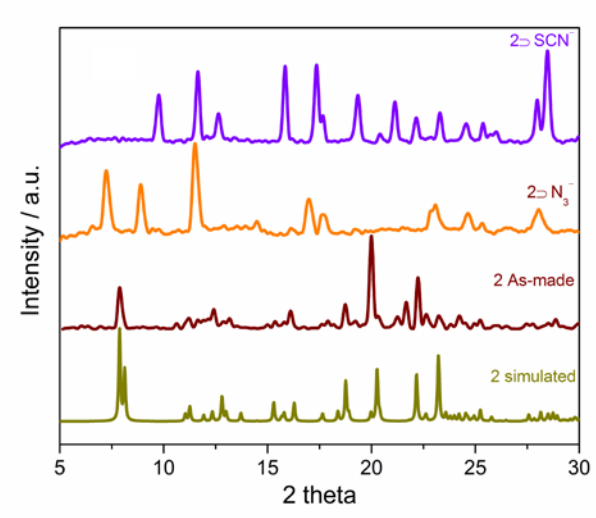

Figure 2.9.2. *PXRD patterns of various anion exchange solids of compound **2**.*

individual anion precursor remain colorless and transparent indicating CP particles did not dissolve and recrystallize from the solvent. Owing to the differential PXRD patterns of anion exchanged products, the compound shows anion-responsive structural dynamism. Reversibility of the anion exchange experiment was also performed by taking a $NaClO_4$ solution (1mM/10mL H_2O). No strong bands at~ 1100 cm^{-1} for ClO_4^- appeared in re exchanged products as revealed in FTIR spectra indicating reversibility could not be achieved in these cases. Encapsulation of a particular anion by a cationic moiety in presence of other competing anions is very important. Hence to perform the guest anion affinity by cationic framework **2**, I investigate anion exchange experiment by taking binary mixture of anions: N_3^-/ SCN^-. In a representative experiment, crystals of compound **2** were immersed in aqueous solution of equimolar mixtures of NaN_3 and KSCN. An investigation of FTIR spectra showed a strong band related to SCN^- at ~ 2080 cm^{-1} suggesting preferential uptake of SCN^- over N_3^- (**Figure 2.9.3**).

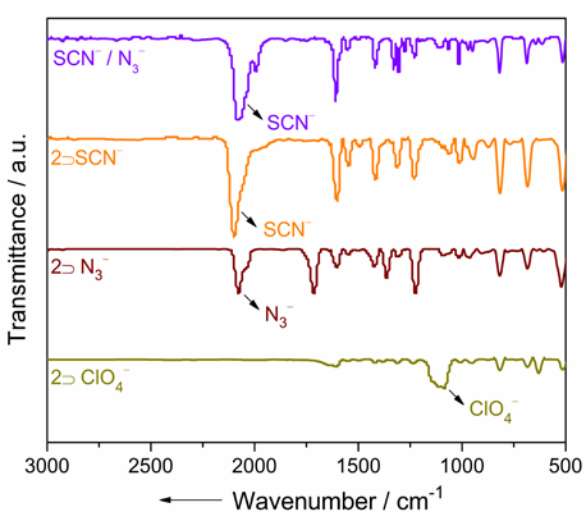

Figure 2.9.3. *FTIR spectra of different binary mixtures of anions of compound* ***2****.*

2.4. Conclusion:

To conclude, a 3D cationic CP has been synthesized using a N-donor ligand. The cationic CP showed inherent dynamic behaviour owing to the loss of low boiling solvent at room temperature. Guest driven dynamic behaviour of the cationic framework has been well validated by SCSC transformation experiment. Apart from the guest driven dynamic behaviour, the cationic CP also exhibited anion-responsive structural dynamism. The compound showed easy anion–exchange behaviour with strongly coordinating anions of different sizes and shapes in aqueous medium. Moreover, different guest anion-affinity was also achieved with the cationic framework.

2.5. References:

(1) (a) Zhou, H.-C.; Long, J. R.; Yaghi, O. M. *Chem. Rev*. **2012**, *112*, 673–674. (b) McKinlay, A. C.; Morris, R. E.; Horcajada, P.; Ferey, G.; Gref, R.; Couvreur, P.; Serre, C. *Angew. Chem. Int. Ed.* **2010**, *49*, 6260–6266. (c) Lee, J. Y. ; Farha, O. K.; Roberts, J.; Scheidt, K. A.; Nguyen, S. T.; Hupp, J. T. *Chem. Soc. Rev.* **2009**, *38*, 1450-1459. (d) Kitagawa, S.; Kitaura, R.; Noro, S. I. *Angew. Chem. Int. Ed.* **2004**, *43*, 2334 – 2375. (e) Park, I. H.; Chanthapally, A.; Zhang, Z.; Lee, S. S.; Zaworotko, M. J.; Vittal, J. J. *Angew. Chem. Int. Ed.* **2014**, *53*, 414 – 419. (f) Shigematsu, A.; Yamada, T.; Kitagawa, H. *J. Am. Chem. Soc.*

2012, *134*, 13145 – 13147.(g) Das, M. C.; Bharadwaj, P. K. *J. Am. Chem. Soc.* **2009**, *131*, 10942–10949.(h) Sen, S.; Neogi, S.; Rissanen, K.; Bharadwaj, P. K. *Chem. Commun*. **2015**, *51*, 3173–3176. (i) Zhang, J.-P.; Liao, P.-Q.; Zhou, H.-L.; Lin, R.-B.; Chen, X.-M. *Chem. Soc. Rev.* **2014**, *43*, 5789-5814.(j) Matsuda, R.; Kitaura, R.; Kitagawa, S.; Kubota, Y.; Kobayashi, T. C.; Horike, S.; Takata, M. *J. Am. Chem. Soc*. **2004**, *126*, 14063–14070. (k) Ghosh, S. K.; Kitagawa, S. *CrystEngComm.* **2008**, *10*, 1739–1742. (l) Chen, B.; Yang, Y.; Zapata, F.; Lin, G.; Qian, G.; Lobkovsky, E. B. *Adv. Mater.* **2007**, *19*, 1693 – 1696. (m) Das, M. C.; Ghosh, S. K.; Sañudo, E. C.; Bharadwaj, P. K. *Dalton Trans*. **2009**, 1644-1658. (n) Zhang, W.; Hu, Y.; Ge, J.; Jiang, H.-L.; Yu, S.-H. *J. Am. Chem. Soc*. **2014**, *136*, 16978-16981. (o) Zhang, J.-W.; Zhang, H.-T.; Du, Z.-Y.; Wang, X.; Yu, S.-H.; Jiang, H.-L. *Chem. Commun.* **2014**, *50*, 1092-1094. (p) Konidaris, K. F.; Morrison, C. N.; Servetas, J.G.; Haukka, M.; Lan, Y.; Powell, A. K.; Plakatouras, J. C.; Kostakis, G. E. *CrystEngComm*. **2012**, *14*, 1842-1849. (q) Asha, K.S.; Bhattacharyya, K.; Mandal, S. *J. Mater. Chem. C*. **2014**, *2*, 10073-10081.

(2) (a) Horike, S.; Shimomura S.; Kitagawa, S. *Nat. Chem.* **2009**, *1*, 695 –704. (b) Ferey, G.; Serre, C. *Chem. Soc. Rev.* **2009**, *38*, 1380–1399. (c) Yanai, N.; Kitayama, K.; Hijikata, Y. ; Sato, H.; Matsuda, R.; Kubota, Y.; Takata, M.; Mizuno, M.; Uemura, T.; Kitagawa, S. *Nat.Mater.* **2011**,*10*,787–793. (d) Thallapally, P.K.; Mcgrail, P.; Dalgrano, S. J.; Schaef, H. T. ; Tian J.; Atwood, J. L. *Nat. Mater.* **2008**, *7*, 146-150. (e) Thallapally, P. K.; Tian, J. ; Kishan, M. R.; Fernandez, C. A. ; Dalgarno, S. J.; McGrail, P. B; Warren, J. E.; Atwood, J. L. *J. Am. Chem. Soc*. **2008**, *130*, 16842–16843.

(3) (a) Serre, C.; Draznieks, C. M.; Surblé, S.; Audebrand, N.; Filinchuk, Y.; Férey, G. *Science.* **2007**, *315*, 1828-1831. (b) Ghosh, S. K. ; Bureekaew, S.; Kitagawa, S. *Angew. Chem. Int. Ed.* **2008**, *47*, 3403 –3406. (c) Ghosh, S. K. ; Zhang, J.-P.; Kitagawa, S. *Angew. Chem. Int. Ed.* **2007**, *46*, 7965–7968. (d) Joarder, B.; Chaudhari, A. K. ; Nagarkar, S. S.; Manna, B.; Ghosh, S. K. *Chem. Eur. J.* **2013**, *19*, 11178 – 11183. (e) Wang, J.-H.; Li, M.; Li, D.; *Chem. Sci*. **2013**, *4*, 1793-1801.

(4) (a) Takashima, Y.; Martinez, V. M. ; Furukawa, S.; Kondo, M.; Shimomura, S.; Uehara, H.; Nakahama, M.; Sugimoto, K. ; Kitagawa, S. *Nat. Commun*. **2011**, *2*, 168. (b) Dybtsev, D. N.; Chun, H.; Kim, K. *Angew. Chem. Int. Ed.* **2004**, *43*, 5033 –5036.

(5) (a) Kondo, A.; Noguchi, H.; Carlucci, L.; Proserpio, D. M. ; Ciani, G.; Kajiro, H.; Ohba, T.; Kanoh, H.; Kaneko, K. *J. Am. Chem. Soc*. **2007**, *129* , 12362–12363. (b) Kondo, A.; Kajiro, H. ; Noguchi, H. ; Carlucci, L. ; Proserpio, D. M. ; Ciani, G.; Kato, K.; Takata, M. ; Seki, H.; Sakamoto, M.; Hattori, Y.; Okino, F.; Maeda, K.; Ohba, T.; Kaneko, K.; Kanoh, H. *J. Am. Chem. Soc*. **2011**, *133*, 10512–10522. (c) Biradha, K. ; Fujita, M. *Angew. Chem. Int. Ed.* **2002**, *41*, 3392-3395. (d) Manna, B.; Chaudhari, A. K.; Joarder, B.; Karmakar, A.; Ghosh, S. K. *Angew. Chem. Int. Ed.* **2013**, *52*, 998–1002. (e) Kotani, R.; Kondo A.; Maeda, K. *Chem. Commun.* **2012**, *48*, 11316–11318.

(6) (a) Maji, T. K.; Matsuda, R.; Kitagawa, S. *Nat. Mater*. **2007**, *6*, 142 –148.

(7) (a) Min, K. S.; Suh, M. P. *J. Am. Chem. Soc.* **2000**, *122*, 6834 – 6840. (b) Chen, Y.-Q.; Li, G.-R.; Chang, Z.; Qu, Y.-K. ; Zhang, Y.-H.; Bu, X.-H. *Chem. Sci*. **2013**, *4*, 3678-3682. (c) Li, X.; Xu, H.; Kong, F.; Wang, R. *Angew.Chem. Int. Ed.* **2013**, *52*, 13769 –13773. (d) Ma, J.-P. ; Yu, Y.; Dong, Y.-B. *Chem. Commun.* **2012**, *48*, 2946 – 2948. (e) Manna, B.; Joarder, B.; Desai, A. V. ; Karmakar, A.; Ghosh, S. K. *Chem. Eur. J.* **2014**, *20*, 12399 – 12404. (e) Muthu, S.; Yip, J. H. K. ; Vittal, J. J.; *J. Chem. Soc. Dalton Trans*. **2001**, 3577 –3584.

(8) (a) Karmakar, A.; Manna, B.; Desai, A.V.; Joarder, B.; Ghosh, S. K. *Inorg. Chem*. **2014**, *53* , 12225–12227. (b) Manna, B.; Singh, S.; Ghosh, S. K. *J. Chem. Sci*. **2014**, *126*, 1417–1422.

(9) (a) Maji, T. K.; Uemura, K.; Chang, H.-C. ; Matsuda, R.; Kitagawa, S. *Angew. Chem. Int. Ed.* **2004**, *43*, 3269–3272. (b) Suh, M. P.; Ko, J. W. ; Choi, H. J. ; *J. Am. Chem. Soc*. **2002**, *124*, 10976–10977. (c) Li, H.-X.; Ren, Z.-G. ; Liu, D.; Chen, Y.; Lang, J.-P.; Cheng, Z.-P.; Zhu, X.-L.; Abrahams, B. F. *Chem. Commun.* **2010**, *46*, 8430–8432. (d) Bloch, W. M.; Sumby, C. J. *Chem. Commun*. **2012**, *48*, 2534-2536. (e) Bloch, W. M.; Burgun, A.; Coghlan, C. J.; Lee, R.; Coote, M. L.; Doonan, C. J.; Sumby, C. J. *Nat. Chem.* **2014**, *6*, 906–912. (f) Cai, Y.-P. ; Zhou, X.-X.; Zhou, Z.-Y.; Zhu, S.-Z. ; Thallapally, P. K.; Liu, J. *Inorg. Chem*. **2009**, *48*, 6341–6343.

(10) Aijaz , A.; Lama, P.; Bharadwaj, P. K. *Inorg. Chem.* **2010**, *49*, 5883–5889.

(11) (a) Manna, B.; Singh, S.; Karmakar, A.; Desai, A. V.; Ghosh, S. K. *Inorg. Chem*. **2015**, *54* , 110–116. (b) Maji, T. K.; Matsuda, R.; Kitagawa, S. *Nat. Mater.* **2007**, *6*, 142– 148. (c) Chen, B.; Wang, L.; Zapata, F.; Qian, G.; Lobkovsky, E. B. *J. Am. Chem. Soc*. **2008**, *130*, 6718–6719.

(12) *SAINT Plus*, (Version 7.03); Bruker AXS Inc.: Madison, WI, **2004**.

(13) Sheldrick, G. M. *SHELXTL*, *Reference Manual*: version 5.1: Bruker AXS; Madison, WI, **1997**.

(14) Sheldrick, G. M. *Acta Crystallogr. Sect. A* **2008**, *112*.

(15) WINGX version 1.80.05 Louis Farrugia, University of Glasgow.

(16) Spek, A. L. PLATON, *A Multipurpose Crystallographic Tool*, Utrecht University, Utrecht, The Netherlands, **2005**.

(17) Ciurtin , D. M.; Dong , Y.-B.; Smith , M. D.; Barclay, T.; Loye, H.-C. Z. *Inorg. Chem*. **2001**, *40* , 2825–2834.

Chapter 3

Anion Responsive Tunable Luminescence and Structural Dynamism of A Flexible Cationic Coordination Polymer

3.1. Introduction:

Microporous metal-organic frameworks (MOFs)/coordination polymers (CPs) are of great current interest, not only due to their fascinating architectures, but also due to their wide range of potential applications especially in gas storage, chemical separation, drug delivery, catalysis, enantioseparation, optical properties, chemosensing etc.[1] Mostly second generation rigid porous materials showed exotic results in the aforementioned areas with their intact stable and rigid porosity of the overall framework.[2] Recently, Kitagawa and others explored the third generation soft materials and their advantages over the rigid porous frameworks.[3] Guest responsive structural dynamism is particularly very important to study such kind of materials. Flexible soft porous materials are sensitive to the chemical environment and undergo structural variations depending upon the nature of guest molecules inside the framework.[4] Among various CPs, cationic CPs have advantages over others to design dynamic frameworks. Cationic CPs are often made with neutral ligands and metal ions, so extra-framework anions usually occupy the framework void or remains weakly coordinated to the metal centers.[5] Exchanging anions inside the framework with other anions of different shape and size may lead to structural changes along with their physical properties.[6] Luminescent CPs with switchable properties are of great interest due to their potential applications in chemical sensors.[7] Luminescent cationic CP with extra framework anions may give us a dynamic framework and tunable luminescent behavior by exchanging framework anions with other foreign anions of different shape, size and coordinating nature. Until now, great progress has been made on separation and other properties of dynamic frameworks, but luminescent response to guest molecules/anions are rarely reported with structural dynamism.[8]

Here, in this chapter, I report a porous CP made of one-dimensional (1D) coordination polymers of Zn^{II} and a newly designed neutral N-donor organic ligand (**L**) with extra-framework nitrate anions, which feature interesting guest and anion dependent structural dynamism. Dynamic structural behavior has been demonstrated by single-crystal-to-single-crystal (SCSC) structural transformation. The compound shows slow opening of the framework upon guest inclusion, and size selective sorption of hydrophobic guest molecules. Anions of the framework are easily exchangeable, and the compound shows interesting anion responsive tunable luminescent behaviors.

3.2. Experimental Section:

3.2.1. General remarks:

3.2.1.1. Materials: All the reagents and solvents were commercially available and used without further purification.

3.2.1.2. Physical measurements: Powder X-ray diffraction (PXRD) patterns were measured on Bruker D8 Advanced X-Ray diffractometer at room temperature using Cu-Kα radiation (λ= 1.5406 Å) with a scan speed of 0.5° min^{-1} and a step size of 0.01° in 2 *theta*. Thermogravimetric analysis was recorded on Perkin-Elmer STA 6000, TGA analyser under N_2 atmosphere with heating rate of 10° C/min. FT-IR spectra were recorded on NICOLET 6700 FT-IR Spectrophotometer using KBr Pellets. The solid state fluorescence spectra were recorded on Fluorolog 3.

3.2.1.3. X-ray Structural Studies: Single-crystal X-ray data of compound **1a** and compound **1** were collected at 150 K on a Bruker KAPPA APEX II CCD Duo diffractometer (operated at 1500 W power: 50 kV, 30 mA) using graphite-monochromated Mo Kα radiation (λ = 0.71073 Å). Crystal was on nylon cryoLoops (Hampton Research) with Paraton-N (Hampton Research) oil. The data integration and reduction were processed with SAINT [9] software. A multi-scan absorption correction was applied to the collected reflections. The structure was solved by the direct method using SHELXTL[10] and was refined on F^2 by full-matrix least-squares technique, using the SHELXL-97[11] program package within the WINGX[12] programme. All non-hydrogen atoms were refined anisotropically. All hydrogen atoms were located in successive difference Fourier maps and they were treated as riding atoms using SHELXL default parameters. The structures were examined using the *Adsym* subroutine of PLATON[13] to assure that no additional symmetry could be applied to the models. **Appendix 3.1-3.2** indicates crystallographic data of compound **1a** (CCDC-883148) and **1** (CCDC-883147), which can be obtained free of charge from The Cambridge Crystallographic Data Centre (via www.ccdc.cam.ac.uk/data_request/cif.).

3.2.2. Synthesis:

3.2.2.1 Synthesis of Ligand L: The condensation of 4,4'-Ethylenedianiline (5gm, 0.0235 mol) & 2-pyridine carboxaldehyde (5.034 gm, 0.047 mol) in (1:1) mixture of EtOH & MeOH for about 3 hrs at 70 °C gives rise to light yellow ppt. The ppt formed, filtered off, washed with EtOH and MeOH, dried under vacuum to afford 7gm of light yellow solid (**Figure 3.1**). For $C_{26}H_{22}N_4$: C, 79.89; H, 5.67; N, 14.33; found: C, 80.40; H, 5.07; N, 14.52. Yield: 76%. ^{1}H-NMR (400 MHz , DMSO-d_6): δ 8.68 (d, J=3.6Hz,2H),δ 8.57 (s,2H),δ 8.12 (d,J=7.8Hz,2H),δ 7.92 (t,J=7.3Hz,2H),δ 7.49 (t, J=6.0Hz,2H),δ 7.28 (q, J=7.2Hz,8H), δ 2.91 (s, 4H) (**Appendix 3.3**). ^{13} C NMR: 160.5,154.7,150.2,148.7,140.9,137.6,129.9,126.1,121.7,121.6,37.0 (A**ppendix 3.4**). HRMS (ESI): Calc. for $C_{26}H_{23}N_4$ $[M+H]^+$: 391.1922; Found: 391.1924.

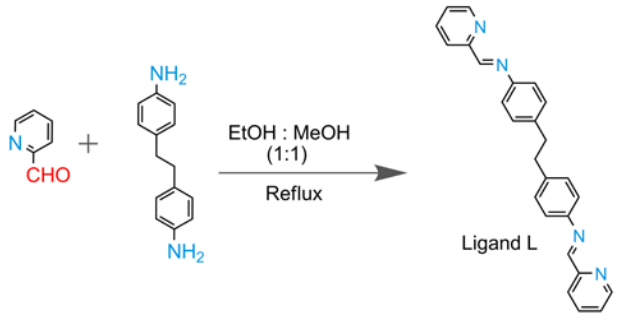

Figure 3.1. *Schematic representation of the ligand **L**.*

3.2.2.2 Synthesis of Compound 1a: DCM solution of the ligand (39 mg, 1mL) was taken into a glass tube, onto that benzene(1mL) carefully layered and over the benzene layer MeOH solution of $Zn(NO_3)_2.6H_2O$ (29.74 mg, 1mL) very carefully layered. Rod like yellow crystals suitable for X-ray studies were obtained after 15 days in 60 % yield.

3.2.2. 3 Synthesis of Compound 1 : When parent crystals are being taken out from the mother liquor and kept in open air for about 1.5 hrs; it gives rise to another type crystals (confirmed by single X-ray studies) compound **1**.FT-IR(KBr pellet, cm^{-1}): 3406.42(m), 2921.91(w), 1630.18(w), 1599.65(m), 1502.91(w), 1384.21(s), 1156.59(w), 1101.12(w), 1019.91(m), 907.19(m), 847.26(m), 775.34(m), 639.08(m), 564.10(m).

3.2.3 Anion exchange study: Solid powder of compound **1** was stirred very slowly in methanolic solutions (1 mmol/10 mL MeOH) of NaN_3, KSCN, $NaClO_4$ and $NaN(CN)_2$

respectively for about 5 days at RT giving rise to the anion exchange product, and characterized by FT-IR, PXRD and solid- state emission spectra.

3.2.4 Reversibility study: Each solid powder of the exchanged compounds was stirred very slowly in separate methanolic solution (10 mL) of tetra butyl ammonium nitrate of two different concentration (0.5 mmol & 1.0 mmol) for about 5 days at RT , filtered off, washed with MeOH several times, and characterized by FT-IR.

3.2.5 Anion selectivity study

3.2.5 a Separation of N_3^- and SCN^- based on 1: Solid powder of compound **1** was stirred very slowly in methanolic solution (10 mL) of equimolar NaN_3 (1 mmol) and KSCN (1 mmol) for about 5 days at RT, giving rise to the anion exchange product, and characterized by FT-IR spectra.

3.2.5 b Separation N_3^- and ClO_4^- based on 1: Solid powder of compound **1** was stirred very slowly in methanolic solution (10mL) of equimolar NaN_3 (1mmol) and $NaClO_4$ (1mmol) for about 5 days at RT, giving rise to the anion exchange product, and characterized by FT-IR spectra.

For $ClO_4^-/N(CN)_2^-$, $SCN^-/N(CN)_2^-$ and $N_3^-/N(CN)_2^-$ combinations, similar experiment was carried out; exchanged products characterized by FT-IR spectra.

3.2.6 Solvent exposure study: Solid powder of compound **1** was exposed to different low boiling solvents (MeOH, EtOH, ACN, Acetone etc) for about 7days and characterized by PXRD.

3.2.7 Sorption Measurements: Solvent sorption measurements were performed using BelSorpmax (Bel Japan). All of the solvents used were of 99.99% purity. The dehydrated sample was obtained by heating as-made sample at 120 °C under vacuum for 3h, and the dehydration was confirmed by TGA and PXRD. Prior to adsorption measurement, the dehydrated sample was pretreated at 120 °C under vacuum for 3h using Bel PrepvacII, and purged with N_2 on cooling. Low pressure gas sorption measurements were performed using Bel Sorpmax (Bel Japan). All of the gases used were of 99.999% purity.

3.3. Result and discussions:

The combination of **L** and $Zn(NO_3)_2$ in CH_2Cl_2/MeOH and benzene solvent system afforded yellow colored rod shaped single-crystals of compound **1a** $[\{Zn(L)(MeOH)_2\}(NO_3)_2 \cdot xG]_n$ (Where G is disordered guest molecules). Single-crystal analysis of the complex revealed the formation of a 1D chain structure. These 1D chains are hydrogen bonded with other chains through uncoordinated anions and solvent molecules leading to H-bonded 3D structure with 1D pore channels. A noteworthy feature of the compound **1a** is that, when crystals of **1a** were left out of mother liquor at room temperature for one hour, it showed drastic structural transformation of the network, without losing crystalline nature. Single-crystal analysis of those crystals revealed large differences in unit-cell parameters and complete structural analysis showed that two coordinated MeOH solvent molecules with each Zn^{II} escaped, and were replaced by two H_2O molecules to form a new phase **1** $[\{Zn(L)(H_2O)_2\}(NO_3)_2 \cdot 2H_2O]_n$. Although the coordination network of complexes **1a** and **1** are very similar but overall structure, shape and size of channels are very different (**Figure 3.2**). Single-crystal X-ray diffraction (SC-XRD) study revealed that compound **1a** crystallized in monoclinic system, space group *C2/c* (**Appendix 3.1**). The asymmetric unit of **1a** consists of one-half of each Zn^{II} and **L**, one coordinated methanol, one disordered nitrate anion and disordered solvents. Each metal ion exhibited six coordinated distorted octahedral geometry with N_4O_2 donor set, bonding from two different **L** with four nitrogen coordinating sites and rest two coordinating sites were occupied by two coordinated methanol molecules. The Zn^{II}–N (pyridine), Zn^{II}–N (aliphatic) and Zn^{II}–O distances are

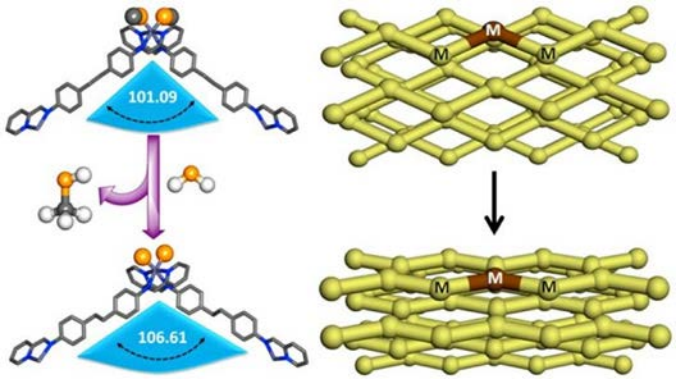

Figure 3.2. *Crystal structures of compound **1a** (above) and **1** (below) showing coordination environment (left) and overall framework (right).*

2.156(3), 2.217(3) and 2.081(3) Å respectively. At both sides of the **L,** nitrogen atom from the ortho position of the aromatic ring and one aliphatic N-atom binds to Zn^{II} in bidentate fashion. Coordination from both sides of the ligand **L** extended the structure to a 1D chain in zigzag manner (**Figure 3.3**).

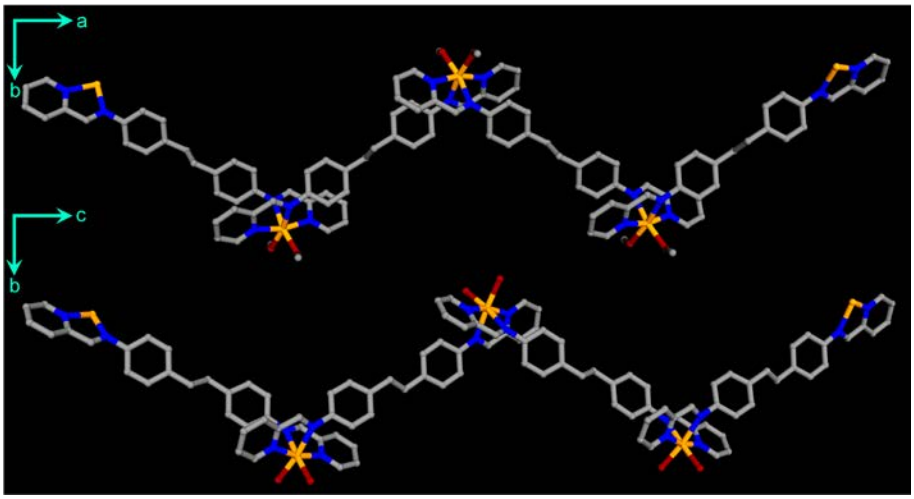

Figure 3.3. *1D chain of both the compounds showing coordination environment around the metal centre; compound **1a** (top); compound **1** (bottom) (colour code; carbon: gray, oxygen: red, nitrogen: blue, zinc: orange).*

Packing diagram of the cationic chains of compound **1a** forms 1D channel along *c* axis, which encapsulates disordered nitrates and solvent molecules. SCSC transformation analysis revealed that crystal system of compound **1** is same as that of **1a** but space group changed to $P2_1/n$ (**Appendix 3.2**). Coordination environment around the Zn^{II} remains almost unchanged with similar N_4O_2 donor set but coordinated methanol solvents are now replaced by water molecules. Bond lengths and angles around Zn^{II} are also very similar. 3D packing structure of cationic chains of **1** show that this compound also form a channel along crystallographic *a* axis, occupied by free nitrates and uncoordinated water molecules. Coordinated water molecules form strong H-bonding with free nitrates and free water molecules, leading to H-bonded 3D structure. Interestingly, close examination of both the structures revealed that during structural transformation M-M-M angle for both the compounds are quite different and expanded from 101.09° (**1a**) to 106.61°(**1**) during structural transformation. This transformation leads to drastic

change in the shape and size of 1D channel (**Figure 3.4**).

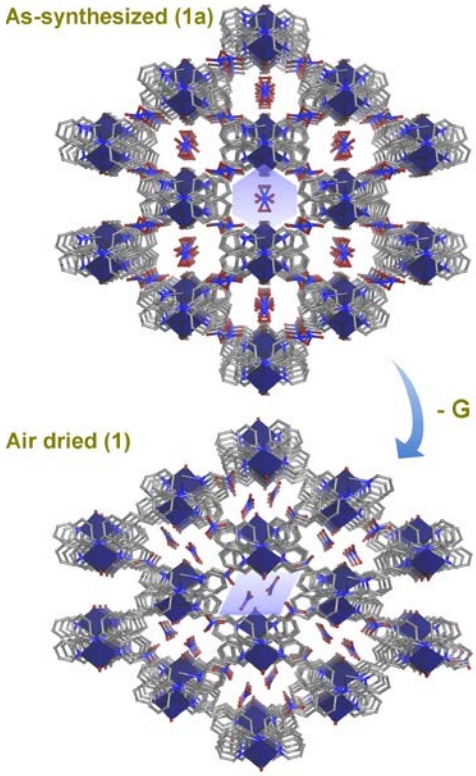

Figure 3.4. *Perspective views of the structural transformation between compound **1a** and **1** (H atoms and free solvent molecules are deleted for clarity).*

Compound **1** is stable at room temperature in single crystal form for several hours, but in powder form, compound is not stable in its original form and changes its structure with time in open air, which is evident from the little variation of powder X-ray diffraction (PXRD) patterns of **1** at different time intervals (**Figure 3.5**). Thermo-gravimetric analysis (TGA) of the powder sample showed ~ 5% wt loss at around 120°C corresponding to ~2 H_2O molecules per formula unit, and further it is stable up to ~ 300°C (**Figure 3.6**). To check the dynamic behavior of the framework, we studied guest inclusion behavior of the dehydrated phase in presence of other guest molecules. In a typical experiment, **1** was exposed to different dry solvents for few days. PXRD analysis revealed structural changes for different vapor exposed compounds, suggesting the flexible behavior of the framework. For small hydrophobic guests (acetone, acetonitrile), PXRD patterns are identical but different from PXRD pattern of **1**, indicating new phases after guest

inclusion. On the other hand, in presence of small hydrophilic guests (ethanol, methanol), similar patterns were observed as that of **1** indicating structural similarity. It suggests different responses of **1** towards two different types of guest molecules (**Figure 3.7**).

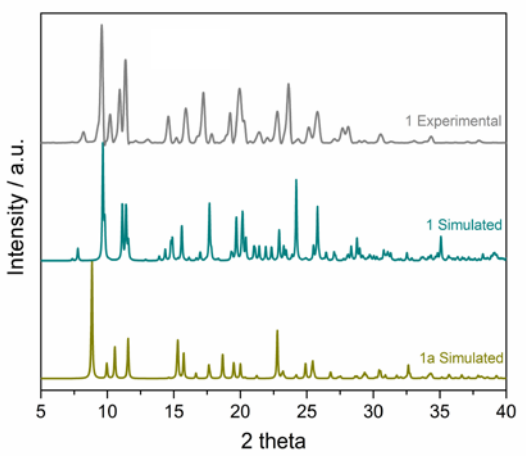

Figure 3.5. *PXRD patterns of (a) Simulated **1a**, (b) Simulated **1**, and (c) **1**experimental.*

To confirm the guest inclusion behavior, solvent sorption experiments were carried out with hydrophobic and hydrophilic guests at 298K.

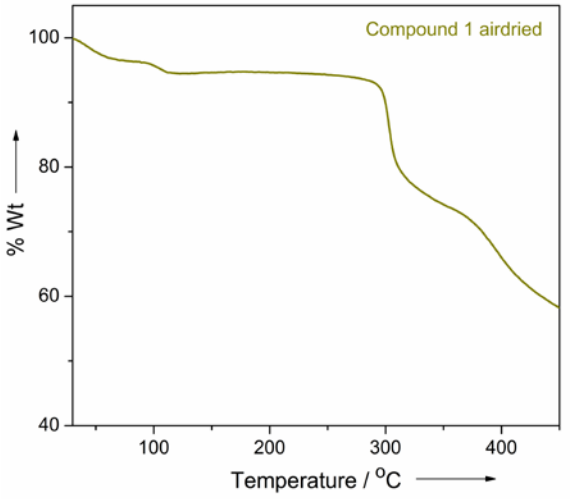

Figure 3.6. *Thermogravimetric analysis profile of compound **1**.*

The dehydrated or guest free phase (**1´**) was generated by heating **1** at 120°C for 3 hours to remove guest H_2O molecules. Dynamic behavior of the framework was very clear from solvent sorption experiments. Small guest molecules of both types showed very similar sorption patterns.

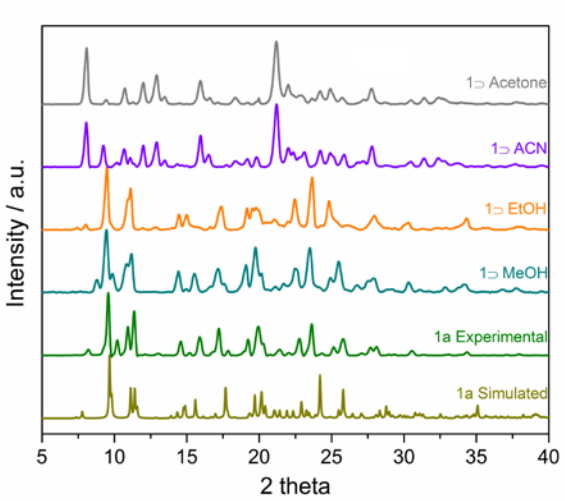

Figure 3.7. *PXRD patterns of different vapor exposed samples of* ***1****.*

The sorption profiles increased slowly with little amount of sorption were observed below P/P_0 = 0.2, but which slowly increased with increasing pressure and all the profiles show hysteric sorption behavior (**Figure 3.8**).

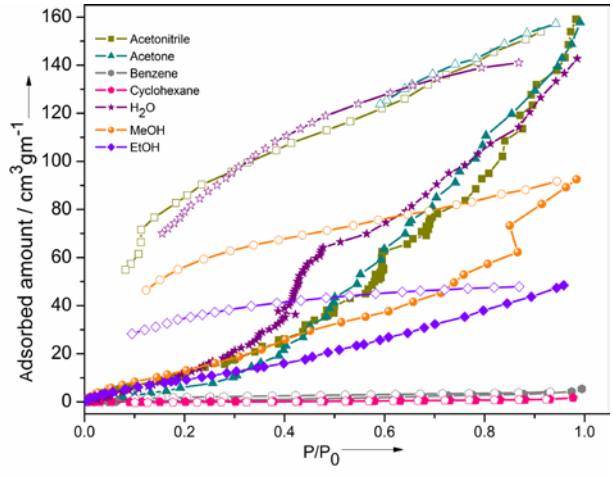

Figure 3.8. *Adsorption and desorption curves of hydrophobic and hydrophilic guest molecules at 298 K.*

Among hydrophilic guest molecules, H_2O showed highest amount uptake (~ 143 ml/gm), whereas methanol (~93ml/gm), ethanol (~ 48ml/gm) showed lesser amount of uptake, which is in accordance to the size of the guest molecules. Small and similar sized hrodrophobic guests (acetonitrile and acetone) showed almost similar amount of uptake (~ 160ml/gm), but large hydrophobic guest molecules (like benzene and cyclohexane) could not enter into the channels due to the insufficient space inside the channels. Flexible nature of the framework is also observed during anion exchange studies. As described above, the compound **1** has 1D channel along *c* axis filled with NO_3^- anions. To check the anion dependent structural dynamism, anion exchange experiments has been performed. For this purpose, I used two types of anions: (1) anions with weak or non-coordinating nature like ClO_4^- and $N(CN)_2^-$ (Type-A), and (2) anions having strong coordinating nature, like N_3^-, SCN^- (Type-B). Crystals of compound **1** were immersed in separate methanolic solutions of excess NaN_3, KSCN, $NaClO_4$ and $NaN(CN)_2$. I monitored anion exchange experiments by FT-IR spectra. It was observed that it needed 5 days for complete exchange of anions. FT-IR spectra of exchanged products showed strong bands associated with exchanged anions and disappearance of bands for nitrate anion. Other peaks in the spectra remain almost unchanged, suggesting that the framework of the complexes remain intact after exchange process (**Figure 3.9**).

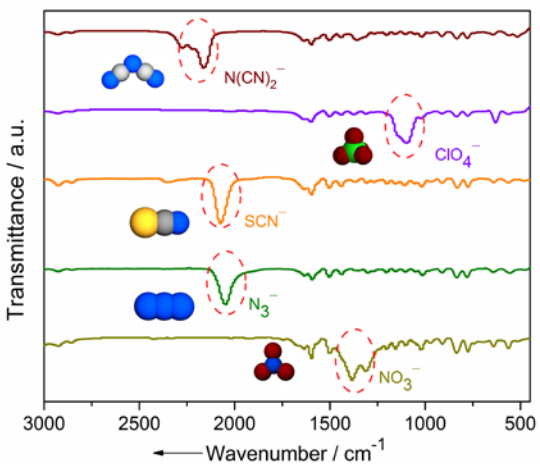

Figure 3.9. *FTIR spectra of anion exchanged compounds with highlighted peak positions of the corresponding anions.*

For compound **1** with NO_3^- anions inside the channels (designated as **1**⊃ NO_3^-) has a strong band at1390 cm^{-1} due to nitrate anion and this band almost completely disappeared in exchanged products and new peaks appeared at ~2050 cm^{-1} (**1**⊃N_3^-) , ~2080 cm^{-1} (**1**⊃SCN^-), ~1100 cm^{-1} (**1**⊃ClO_4^-), and at ~ 2160 cm^{-1} (**1**⊃$N(CN)_2^-$) as expected for different anions. Due to the different shape, size and coordinating tendency, PXRD patterns of exchanged products are different for each anion, showing the highly flexible nature of the framework. Due to the dynamic nature, framework can easily adjust its channel dimension to encapsulate different guest anions (**Figure 3.9.1**). Anion reversibility was performed in a two stage experiment with (0.5 mM/10 ml MeOH) and (1.0mM/10 ml MeOH) concentrations of tetrabuylammonium nitrate (see experimental details). FT-IR spectra reveals that at 0.5mM/10mlMeOH concentration, ClO_4^- was completely exchanged by NO_3^-, while no anion exchange was observed in the rest of the three compounds.

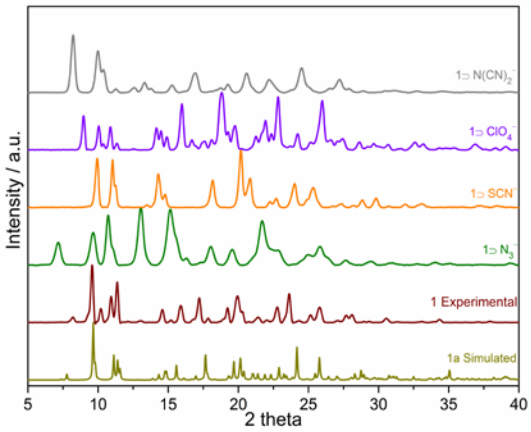

Figure 3.9.1. *PXRD patterns of various anion exchanged solids of compound **1**.*

In second stage of experiment; at concentration 1.0 mM/ 10ml MeOH, liitle exchange by NO_3^- anion in **1**⊃$N(CN)_2^-$ was confirmed by the presence of NO_3^- peak in the FT-IR spectrum and slightly reduced peak intensity of the $N(CN)_2^-$was observed. On the other hand, for **1**⊃N_3^- and **1**⊃SCN^- compounds, no NO_3^- uptake was observed suggesting the strong interactions of the N_3^-, SCN^-anions with the framework. Whereas **1**⊃ClO_4^- is completely exchangeable as previous one (**Figure 3.9.2**). Selective anion exchange experiment with the framework was

checked by performing anion exchange experiments in several binary anionic mixtures. Five different binary combinations were used to check affinity *viz*. N_3^-/SCN^-, N_3^-/ClO_4^-, $N_3^-/N(CN)_2^-$, $ClO_4^-/N(CN)_2^-$,and $SCN^-/N(CN)_2^-$.

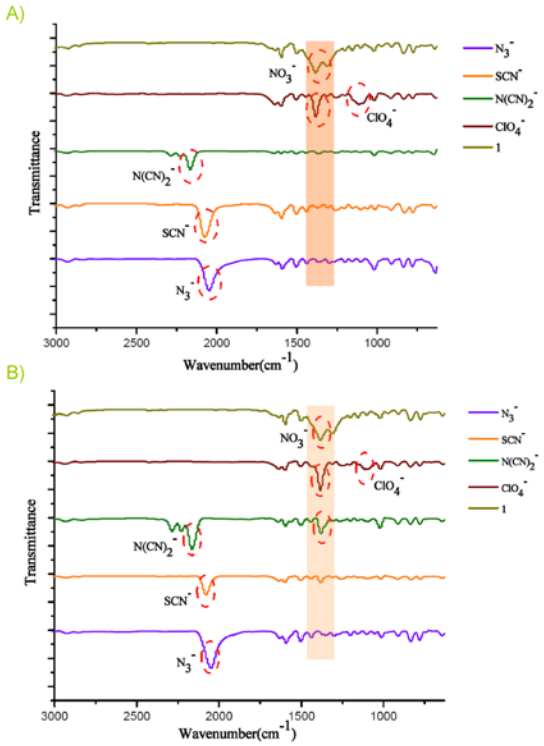

Figure 3.9.2. *FTIR spectra of reversible anion exchange of compound **1**; A) with 0.5mm conc. of tetra butyl ammonium nitrate, B) with 1mm conc. of tetra butyl ammonium nitrate.*

In a typical experiment, crystals of **1** were immersed in methanolic solution of mixed anions having equimolar concentrations (**experimental details**). The exchanged compounds were further monitored by FT-IR analysis to check the preferencial exchange from the mixture. Among the five combinations, N_3^-/SCN^- and N_3^-/ClO_4^- showed the selective anion exchange by the framework,where from first one it exchanged with $SCN^-$and from the another mixture, it got exchanged with N_3^- (**Figure 3.9.3**). Rest of the three combinations showed the presence of both the anions inside the framework with presence of their respective IR frequencies (**Appendix 3.5-3.8**). It is worth noting that, reversibile anion exchange of **1**⊃ SCN^- and **1**⊃ N_3^- with NO_3^- could not be achieved due to effective coordinating tendency of the corresponding anions.

Hence, above experiments reveal the order of affinity of guest anions for the framework is SCN^- > N_3^- > $N(CN)_2^-$ > ClO_4^- (**Figure 3.9.4**).

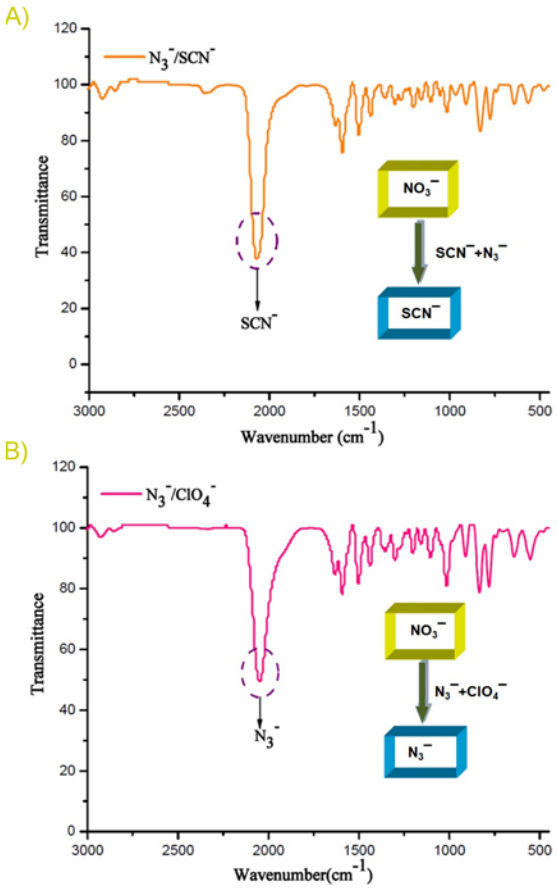

Figure 3.9.3. *FTIR spectra of anion selectivity test; A) SCN^- selectively adsorbed from N_3^- / SCN^- mixture, B) N_3^- taken up by the framework from N_3^- / ClO_4^- mixture.*

This above order of affinity arises from several properties of anions like their size, shape, geometry, their coordinating tendencies to Zn(II), and also their different π-π interaction and hydrogen bonding abilities with the framework. Anion exchanged materials showed interesting anion-responsive luminescent behavior. Solid state UV absorptions were measured for all anion exchanged compounds which showed almost very similar to the compound **1** (**Figure 3.9.5**).

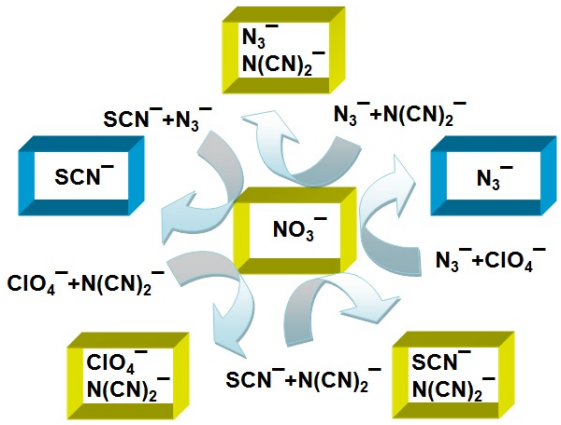

Figure 3.9.4. *Schematic representation depicting anion selectivity from the combinations of various anions.*

Further to this, solid state emission spectra were recorded for powder samples at room temperature for **L**, **1** and all anion exchanged compounds. Upon excitation at 394 nm, **L** shows two emission bands, at 512 nm and 533 nm, L is weakly fluorescent compared to other samples.

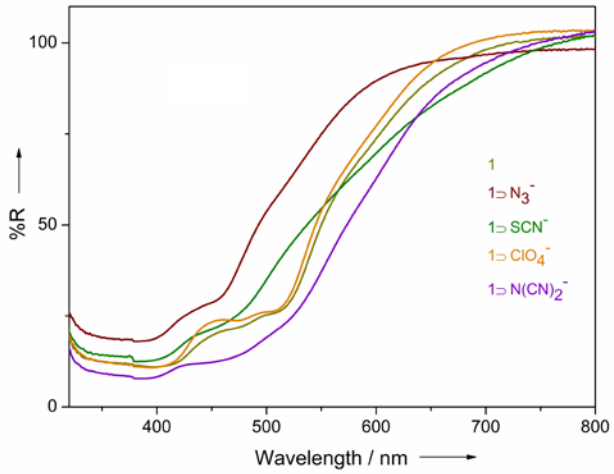

Figure 3.9.5. *Reflectance spectra of compound **1** and various exchanged phases at room temperature.*

1 showed an intense band at 541 nm with red shift with respect to **L** emission. This may be attributed to the coordinating effect of **L** to the Zn^{II}. Anion exchanged compounds **1**⊃N_3^-, **1**⊃SCN, **1**⊃$N(CN)_2^-$and **1**⊃ClO_4^- display broad peaks with intensity maxima at 514 nm, 542 nm, 543 nm and 536 nm respectively. **1**⊃N_3^- exchanged compound showed a blue shift with respect to **L** and **1** emission (**Figure 3.9.6**).

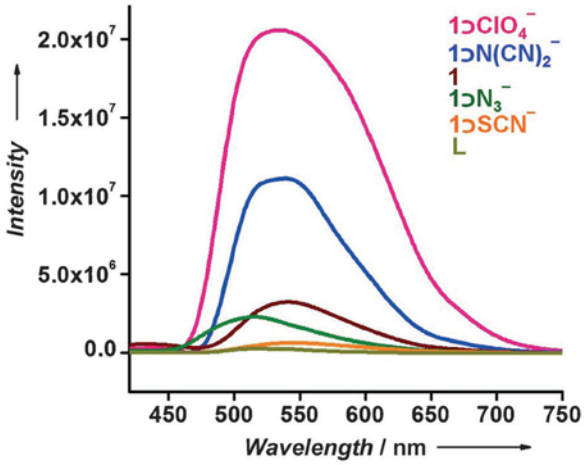

Figure 3.9.6. *Solid state emission spectra of compound **1** and various exchanged phases at room temperature.*

In case of compound **1,** π*-n or π*-π *i.e.* intraligand transitions are possible. The emission intensity of exchanged compounds showed very drastic difference as compared to **1**. For A type anions exchanged compounds i.e. **1**⊃$N(CN)_2^-$and **1**⊃ClO_4^-, high fluorescence enhancement observed (70.72 and 84.14% respectively), on the other hand considerable quenching was observed for B-type anion exchanged compounds i.e. **1**⊃$N_3^-$and **1**⊃SCN^- (29.53% and 80.36% respectively)(**Figure 3.9.7**). Here, the reason for the order of observed luminescence changes with the different anions are not very obvious, but probably due to the various electronic interactions with the framework walls and Zn(II) centre depending upon their size, shape, geometry and coordinating tendencies. As ClO_4^- and the $N(CN)_2^-$ are weakly coordinating so they can accomodate in different places within the dynamic framework after exchange with NO_3^-, which may help to change the framework such way that intraligand interactions may increase and subsequently it may enhance

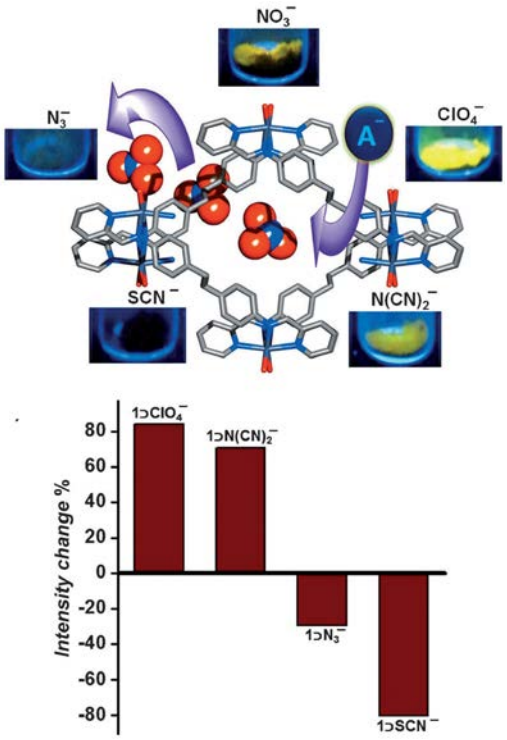

Figure 3.9.7. *Solid state anion exchange effects on the luminescence properties of **1**; A1: $(ClO_4)^-$; A2: $N(CN)_2^-$; B1: N_3^-; B2: SCN^-(top); Bar diagram showing % enhancement and quenching with respect to **1**(bottom).*

---

the luminescence. In case of N_3^- and SCN^-, both can strongly coordinate with the Zn(II) so after coordination, it can make drastic structural change (also observed in PXRD **Figure 3.9.1**) which may diminish intraligand interactions within the framework, and that may reduce luminiscence intensity compared to compound **1.**

3.4. Conclusion:

In conclusion, a dynamic luminescent cationic porous framework has been synthesized using a newly designed chelating N-donor ligand. The compound shows guest as well as anion dependent structural dynamic behavior. Guest dependent dynamic behavior has been demonstrated by SCSC experiment. Anions of the compound lying in the channels are completely exchangeable by other incursive anions. Depending upon anions nature complete reversible, partial reversible and non reversible anion exchange was observed. Different kind of

affinity of the anions toward the framework was observed. Anion exchanged compounds showed interesting anion-responsive tunable luminescent properties, which might have important biological and environmental applications.

3.5. References:

(1) a) Zhou, H. –C,; Long, J. R.; Yaghi, O. M. *Chem. Rev.* **2012,** *112*, 673-674. b) Liu, Q.-K.; Ma, J.-P.; Dong, Y.-B. *J. Am. Chem. Soc.* **2010**, *132*, 7005–7017. c) McKinlay, A. C.; Morris, R. E.; Horcajada, P.; Ferey, G.; Gref, R.; Couvreur, P.; Serre, C. *Angew. Chem. Int. Ed*. **2010**, *49*, 6260 – 6266. d) An, J.; Geib, S. J.; Rosi, N. L. *J. Am. Chem. Soc.*, **2009**, *131* , 8376–8377. f) Lee, J.Y.; Farha, O. K.; Roberts, J.; Scheidt, K. A.; Nguyen, S. T.; Hupp, J. T. *Chem. Soc. Rev*. **2009**, *38*, 1450–1459. g) Ma, L.; Falkowski, J. M.; Abney , C.; Lin, W. *Nat. Chem.* **2010,** *2*, 838-846. h) Guo, Z.; Cao, R.; Wang, X.; Li, H.; Yuan, W.; Wang, G.; Wu, H.; Li, J. *J. Am. Chem. Soc.* **2009**, *131*, 6894–6895. i) Li, G.; Yu, W.; Cui, Y. *J. Am. Chem. Soc.* **2008**, *130*, 4582-4583.

(2) a) Millward, A. R.; Yaghi, O. M. *J. Am. Chem. Soc.* **2005**, *127*, 17998-17999. b) Humphrey, S. M.; Chang, J.-S.; Jhung, S. H.; Yoon, J. W.; Wood, P. T. *Angew. Chem. Int. Ed*. **2007**, *46*, 272 –275.

(3) Horike, S.; Shimomura, S.; Kitagawa, S. *Nat. Chem.* **2009,** *1*, 695-704.

(4) a) Yanai, N.; Kitayama, K.; Hijikata, Y.; Sato, H.; Matsuda, R.; Kubota, Y.; Takata,; Mizuno, M. M.; Uemura, T.; Kitagawa, S. *Nat. Mater.* **2011,** *10*, 787–793. b) Chen, C.-L.; Beatty, A. M. *J. Am. Chem. Soc*. **2008**, *130*, 17222–17223. c) Zhang , J.-P.; Chen, X.-M. *J. Am. Chem. Soc*. **2008**, *130*, 6010–6017. d) Yanai, N.; Uemura, T.; Inoue, M.; Matsuda, R.; Fukushima, T.; Tsujimoto, M.; Isoda, S.; Kitagawa, S. *J. Am. Chem. Soc*. **2012**, *134*, 4501−4504.

(5) a) Min, K. S.; Suh, M. P. *J. Am. Chem. Soc.* **2000,** *122*, 6834-6840 . b) Tzeng, B.-C.; Chiu, T.-H.; Chen, B.-S.; Lee, G.-H. *Chem. Eur. J.* **2008**, *14*, 5237 – 5245. c) Yang, Q.-Y.; Li, K.; Luo, J.; Pana, M.; Su, C.-Y. *Chem. Commun*., **2011**, *47*, 4234–4236.

(6) a) Maji**,** T.K.; Matsuda**,** R.; Kitagawa, S. *Nat. Mater.* **2007**, *6*, 142-148. b) Ma, J.-P.; Yu, Y.; Dong, Y.-B. *Chem. Commun.*, **2012**, *48*, 2946–2948.

(7) a) Cui, Y.; Xu, H.; Yue, Y.; Guo, Z.; Yu, J.; Chen, Z.; Gao, J.; Yang, Y.; Qian, G.; Chen, B. *J. Am. Chem. Soc.* **2012**, *134*, 3979–3982. b) Wang , C.; Lin, W. *J. Am. Chem. Soc*. **2011**, *133*,

4232–4235. c) An ,J.; Shade, C. M.; C.-Czegan, D. A.; Petoud, S.; Rosi, N. L. *J. Am. Chem. Soc.*, **2011**, *133* , 1220–1223.

(8) Takashima, Y.; Martínez , V. M.; Furukawa , S.; Kondo , M.; Shimomura , S.; Uehara , H.; Nakahama, M.; Sugimoto, K.; Kitagawa, S. *Nat. Commun.* **2011,** *2*,168.

(9) *SAINT Plus*, (Version 7.03); Bruker AXS Inc.: Madison, WI, **2004**.

(10) Sheldrick, G. M. *SHELXTL, Reference Manual*: version 5.1: Bruker AXS; Madison, WI, **1997**.

(11) Sheldrick, G. M. *Acta Crystallogr. Sect. A* **2008**, *112*.

(12) *WINGX version 1.80.05 Louis Farrugia, University of Glasgow.*

(13) Spek, A. L. PLATON, *A Multipurpose Crystallographic Tool*, Utrecht University, Utrecht, The Netherlands, **2005**.

Chapter 4

Anion Triggered Tunable Bulk Phase Homochirality and Luminescence of A Cationic Coordination Polymer

4.1. Introduction:

Homochiral coordination polymers (CPs) / metal-organic frameworks (MOFs) have found great attention due to their potential applications in the field of enantioselective catalysis[1] and separation.[2] The synthetic schemes of the rational design of such homochiral frameworks can be classified into three types: (1) spontaneous chiral resolution, (2) chiral induction, and (3) use of enantiopure ligands. Chiral induction and use of enantiopure ligands are the common strategy to generate homochiral frameworks.[3] Generation of spontaneous homochirality in CPs using achiral ligands is seldom studied [4] and retention of the same in bulk phase is quite rare and challenging.[5] Additionally , it has been found that the judiciously chosen achiral N-donor ligand upon coordination with metal ion enhances the chance to create homochiral framework. Employing neutral N-donor ligands often imparts a cationic character to the framework.[6] Consequently, the anions within the framework reside in the porous channels or are weakly coordinated to the metal centers. Efficient substitution of these anions in the framework can aid in tuning the functionality of the host system and often makes a framework dynamic.[7] Taking advantage of such dynamism of a cationic homochiral framework, bulk phase homochirality can be tuned by varying anions in the framework. Conjunction of d^{10} metal ion with neutral N-donor ligand provides a luminescent cationic framework.[8] Anion-responsive tunable luminescence is a key outcome of constructing such cationic matrices.[7b] Sorption behavior of these cationic frameworks can also be tuned by exchanging host anions with other guest anions of different size and shape owing to differential interactions with the incoming adsorptive guests.[7a] By combining altogether in a single species a smart multifunctional material can be developed.[9]

It has been observed that 2,2′-pyridyl like functionality of a N-donor ligand affords helicity to their packing which eventually yields an homochiral framework.[10] Hence, strategically a N-donor ligand of the above functionality has been chosen to generate a homochiral cationic framework. In the present report, I have explored a cationic one dimensional (1D) coordination polymer having six fold helices resulted to a homochiral framework. The framework is built from an achiral neutral N-donor ligand (L) having 2,2′-pyridyl like coordination sites and zinc nitrate, wherein, free nitrate ions are encapsulated in the voids of the resultant cationic framework. The compound is found to exhibit bulk-phase homochirality. Facile exchange of the size-selective non-coordinated anions in the parent compound could be accomplished, which has

been demonstrated by solid state structural transformation based experiments. Interestingly, the framework demonstrated retention of bulk-phase homochirality in the anion-exchanged compounds. Framework has also been found to display anion responsive tunable luminescence and size dependent guest inclusion behaviors (**Figure 4.1**).

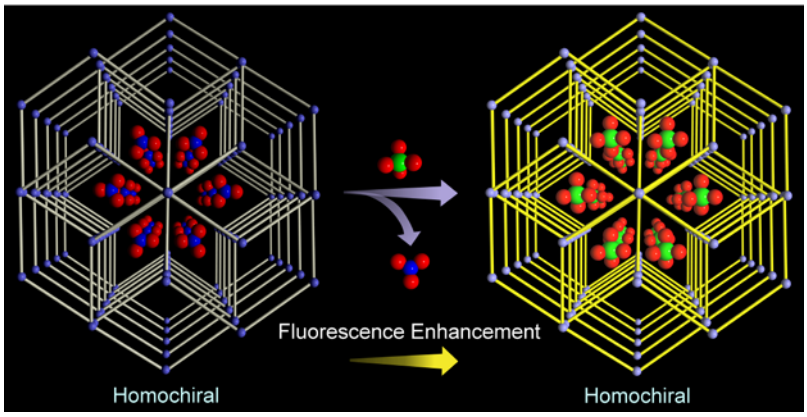

Figure 4.1. *Schematic representation of anion-induced fluorescence enhancement in a SCSC manner from compound* ***1*** $\supset NO_3^-$ *(left) to compound* ***1*** $\supset ClO_4^-$ *(right) maintaining framework homochirality.*

4.2. Experimental Section:

4.2.1. General remarks:

4.2.1.1. Materials: All the reagents and solvents were commercially available and used without further purification.

4.2.1.2. Physical measurements: Powder X-ray diffraction (PXRD) patterns were measured on Bruker D8 Advanced X-Ray diffractometer at room temperature using Cu-Kα radiation (λ= 1.5406 Å) with a scan speed of 0.5° min^{-1} and a step size of 0.01° in 2 *theta*. Thermogravimetric analysis was recorded on Perkin-Elmer STA 6000, TGA analyser under N_2 atmosphere with heating rate of 10° C/min. FT-IR spectra were recorded on NICOLET 6700 FT-IR Spectrophotometer using KBr Pellets. The solid state fluorescence spectra recorded on Fluorolog

3. Solid state CD spectra were measured in JASCO J815 spectrometer in the range 600 nm – 200 nm.

4.2.1.3. X-ray Structural Studies: Single-crystal X-ray data of compound **1**⊃ NO_3^- and compound **1**⊃ ClO_4^- were collected at 150 K on a Bruker KAPPA APEX II CCD Duo diffractometer (operated at 1500 W power: 50 kV, 30 mA) using graphite-monochromated Mo Kα radiation (λ = 0.71073 Å). Crystal was on nylon CryoLoops (Hampton Research) with Paraton-N (Hampton Research) oil. The data integration and reduction were processed with SAINT[11] software. A multi-scan absorption correction was applied to the collected reflections. The structure was solved by the direct method using SHELXTL[12] and was refined on F^2 by full-matrix least-squares technique using the SHELXL-97[13] program package within the WINGX[14] programme. All non-hydrogen atoms were refined anisotropically. All hydrogen atoms were located in successive difference Fourier maps and they were treated as riding atoms using SHELXL default parameters. The structures were examined using the *Adsym* subroutine of PLATON[15] to assure that no additional symmetry could be applied to the models. **Appendix 4.1-4.2** indicate crystallographic data of compound **1**⊃ NO_3^- (CCDC-992985) and **1**⊃ ClO_4^- (CCDC 992986), which can be obtained free of charge from The Cambridge Crystallographic Data Centre (via www.ccdc.cam.ac.uk/data_request/cif.).

4.2.2. Synthesis:

4.2.2. 1 Synthesis of Compound 1⊃ NO_3^-: DCM solution of the ligand (L) (39 mg, 1mL) was taken into a glass tube, onto that benzene(1mL) was carefully layered and over the benzene layer (1:9 H_2O & EtOH) solution of $Zn(NO_3)_2.6H_2O$ (29.74 mg, 1mL) was very carefully layered. Block shaped yellow crystals suitable for X-ray studies were obtained after 15 days in 60 % yield. Compound **1**⊃ NO_3^-. FT-IR(KBr pellet, cm^{-1}): 3431.90(m), 3035.84(w), 2927(w), 1764.52(w), 1592.94(m), 1512.07(m), 1381.31(s), 1199.90(w), 1156.82(w), 1106.93(w), 1019.26(m), 913.44(w), 826.52(m), 771.34(m), 644.36(w), 558.199(m). Elemental analysis (%) calcd for C_{29} H_{31} N_6 O_{10} Zn: C 50.5, H 4.49, N 12.19. Found: C 47.79, H 3.92, N 11.65.

4.2.2. 3 Synthesis of Compound 1⊃ ClO_4^- : Crystals of compound **1**⊃ NO_3^- dipped into an aqueous solution (1 mmol/10 mL H_2O) of $NaClO_4$ for about 5 days to get compound **1**⊃ ClO_4, Confirmed from SC-XRD study. Elemental analysis (%) calcd for C_{26} H_{30} N_4 Cl_2 O_{12} Zn: C 42.92, H 4.16, N 7.70. Found: C 45.07, H 3.93, N 7.96.

4.2.2 Anion exchange study: Solid crystalline powder of compound **1**⊃ NO_3^- was slowly stirred in aquous solutions (1 mmol/10 mL H_2O) of NaN_3, KSCN, $NaN(CN)_2$, $NaClO_4$, $NaBF_4$, $NaPF_6$ and $NaCF_3SO_3$ respectively for about 5 days at RT giving rise to the anion exchanged product, characterized by FT-IR, XPRD, TGA, solid- state UV and solid-state emission spectra. Elemental analysis (%) Found for **1**⊃ BF_4: C 46.54, H 3.37, N 8.04. For **1**⊃ PF_6: C 46.2, H 3.35, N 8.0. For **1**⊃ CF_3SO_3: C 47.01, H 2.9, N 7.60.

4.2.3 Anion selectivity study

4.2.3 a Separation of ClO_4^- and BF_4^- based on 1⊃ NO_3^-: solid crystalline powder of compound **1**⊃ NO_3^- was stirred very slowly in aqueous solution (10 mL) of equimolar $NaClO_4$ (1 mmol) and $NaBF_4$ (1 mmol) for about 5 days at RT giving rise to the anion exchanged product, characterized by FT-IR spectra.

4.2.3 b Separation ClO_4^- and $CF_3SO_3^-$ based on 1⊃ NO_3^- : solid crystalline powder of compound **1**⊃ NO_3^- was stirred very slowly in methanolic solution (10mL) of equimolar $NaClO_4$ (1mmol) and $NaCF_3SO_3$ (1mmol) for about 5 days at RT, giving rise to the anion exchanged products, characterized by FT-IR spectra.

For $BF4^-/PF_6^-$, $PF_6^-/CF_3SO_3^-$ and ClO_4^-/PF_6^- combinations, similar experiment was carried out, and exchanged products characterized by FT-IR spectra.

4.2.4 Solvent exposure study: Solid powder of compound **1′** was exposed to different hydrophilic solvents (H_2O, MeOH and EtOH etc) for about 7days, and characterized by PXRD.

4.2.5 Sorption Measurements: Solvent sorption measurements were performed using BelSorpmax (Bel Japan). All of the solvents used were of 99.99% purity. The desolvated

samples were obtained by heating compound **1**⊃ NO_3^- and **1**⊃ ClO_4^- at 110 °C under vacuum for 12hrs and the desolvation was confirmed by TGA and PXRD. Prior to adsorption measurement the desolvated samples were pretreated at 110 °C under vacuum for 5h using Bel PrepvacII and purged with N_2 on cooling. Low pressure gas sorption measurements were performed using Bel Sorpmax (Bel Japan). All of the gases used were of 99.999% purity.

4.3. Result and discussions:

The combination of L^{7b} (4,4'-(ethane-1,2-diyl)bis(N-(pyridin-2-ylmethylene)aniline) (**Figure 4.2**) and $Zn(NO_3)_2$ in a solvent system of CH_2Cl_2/EtOH, H_2O and benzene yielded yellow colored block-shaped single crystals of compound **1**⊃ NO_3^- $[\{Zn(L)(OH_2)_2\}(NO_3)_2 \cdot xG]_n$ (in which G are disordered guest molecules) (**Figure 4.3 and Appendix 4.3**).

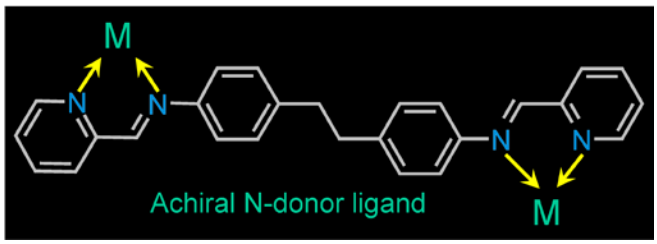

Figure 4.2. *Achiral N-donor ligand showing bichelating metal binding sites at both ends.*

Single-crystal X-ray diffraction (SC-XRD) analysis revealed that **1**⊃ NO_3^- crystallized in chiral hexagonal space group *$P6_522$* with a flack parameter of 0.06(3) (**Appendix 4.1**). Solid state CD spectral analysis revealed that the overall framework is homochiral. Asymmetric unit of **1**⊃ NO_3^- contains one-half Zn^{II}, one-half L, one coordinated water, two disordered nitrate anions (with half occupancy each), and disordered solvents (**Appendix 4.4**). Each metal ion is octahedrally coordinated to four nitrogen atoms from two different L and two oxygen atoms of two water molecules. The Zn(II)-N(pyridine), Zn-N(aliphatic) , and Zn(II)-O(water) distances are 2.141(3), 2.226(3), and 2.091(3) Å respectively. Two nitrogen atoms; one from ortho position of aromatic ring and another from the aliphatic ring bind to Zn (II) in a bidentate fashion. Similarly, other two nitrogen atoms at the other side of the same ligand (L) bind to another metal centre (**Appendix 4.5**). Twisted orientation around C-C single bond in the

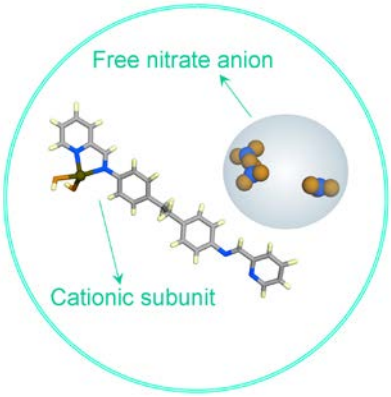

Figure 4.3. *Formula unit of compound* ***1*** $\supset NO_3^-$ *showing cationic subunit and free anions.*

ligand structure is observed in the framework. As a matter of fact N,N-chelating donor sites at both sides of the ligand anchor to each metal in a distorted *syn* conformation, and eventually giving rise a helical arrangement to the structure. Thus extending the coordination at both ends of the ligand furnishes an infinite 1D helical chain with pitch of 44.042Å running along *b* axis (**Appendix 4.6**). These 1D chains form H-bonds with like chains in the vicinity, via free nitrate ions, coordinated water molecules and solvent molecules. Adjacent helices were stabilized by CH-π interactions between H-atoms of CH_2 group and aromatic pyridyl rings of the ligand (**Figure 4.4**).

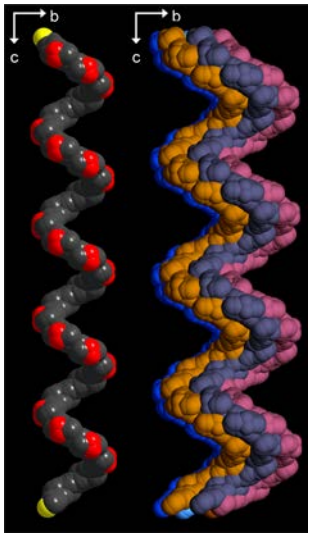

Figure 4.4. *Single helical chain of compound* ***1*** $\supset NO_3^-$ *(left); six adjacent helices (each shown in different color) (right).*

Such binding modes consequently lead to H-bond based 3D packing with free nitrate and disordered solvent molecules in the interstitial positions of the framework (**Figure 4.5**).

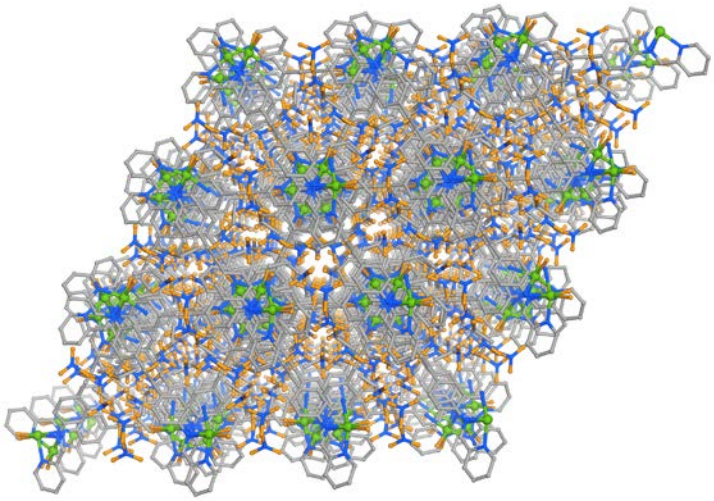

Figure 4.5. *Perspective view of overall packing in compound* ***1***$\supset NO_3^-$.

Recently, Vittal *et al*. clearly explained in their chemical review how the supramolecular/ intermolecular interactions are responsible for the self assembly of a single stranded helix to multiple stranded helices .[16] Thus here, each left-handed helix aligns parallel to the adjacent helix and assembles to multiple stranded helices through intermolecular CH-π interactions and inter-chain H-bonding (**Figure 4.4**). A noteworthy feature of this structure is the six fold helical packing of the framework. Careful analysis of the structure reveals that each left handed helix is interweaved by six similar helices, and the central one is in H-bonded with six similar helices. This gives rise to a homochiral framework originating from six fold interwoven helices (**Figure 4.6**). Overall packing of compound **1**$\supset NO_3^-$ showed presence of free nitrate ions in the framework. The presence of free anions in **1**$\supset NO_3^-$motivated us to perform anion exchange experiments. Two kinds of anions were employed for these studies:1) anions with strong coordinating ability such as N_3^- , SCN^- and $N(CN)_2^-$ (type A) and 2) anions with non-coordinating or weakly coordinating nature viz. ClO_4^-, BF_4^-, PF_6^- and $CF_3SO_3^-$(type B). In a typical experiment crystals of **1**$\supset NO_3^-$ were immersed in separate aqueous solutions of NaN_3,

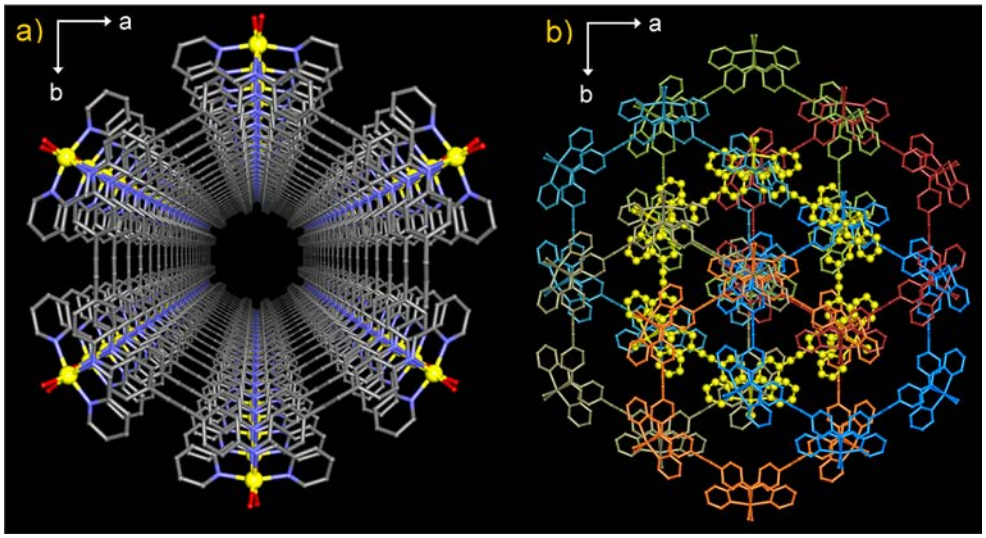

Figure 4.6. *Perspective view of left handed helix of compound* ***1***$\supset NO_3^-$ *(a);six fold helical packing of* ***1***$\supset NO_3^-$ *(shown in different colors)(b).*

KSCN, $NaN(CN)_2$, $NaClO_4$, $NaBF_4$, $NaPF_6$ and $NaCF_3SO_3$ respectively (experimental details) . FT-IR spectroscopic tool was used to monitor these exchange experiments. Elemental analysis and FT-IR spectra suggested that 5-6 days were required for more than 95% exchange. The exchanged compounds were devoid of the peak associated with NO_3^- but the peaks for the corresponding anions could be observed. Rest of the bands remained unaltered. To extrapolate this observation, the strong band observed for NO_3^- in compound **1** at 1384 cm^{-1} (**1**$\supset NO_3^-$) almost disappeared with new peaks at ≈ 2050 cm^{-1} for **1**$\supset N_3^-$, ≈2080 cm^{-1} for **1**$\supset SCN^-$, ≈2160 cm^{-1} for **1**$\supset N(CN)_2^-$, ≈1100cm^{-1} for **1**$\supset ClO_4^-$, ≈1080cm^{-1} for **1**$\supset BF_4^-$, ≈850cm^{-1} for **1**$\supset PF_6^-$ and ≈1272cm^{-1} for **1**$\supset CF_3SO_3^-$ appearing for respective anion exchanged compounds (**Figure 4.7**). Powder-X-ray diffraction (PXRD) patterns of anion exchanged compounds for type A anions showed structural changes in the three cases. However, for type B anions PXRD patterns were quite similar to that of 1$\supset NO_3^-$, indicating framework integrity towards the exchange process for such kind of anions (**Figure 4.8**). Solid state CD spectral analysis of **1**$\supset NO_3^-$ substantiated its bulk phase homochirality and enantiomeric excess nature as it exhibits positive cotton effect at 198nm (**Appendix 4.7**). To check enantiomeric excess, 10 randomly

picked single crystals (one single crystal as sample each) of **1**⊃NO_3^- were analyzed by CD spectroscopy.

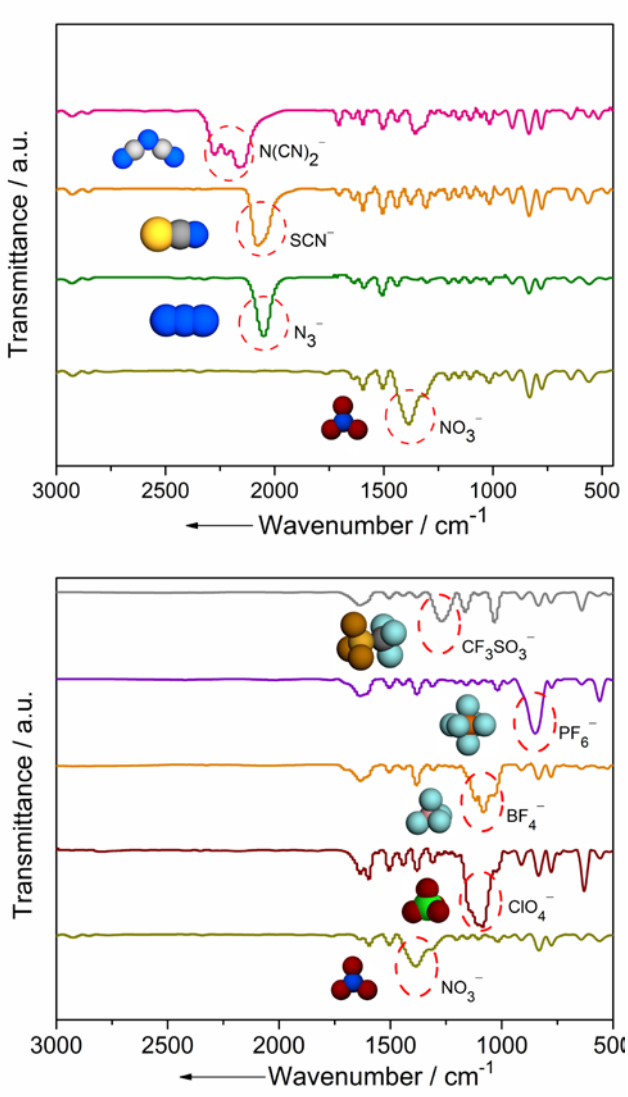

Figure 4.7. *FT-IR spectra of the anion exchanged solids showing bands for respective anions: with strongly coordinating anions (top); with non – coordinating or weakly coordinating anions (bottom).*

Out of 10 samples, 8 showed positive cotton effect and 2 of which showed negative cotton effect. This indicates that **1**⊃NO_3^- exhibits enantiomeric excess in its bulk phase (**Figure 4.9**). More interestingly, bulk homochirality was retained in anion exchanged compounds of B type anions,

which was supported by solid state CD spectra. Solid state CD spectral analysis showed positive cotton effect for all the anion exchanged compounds. The effect was observed for **1**⊃ClO_4^-, **1**⊃BF_4^-, **1**⊃PF_6^- and **1**⊃$CF_3SO_3^-$ at 200nm, 197nm, 205 nm and 203nm respectively

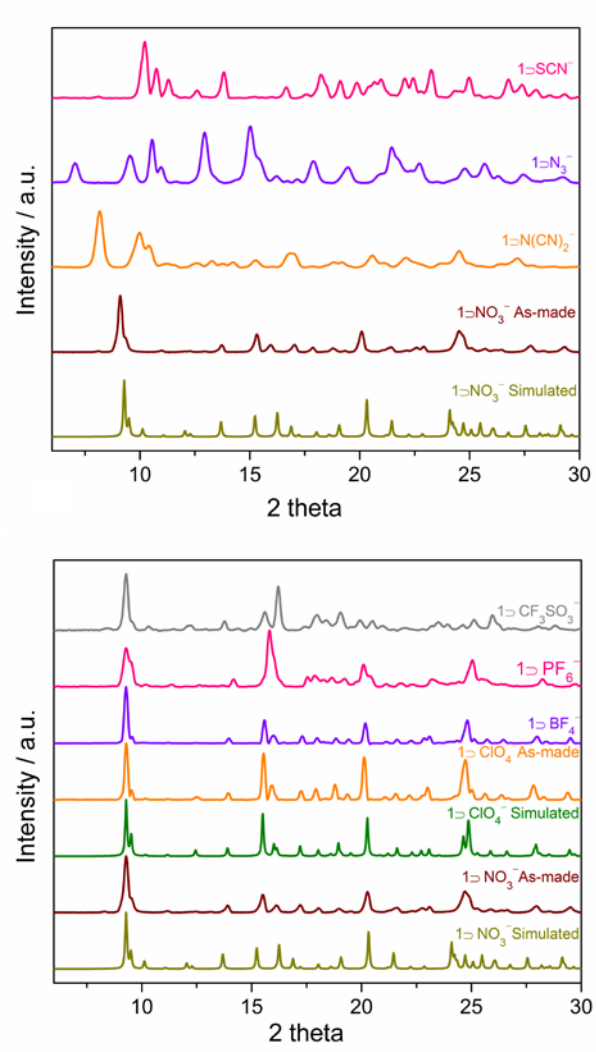

Figure 4.8. *PXRD patterns of the anion exchanged solids: with strongly coordinating anions (top); with non – coordinating or weakly coordinating anions (bottom).*

(**Figure 4.9**). Interestingly, no other examples of showing such tuning of bulk phase homochirality by varying anions are reported. Selective anion exchange experiment was also performed with 1⊃ NO_3^-. To understand the affinity preference of type B anions, five distinct binary combinations *viz.* ClO_4^-/BF_4^-, BF_4^-/PF_6^-, $PF_6^-/CF_3SO_3^-$, ClO_4^-/PF_6^- and

ClO_4^-/$CF_3SO_3^-$ were used for the investigation. Crystals of **1**⊃ NO_3^- were immersed in an aqueous solution of mixed anions in equimolar concentrations (**experimental section**). FT-IR spectral analysis suggested preferential uptake of ClO_4^- over competing anions in ClO_4^-/BF_4^-

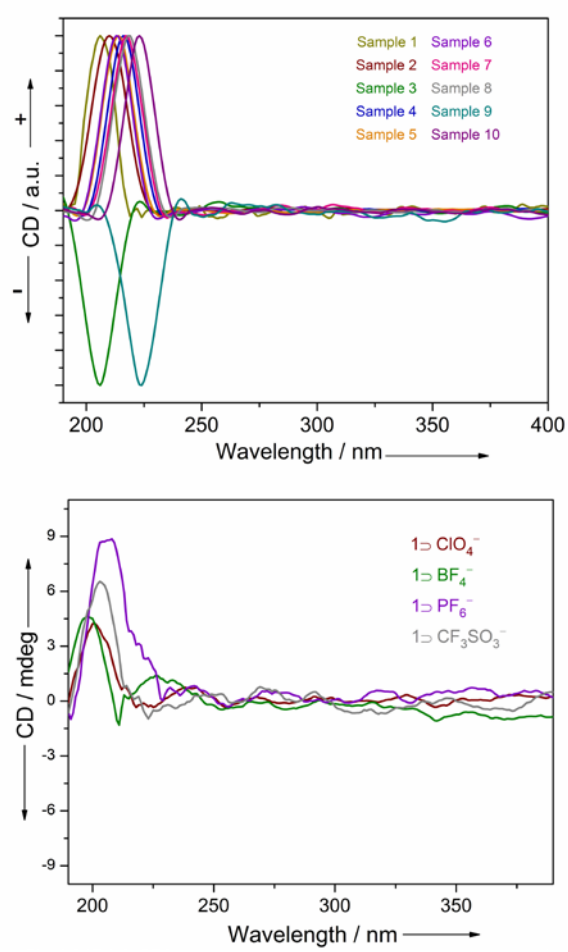

Figure 4.9. *Solid state CD spectra of various compounds: 10 randomly picked crystals of compound* ***1***⊃ *NO_3^-(top); anion exchanged compounds for weakly coordinating anions (bottom).*

and ClO_4^-/$CF_3SO_3^-$ combinations. In all other combinations presence of both anions inside the framework was indicated by their respective IR bands. FT-IR spectral analysis revealed that the combinations BF_4^-/PF_6^- and PF_6^-/$CF_3SO_3^-$ showed more intense bands of PF_6^- over $BF_4^-$and $CF_3SO_3^-$ respectively. The selective affinity experiment led to the following inference of guest anion affinity: ClO_4^-> PF_6^-> BF_4^-≈ $CF_3SO_3^-$(**Figure 4.9.1**). During anion exchange

experiments, X-ray quality single crystals were obtained only in the case of **1**⊃ClO_4^-. Single-crystal structural analysis revealed the replacement of free nitrate anions in **1**⊃ NO_3^- with ClO_4^- ions (**Figure 4.9.2**). The overall framework integrity was maintained as illustrated by $[\{Zn(L)(H_2O)_2\}(ClO_4)_2.(H_2O)_2]_n$.

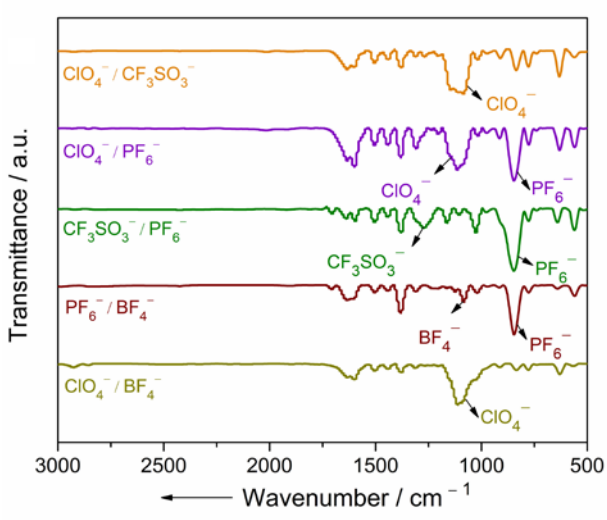

Figure 4.9.1. *FT-IR spectra of various anion exchanged solids taking binary mixture of anions.*

Moreover unit cell parameters of compound **1**⊃ ClO_4^- displayed only a subtle variation as compared to **1**⊃ NO_3^-.

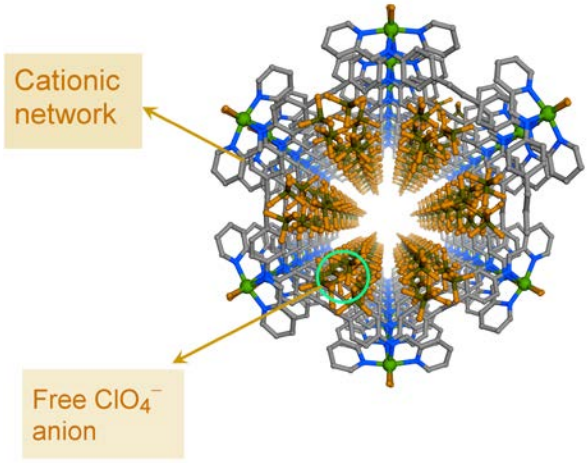

Figure 4.9.2 *Crystal structures of compound* ***1***⊃ ClO_4^- *showing cationic network and free* ClO_4^- *anions.*

The overall structure of **1**⊃ ClO_4^- is very similar to that of **1**⊃ NO_3^- with change in the left handed helical pitch from 44.042Å to 43.105Å (**Figure 4.9.3**). Such helical pitch tuning by anion variation was also explained by Mak *et al*.[17] Powder X-ray diffraction patterns of **1**⊃ NO_3^- confirm its bulk phase purity and intactness of the framework. **1**⊃ ClO_4^- displays very similar

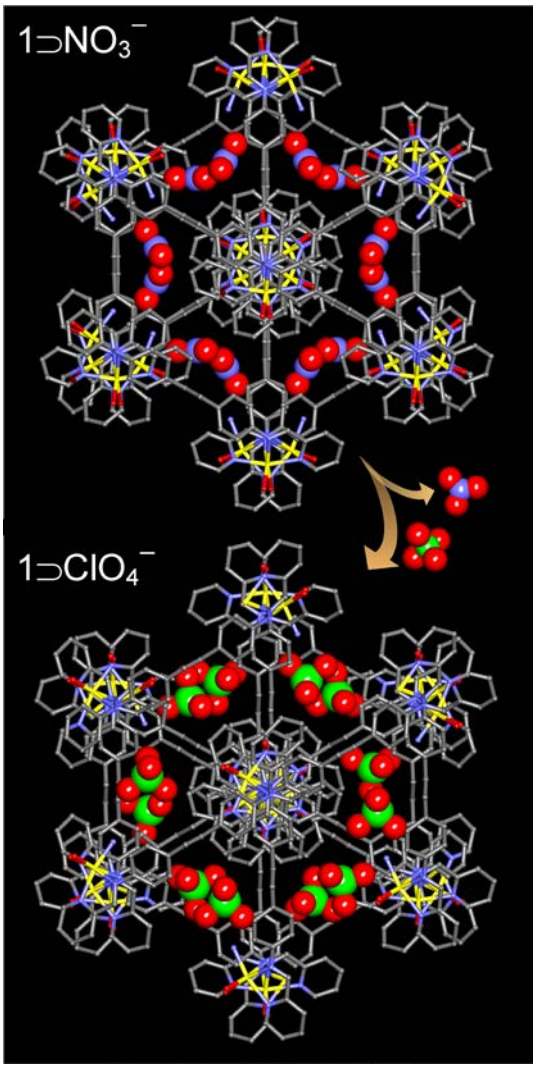

Figure 4.9.3 *Single crystal to single crystal structural transformation from compound* ***1***⊃ NO_3 *to* ***1***⊃ ClO_4 *upon anion exchange.*

PXRD patterns as **1**⊃ NO_3^-, indicating structural integrity after guest anion exchange (**Figure 4.8**).

Thermo-gravimetric analysis (TGA) of **1**⊃ NO_3^- reveals an approximate 8% weight loss at ~ 70º C, corresponding to 2 coordinated water & disordered guest molecules per formula unit and is further stable up to 300º C (**Figure 4.9.4**). **1**⊃ ClO_4^- showed weight loss of ~ 7 % at around 105ºC which corresponds to 2 water molecules per formula unit and is further stable up to 280ºC (**Figure 4.9.4**). Generally variable sorption behavior in a cationic framework arises from the differences in interactions between host anions of different sizes and adsorptive guests. To examine this, the guest inclusion behavior of **1**⊃ NO_3^- and **1**⊃ ClO_4^-, solvent sorption experiments were performed with hydrophilic and hydrophobic solvents at 298 K. Guest free

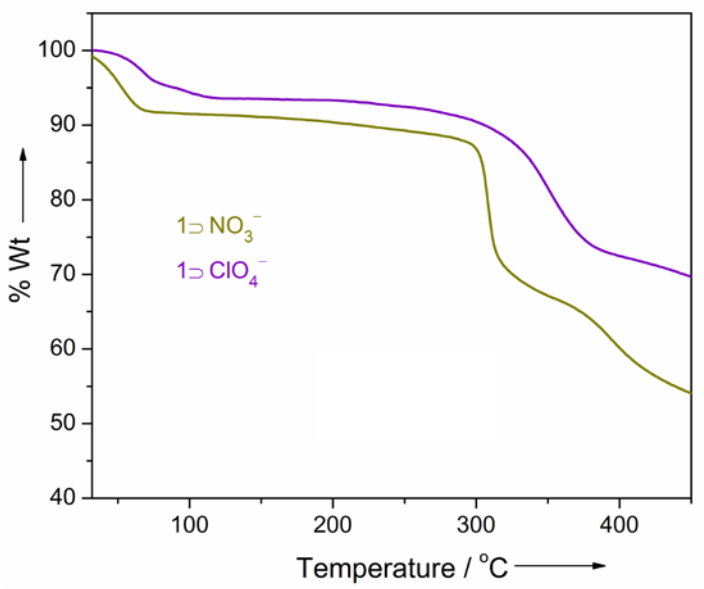

Figure 4.9.4. *TGA plots of compound* ***1***⊃ NO_3 *and* ***1***⊃ ClO_4.

phases **1´** and **2´** were generated by heating **1**⊃ NO_3^- and **1**⊃ ClO_4^- at 110ºC for 12 hours. Sharp peaks of **1´** and **2´** in PXRD patterns indicate the high crystalline nature of the desolvated phases. Amongst the hydrophilic guests for **1´**, H_2O showed the highest uptake amount (10 $mmoLg^{-1}$) with a gate opening behavior (P/P_0 =0.3). EtOH also showed gate opening behavior (P/P_0 = 0.65) but with a lesser uptake amount of 2.3 $mmolg^{-1}$. No uptake was observed for larger hydrophobic guest like benzene. These observations are in accordance with the size of the guest

adsorptive molecule (**Figure 4.9.5 top**). The hysteric adsorption profile in conjuncture with gate adsorption behavior affirms the framework flexibility towards hydrophilic guest molecules. [18] Dynamic nature of framework **1**⊃ NO_3^- was reiterated from the slight variation in PXRD patterns of **1´** upon hydrophilic guest inclusion (**Figure 4.9.6**). In the case of 2´ the order of uptake amount is: H_2O (5 $mmolg^{-1}$) >EtOH (2.5 $mmolg^{-1}$) > Benzene (1 $mmolg^{-1}$) which follows the size dependent guest inclusion trend. Noticeably, the sorption behaviors of both the

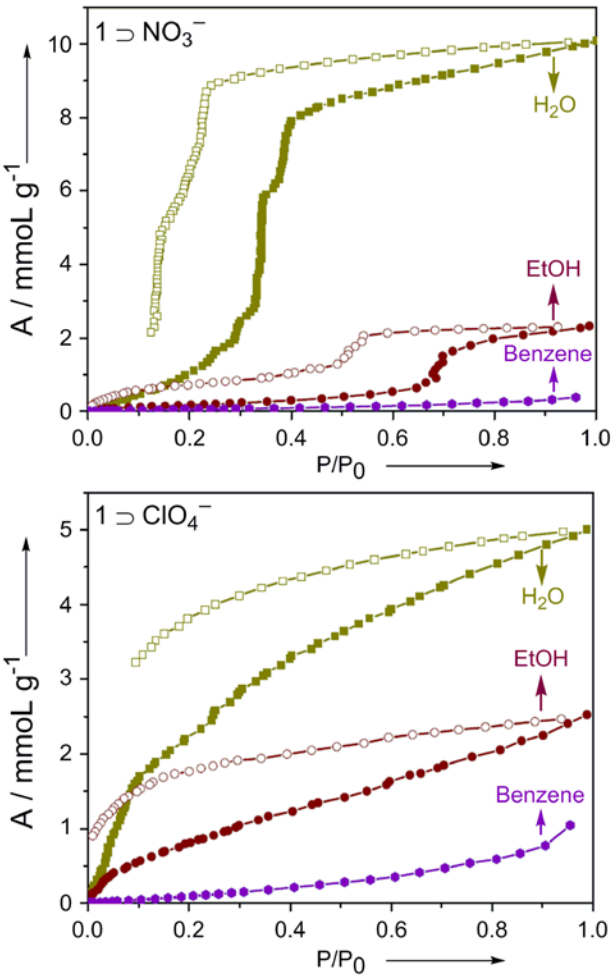

Figure 4.9.5. *Solvent sorption behavior of compounds* ***1***⊃ NO_3^- *and* ***1***⊃ ClO_4^- at 298K.

compounds are quite different and the variations in the uptake amount can probably be ascribed to the difference in interactions of the guest with free anions of different sizes (**Figure 4.9.5 bottom**). Moreover, anion-exchanged products show anion responsive luminescence. To check

excitation wavelength of the compounds, solid-state UV absorptions were measured for **1**⊃ NO_3^- and all anion exchanged products at room temperature. The absorption curves for the parent compound and other anion exchanged compounds exhibited a similar trend (**Figure 4.9.7**). Solid-state emission spectra were also measured for L, **1**⊃ NO_3^- and anion exchanged compounds at room temperature. On exciting at 405nm weak fluorescence of L displayed two emission maxima at 512 nm and 530 nm respectively. **1**⊃ NO_3^- showed an intense band at wavelength 533nm which can be ascribed as π*-n or π*-π intraligand (IL) transitions. **1**⊃ ClO_4^-,

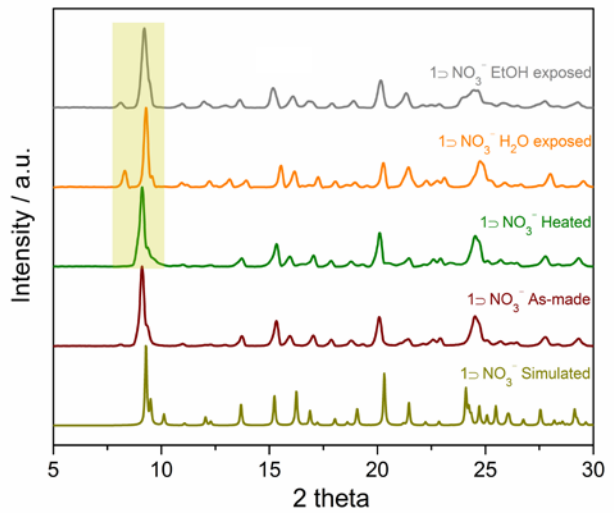

Figure 4.9.6. *PXRD patterns of different solvent exposed phases of compounds* ***1***⊃ NO_3^-.

1⊃BF_4^-, **1**⊃PF_6^- and **1**⊃$CF_3SO_3^-$ displayed broad bands with emission maxima at 531 nm, 528 nm, 532 nm and 531 nm respectively. It is worth noting that the desolvated form of **1**⊃ NO_3^- showed the most intense band observed at 537 nm. This can be attributed to the fact that since, the desolvated phase is devoid of free solvent molecules, relatively higher number of IL transitions are possible in this case. The emission intensities of anion exchanged samples were much different from **1**⊃ NO_3. **1**⊃ClO_4^- showed the highest enhancement in fluorescent intensity when compared to **1**⊃ NO_3^-.

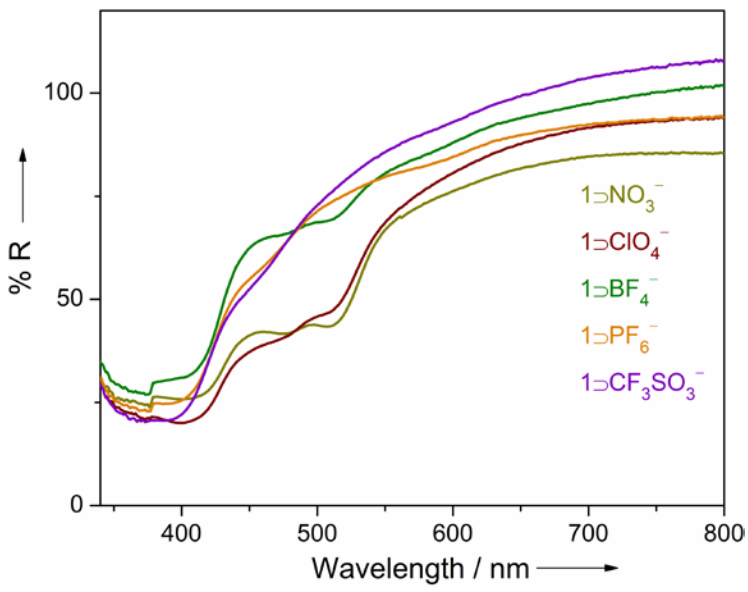

Figure 4.9.7. *Solid state reflectance spectra of* ***1***$\supset NO_3^-$ *and all other exchanged solids* at 298K.

A similar enhancement was observed for **1**$\supset PF_6^-$ and **1**$\supset CF_3SO_3^-$, whereas, **1**$\supset BF_4^-$showed lowest enhancement in fluorescent intensity with respect to **1**$\supset NO_3^-$ (**Figure 4.9.8**).

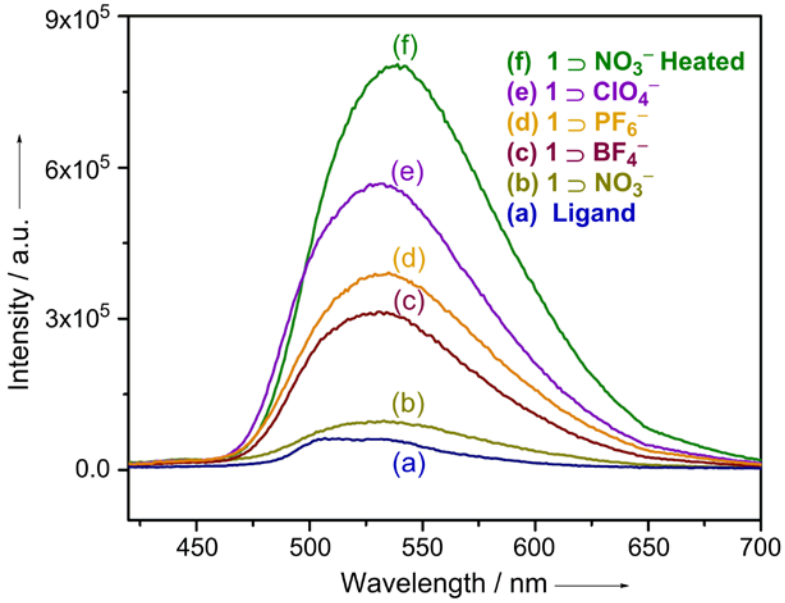

Figure 4.9.8. *Solid state emission spectra of* ***1***$\supset NO_3^-$ *and all other exchanged solids* at 298K.

These differences in emission intensities of various anion exchanged samples may be due to different electronic interactions of guest anions with framework and Zn(II) centre depending upon size shape and geometry of anions.

4.4. Conclusion:

To conclude, a homochiral cationic framework has been successfully synthesized which exhibits bulk phase homochirality. The overall framework showed six-fold interwoven helical packing. The anions in the framework can be quantitatively exchanged with other non-coordinating or weakly coordinating anions. This anion exchange behavior of the compound has been well demonstrated by SCSC experiment. Interestingly, the cationic framework exhibited anion-responsive tunable bulk phase homochirality. The compound displayed anion dependent variable sorption behavior for hydrophilic guest adsorptive. Different kinds of affinities towards various guest anions were also observed for the framework. The compound also showed anion dependent tunable luminescence. The bulk phase homochirality along with anion-responsive tunable chiral and luminescent properties of CPs / MOFs may find potential biological and industrial applications.

4.5. References:

(1) a) Seo, J. S.; Whang, D.; Lee, H.; Jun, S. I.; Oh, J.; Y. Jeon, J.; Kim, K. *Nature.* **2000**, *404*, 982-986. b) Hu, A.; Ngo, H. L.; Lin, W. *J.Am. Chem. Soc.* **2003**, *125*, 11490-11491.

(2) a) Jeong, K. S.; Go, Y. B.; Shin, S. M.; Lee, S. J.; Kim, J.; Yaghi, O. M.; Jeong, N. *Chem. Sci*. **2011**, *2*, 877-882. b) Ma, L.; Falkowski, J. M.; Abney, C.; Lin, W. *Nat. Chem.* **2010**, *2*, 838-846. c) Song, F.; Wang, C.; Falkowski, J. M.; Ma , L.; Lin, W. *J. Am.Chem.Soc.* **2010**, *132*, 15390-15398. d) Dang, D.; Wu, P.; He, C.; Xie , Z.; Duan, C. *J. Am. Chem. Soc.* **2010**, *132*, 14321-14323.

(3) a) Sun, X.-L.; Song, W.-C.; Zang, S.-Q.; Du, C.-X.; Hou , H.-W.; Mak, T. C. W. *Chem. Commun.* **2012**, *48*, 2113-2115. b) Wei, K.; Ni, J.; Min, Y.; Chen , S.; Liu , Y. *Chem. Commun.* **2013**, *49*, 8220-8222. c) Bisht, K. K.; Suresh, E. *J. Am. Chem. Soc.* **2013**, *135* , 15690–15693. d) Joarder, B.; Chaudhari, A.K.; Ghosh, S.K. *Inorg. Chem.* **2012**, *51*,

4644-4649. e) Joarder, B. Chaudhari, A.K.; Nagarkar, S.S.; Manna, B.; Ghosh, S.K. *Chem. Eur. J.* **2013**, *19*, 11178 – 11183.

(4) a) García , L. P.; Amabilino, D. B. *Chem. Soc. Rev*. **2002**, *31*, 342-356 . b) Gao, E.–Q.; Yue, Y. –F.; Bai, S. –Q.; He, Z.; Yan, C. –H. J. *Am. Chem. Soc.* **2004**, 126, 1419–1429. c) Tong, X.–L.; Hu ,T. –L.; Zhao, J. –P.; Wang, Y. –K.; Zhang, H.; Bu, X. –H. *Chem.Commun*. **2010**, *46*, 8543–8545.

(5) a) Kondepudi, D. K.; Kaufman, R. J.; Singh, N. *Science*. **1990**, *250*,975-976. b) Endo, T. K.; Aoyama, Y. *J. Am. Chem. Soc.***1999**, *121*, 3279-3283. c) Wu, S.-T.; Wu, Y.-R.; Kang, Q.-Q.; Zhang, H.; Long, L.-S.; Zheng, Z.; Huang, R.-B.; Zheng, L.-S. *Angew. Chem. Int. Ed*. **2007**, *46*, 8475-8479. d) Zhang, J.; Chen, S.; Nieto, R. A.; Wu, T.; Feng, P.; Bu, X.-H. *Angew. Chem. Int. Ed*. **2010**, *49*, 1267 –1270. e) Tong, X.; Yan, W.; Yu, J.; Xu , R. *Chem. Commun.* **2013**, *49*, 11287-11289.

(6) a) Min, K. S.; Suh, M. P. *J. Am. Chem. Soc*. **2000**, *122*, 6834 – 6840. b) Li, X.; Xu, H.; Kong, F.; Wang, R. *Angew. Chem. Int. Ed*. **2013**, *52*, 13769 –13773. c) Muthu, S.; Yip, J. H. K.; Vittal , J. J. *Dalton Trans*. **2001**, 3577–3584.

(7) a) Maji, T. K.; Matsuda, R.; Kitagawa, S. *Nat. Mater*. **2007**, *6*, 142 –148. b) Manna, B.; Chaudhari, A. K.; Joarder, B.; Karmakar, A.; Ghosh, S. K. *Angew. Chem. Int. Ed*. **2013**, *52*, 998 – 1002. c) Wang, J.-H.; Li, M.; Li, D. *Chem sci.* **2013,** *4*, 1793-1801.

(8) a) Hou, S.; Liu, Q.-K.; Ma, J.-P.; Dong, Y.-B. *Inorg. Chem.* **2013**, *52* , 3225–3235. b) Chen, Y.-Q.; Li, G.-R.; Chang, Z.; Qu,Y.-K.; Zhang, Y.-H.; Bu, X.-H. *Chem. Sci.* **2013**, *4*, 3678-3682.

(9) a) Park, I. –H.; Chanthapally, A.; Zhang, Z.; Lee, S. S.; Zaworotko, M. J.; Vittal, J. J. *Angew. Chem. Int. Ed*. **2014**, *53*, 414 –419. b) Shigematsu, A.; Yamada, T.; Kitagawa, H. *J. Am. Chem. Soc.* **2012**, *134* , 13145–13147 c) Cui, Y.; Xu, H.; Yue, Y.; Guo, Z.; Yu, J.; Chen, Z.; Gao, J.; Yang, Y.; Qian, G.; Chen, B. *J. Am. Chem. Soc*. **2012**, *134*, 3979 – 3982. d) Chen, B.; Yang, Y.; Zapata, F.; Lin, G.; Qian, G.; Lobkovsky, E. B. *Adv. Mater*. **2007**, *19*, 1693–1696. e) Das, M. C.; Bharadwaj, P. K. *J. Am. Chem. Soc*. **2009**, *131*, 10942–10949.

(10) a) Yoshida, N.; Ichikawa, K. *Chem. Commun.* **1997**, 1091-1092. b) Li, S.; Jia, C.; Wu, B.; Luo, Q.; Huang, X.; Yang, Z.; Li, Q.-S.; Yang, X.-J. *Angew. Chem. Int. Ed*. **2011**, *50*, 5721 –5724.

(11) *SAINT Plus*, (Version 7.03); Bruker AXS Inc.: Madison, WI, **2004**.

(12) Sheldrick, G. M. *SHELXTL*, *Reference Manual*: version 5.1: Bruker AXS; Madison, WI, **1997**.

(13) Sheldrick, G. M. *Acta Crystallogr. Sect. A* **2008**, *112*.

(14) *WINGX version 1.80.05 Louis Farrugia, University of Glasgow.*

(15) Spek, A. L. PLATON, *A Multipurpose Crystallographic Tool*, Utrecht University, Utrecht, The Netherlands, **2005**.

(16) Leong , W. L.; Vittal , J. J. *Chem. Rev.* **2011,** *111*, 688–764.

(17) Chen , X-D.; Mak , T. C. W. *Dalton Trans.* **2005**, 3646-3652.

(18) Horike, S.; Shimomura, S.; Kitagawa, S. *Nat. Chem*. **2009**, *1*, 695 –704.

Chapter 5

Rational Integration of Water Array and Protonated Amine in An Anionic Coordination Polymer for Proton Conduction

5.1. Introduction:

Coordination polymers (CPs) / metal-organic frameworks (MOFs) are highly crystalline materials which manifest tailorable functions owing to facile customization of their framework structures.[1] Among various facets, proton conduction in CPs is seeking much attention in recent years on account of its potential application as solid state electrolyte in fuel cell.[2] Generally proton conductivity in CPs can be obtained in two ways. In the first instance, acidic / hydrophilic functionalities are introduced into the framework externally, while by the second route the proton source and ordered carrier molecules are simulataneously present in the framework structure.[2a] The information concerning molecular level ion-conduction pathway can be communicated due to the complementary presence of a well ordered network in such materials. Recently, various functional CPs have been reported as proton conducting materials.[3] Among them, metal-oxalate/phosphate based coordination polymers have been commonly studied for anhydrous and water mediated proton conduction.[4] Hence, for further development and comprehensive understanding of solid state proton conducting materials , investigation of other metal-anion based CPs is pertinently important. Intriguingly metal-sulfate based CPs have not been explored as solid state proton conductors, although it is well known about the facile formation of anionic frameworks by combining metal ions and sulfate anions.[5] Extra -framework cations are required for balancing the charge of such anionic chains.

Use of organic amine in such reaction medium can provide the extra-framework cation in the form of protonated organic amine (**Figure 5.1**).[6] In case of participation by nitrogen-rich aromatic amine, efficient movement of proton in its cationic form might be facilitated. Employment of water medium in such reactions often can lead to the entrapment of water molecules in the crystal lattice owing to hydrophilic nature of such host framework.[7] The complementary presence of such free lattice water molecules along with nitrogen-rich aromatic protonated amine can help in formation of extensive H-bonding array of lattice water molecules along the metal – sulfate chain. This H-bonding array of water molecules in colligation with protonated aromatic amines may render an effective proton hopping pathway which eventually can lead to fabrication of an effective solid state proton conducting material. Thus such H-bonded sulfate based CPs may find an avenue in the further development of solid state proton conductors. Here, $In_2(SO_4)_3$–melamine and water system were chosen to develop a sulfate based

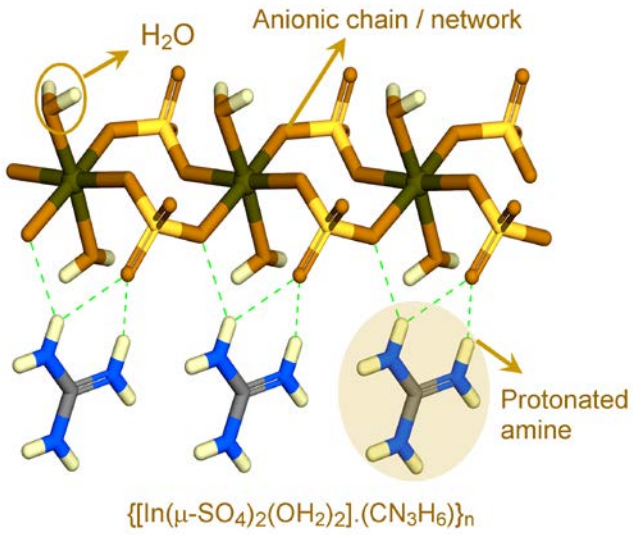

Figure 5.1. *Anionic chain and protonated organic cation of a coordination polymer.*

coordination polymer forming H-bonded 3D network for proton conduction. Simultaneous presence of nitrogen-rich aromatic cation (protonated melamine) and continuous array of water molecules in the CP described a H-bonding pathway and thereby favours the water assisted proton conduction in the polymer (**Figure 5.2**).

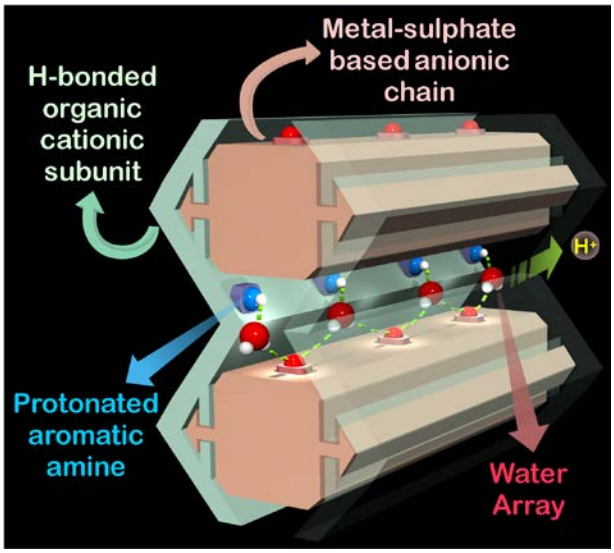

Figure 5.2. *Schematic overview of H-bonded metal-sulfate based coordination polymer for water mediated proton conduction.*

To the best of our knowledge, this is the first report of metal- sulfate based CP carrying a continuous water array functioning as a solid state proton conductor.

5.2. Experimental Section:

5.2.1. General remarks:

5.2.1.1. Materials: All the reagents and solvents were commercially available and used without further purification.

5.2.1.2. Physical measurements: Powder X-ray diffraction (PXRD) patterns were measured on Bruker D8 Advanced X-Ray diffractometer at room temperature using Cu-Kα radiation (λ= 1.5406 Å) with a scan speed of 0.5° min^{-1} and a step size of 0.01° in 2 *theta*. Thermogravimetric analysis was recorded on Perkin-Elmer STA 6000, TGA analyser under N_2 atmosphere with heating rate of 10° C/min. FT-IR spectra were recorded on NICOLET 6700 FT-IR Spectrophotometer using KBr Pellets.

5.2.1.3. X-ray Structural Studies: Single-crystal X-ray data of compound **1** was collected at 100 K on a Bruker KAPPA APEX II CCD Duo diffractometer (operated at 1500 W power: 50 kV, 30 mA) using graphite-monochromated Mo Kα radiation (λ = 0.71073 Å). Crystal was on nylon CryoLoops (Hampton Research) with Paraton-N (Hampton Research). The data integration and reduction were processed with SAINT[8] software. A multi-scan absorption correction was applied to the collected reflections. The structure was solved by the direct method using SHELXTL[9] and was refined on F^2 by full-matrix least-squares technique using the SHELXL-97[10] program package within the WINGX[11] programme. All non-hydrogen atoms were refined anisotropically. All hydrogen atoms were located in successive difference Fourier maps and they were treated as riding atoms using SHELXL default parameters. The structures were examined using the *Adsym* subroutine of PLATON[12] to assure that no additional symmetry could be applied to the models. **Appendix 5.1** shows the crystallographic data for the **1** (CCDC-1033011) , which can be obtained free of charge from The Cambridge Crystallographic Data Centre (via www.ccdc.cam.ac.uk/data_request/cif.).

5.2.1.4 Impedance Analysis: Impedance analysis of the samples was carried out in Bio-Logic VMP-3. Measurements were done in a two-electrode assembly with stainless steel discs as electrode and samples were kept in between them in the form of solid pellets by applying a spring load of 0.5 N/m^2. The whole cell assembly was kept in Espec environmental test chamber to control the temperature and humidity. Applied frequency range for the measurement was from10^6 to 0.01 Hz against the open circuit potential with sinus amplitude of 10 mV. All the EIS data were fitted using an EC-Lab Software V10.19 using equivalent circuit as shown below Where R_b is the bulk resistance (Ω) of the pellet, CPE-1 and CPE-2 is the constant phase element having a dimension in capacitance (F).Further, R_b is used to find the conductivity of the sample by considering the area and thickness of the sample (**Figure 5.3**).

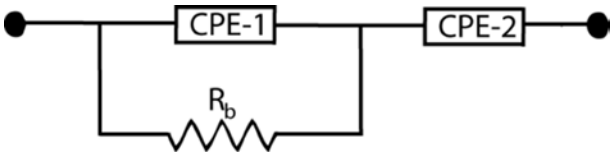

Figure 5.3. *Representative equivalent circuit showing bulk resistance (R_b) of the sample.*

5.2.1.5 Sorption Measurements: Solvent sorption measurements were performed using BelSorpmax (Bel Japan). The solvent was of 99.99% purity. The desolvated samples were obtained by heating compound **1** 110 °C under vacuum for 12hrs and the desolvation was confirmed by TGA and PXRD. Prior to adsorption measurement the desolvated samples were pretreated at 110 °C under vacuum for 5h using Bel PrepvacII and purged with N_2 on cooling. Low pressure gas sorption measurements were performed using Bel Sorpmax (Bel Japan). All of the gases used were of 99.999% purity.

5.2.2. Synthesis:

5.2.2. 1 Synthesis of Compound 1: Single crystals of compound **1** were synthesized by reacting $In_2(SO_4)_3$ (0.0427 g, 0.0825 mmol), melamine (0.0315 g, 0.25 mmol) in H_2O (2 mL) and 1-butanol (1mL) in a 5 ml screw-capped vial. The vial was heated to 110 °C for 26 h under

autogenous pressure and then cooled to RT over 14 h. The colorless rod shaped single crystals of compound **1** were obtained with ~70% yield.

5.3. Result and discussions:

Reaction of melamine (L) with $In_2(SO_4)_3$ in water medium under solvothermal condition gave rod shaped colourless single crystals of compound **1** $[\{In_2(\mu\text{-}OH)_2(SO_4)_4\}.\{(LH)_4\}.nH_2O]_n$. LH represent protonated melamine (**Figure 5.4**).

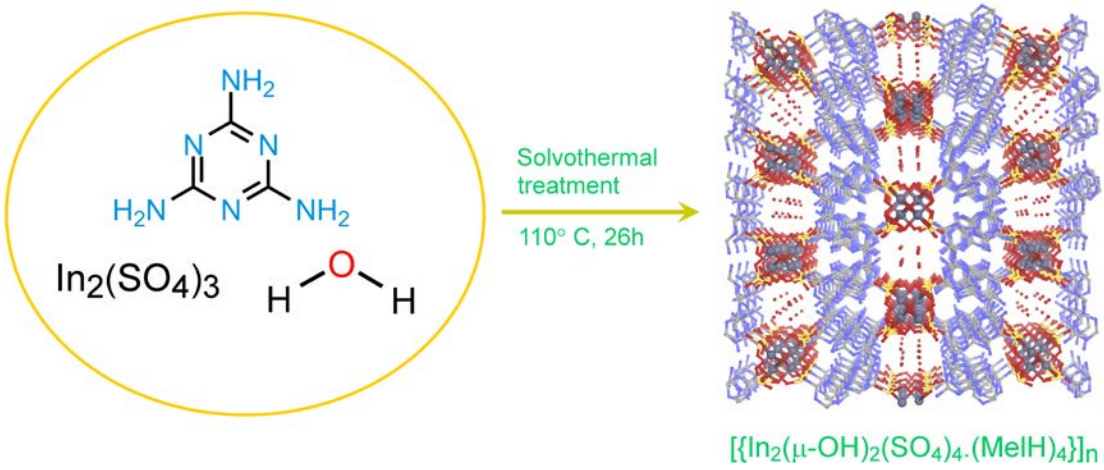

Figure 5.4. *Synthetic scheme of the anionic coordination polymer**1**.*

Single crystal analysis of the compound revealed the generation of 1D anionic coordination polymer chain (**Appendix 5.2**), which are further hydrogen-bonded with protonated aromatic amine and lattice water molecules to render H-bonded 3D network with 1D pore channel. A single crystal X-ray diffraction (SC-XRD) study of the compound showed that it crystallizes in monoclinic crystal system with space group *P*21/n (**Appendix 5.1**). An asymmetric unit of the compound **1(Appendix 5.3)** is made of anionic chain $[\{In_2(\mu\text{-}OH)_2(SO_4)_4\}]^{4-}$, organic cationic amine $[(LH)_4]^{4+}$, and free lattice water molecules (**Figure 5.5**). Each metal centre is octahedrally connected to six oxygen donor atoms. Out of the six O-donor atoms, four of them come from four sulfate groups and rest of the two are bridging –hydroxy groups. The anionic subunit of the asymmetric unit consist of 4 SO_4^{2-}, 2 OH^- and 2 In metal centres and contains overall tetra negative charge on it (4-). Hence each In metal centre shows +3 oxidation state to make overall

asymmetric unit neutral. Each In (III) exhibits distorted octahedral geometry by the coordination of 4 sulfate oxygen atoms (3 equatorial and 1 axial) 2 hydroxy oxygen atoms (1 equatorial, 1 axial). Each sulfate ion connects two adjacent metal

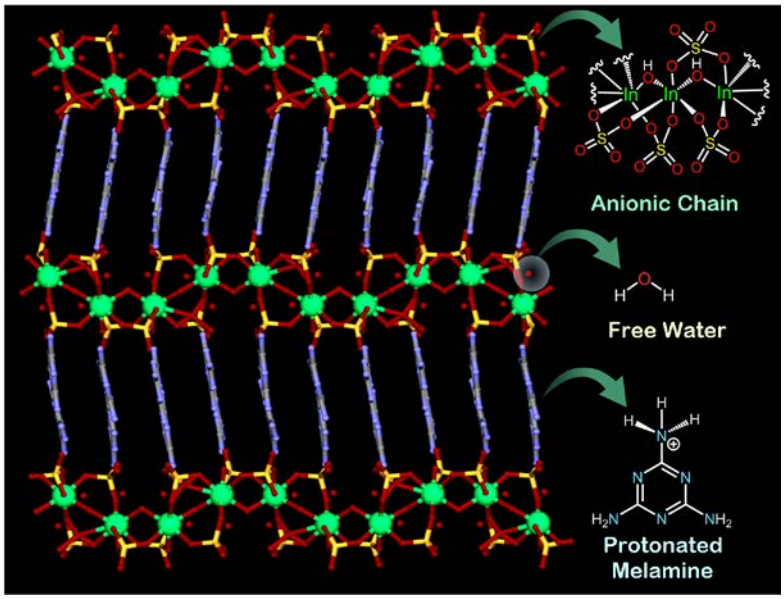

Figure 5.5. *Overall packing of compound **1** along a axis showing anionic chain, protonated melamine and free water molecules.*

centres via two oxygens of it in a bidentate fashion. Thus ligation of SO_4^{2-}in bidentate manner along with μ- hydroxy coordination creates 1D anionic chain of $[\{In_2(\mu\text{-}OH)_2(SO_4)_4\}]_n^{4-}$. These 1D anionic chains form extensive H-bond with organic cationic ammine, free lattice water molecules to create H-bonded CP (**Appendix 5.4**). Free water molecules in the compound also form H-bonding 1D array in between two adjacent anionic chains (**Figure.5.6**). Powder X-ray diffraction (PXRD) patterns of ground sample matched well with its simulated patterns, indicating bulk-phase purity of compound **1** (**Figure. 5.7**). Thermogravimetric analysis (TGA) of powder sample of compound **1** suggested a continuous initial loss due to the presence of strongly hydrogen bonded water molecules in the structure (**Figure. 5.8**). Structural integrity of the compound **1** was maintained even at elevated temperatures as revealed by variable temperature PXRD diffraction patterns (**Figure. 5.9**). The extensive H-bonded network present in the above mentioned coordination polymer is crucial and often required for proton conduction. Hence, the

H-bonded 3D network composed of metal- sulfate based anionic chain and protonated melamine with continuous array of water molecules may act as a potential proton conducting material. Very recently, portable fuel cells which are working in low temperatures and humidified conditions are

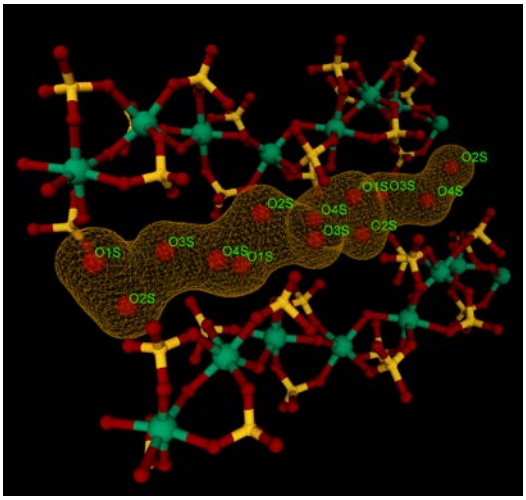

Figure 5.6. *Hydrogen bonded water molecules' chain in compound **1** (shown in wire mesh view).*

seeking much attention as clean energy sources. Proton conductivity of compound **1** was measured by using Electrochemical Impedance Spectroscopy (EIS) technique by controlling

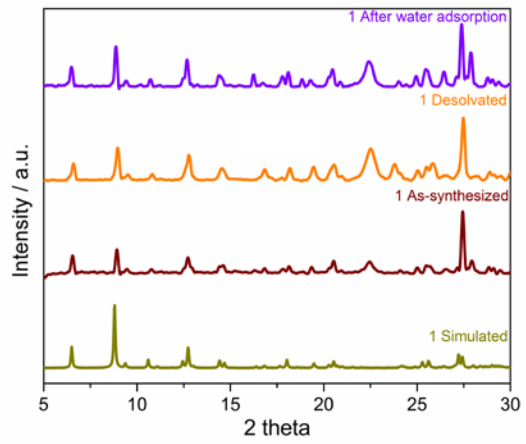

Figure 5.7. *PXRD patterns of simulated, as-synthesized, desolvated and post water adsorption phases of compound **1**.*

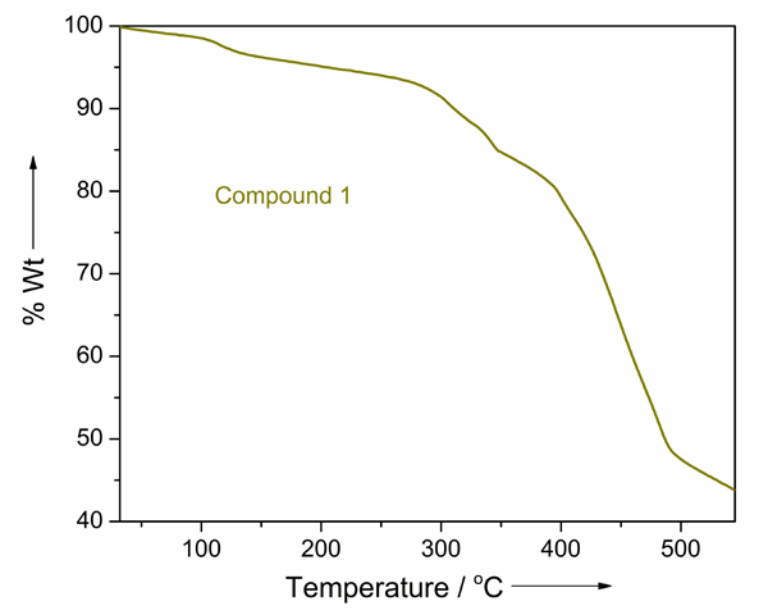

Figure 5.8. *TGA plot of compound **1**.*

humidity as well as temperature. Nyquist plot of the compound **1** measured at 98 % RH and 30^{o}C is shown in the **Figure 5.9.1**. A semi-circle at the high frequency region represents the bulk

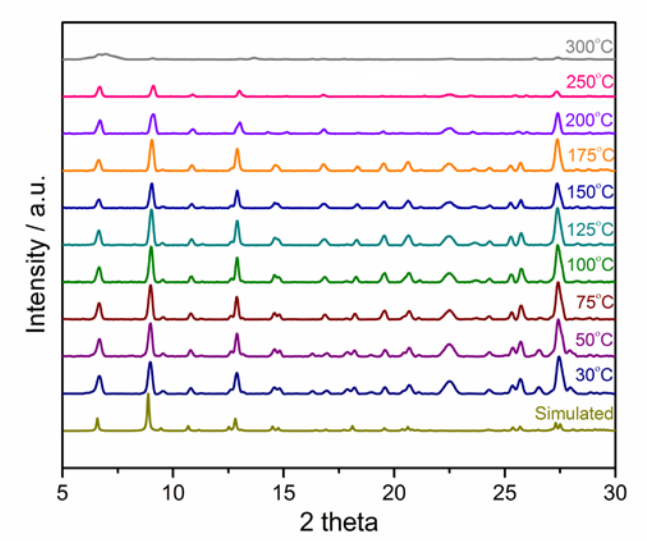

Figure 5.9. *Variable temperature PXRD patterns of compound **1**.*

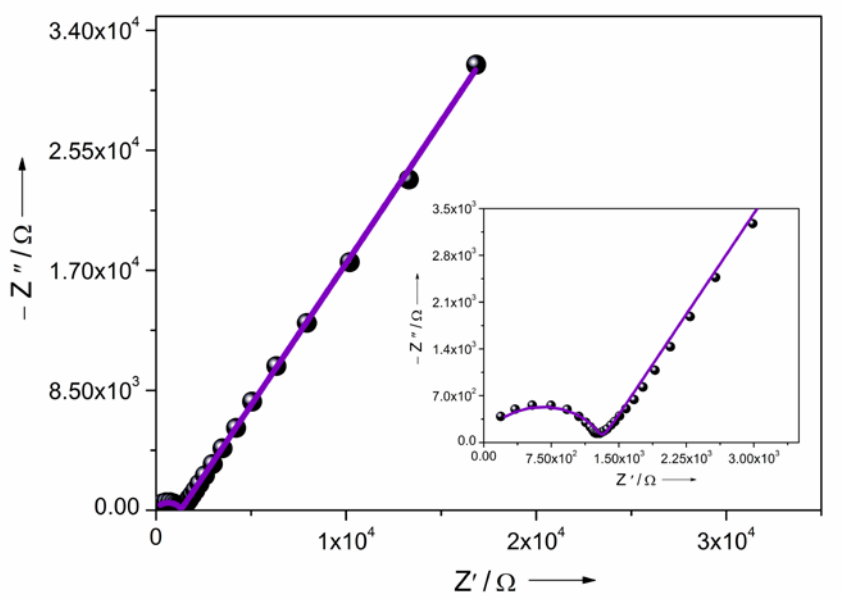

Figure 5.9.1. *Nyquist plot of compound **1** at 98% RH and 30℃. Inset showing zoomed view of high frequency region.*

electrolyte resistance in parallel with a constant phase element (CPE) as found by fitting the EIS spectra (**details are given in the experimental part**). While at the low frequency region the tail

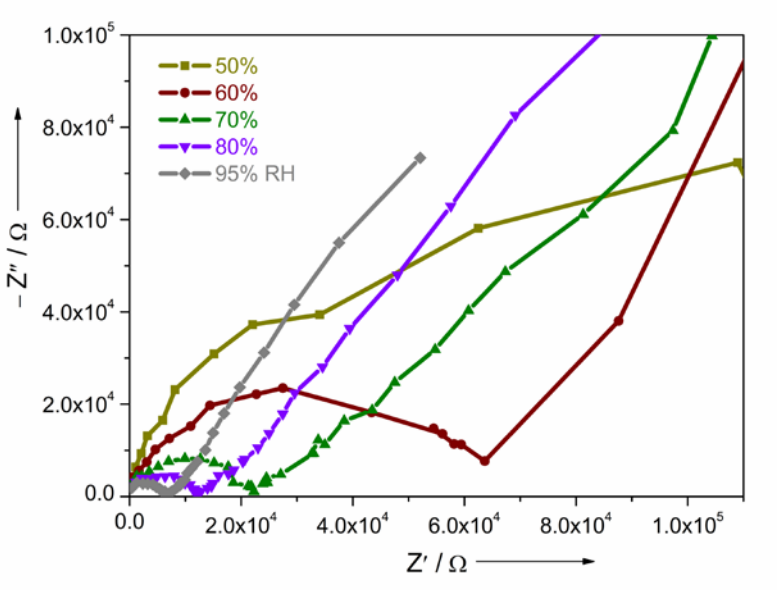

Figure 5.9.2. *Humidity dependent impedance spectra of compound **1**.*

indicates the diffusion resistance of the mobile ions at the electrode-electrolyte interface. From the varied humidity dependant EIS measurement it is found that Compound **1** shows humidity dependant conductivity, where at 50%RH, conductivity was in the order of 10^{-7} Scm^{-1}(**Figure. 5.9.2**). Conductivity is found to be increasing as expected with increasing humidity and reached $1.0x10^{-5}$ Scm^{-1}at 95 % RH (**Figure. 5.9.2**). The conductivity became maximum at 98% RH with the value of $4.4x\ 10^{-5}$ Scm^{-1}. It is worth noting that conductivity of compound **1**increases gradually with increase in humidity up to 95% RH, but a sudden and jump in conductivity at 98% RH is observed (**Figure. 5.9.3**).

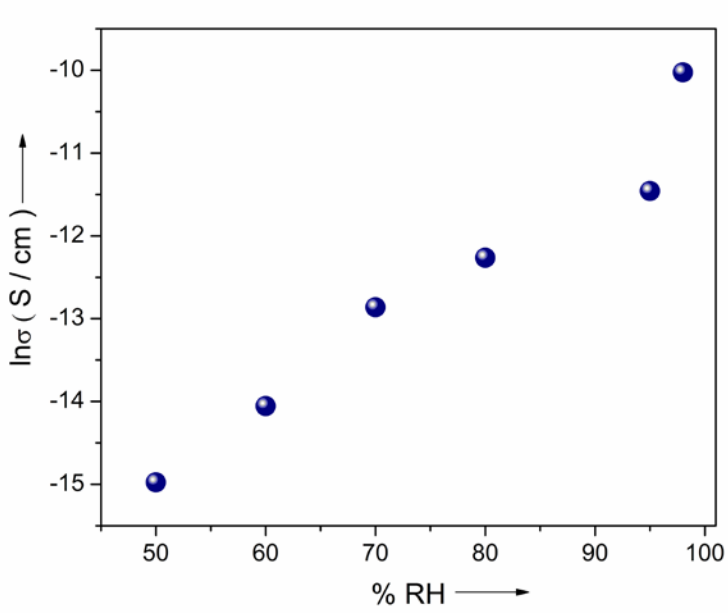

Figure 5.9.3. *Conductivity vs %RH of compound **1** at 30℃.*

Such increase in conductivity beyond 95% RH may be attributed to the presence of large number of water molecules, forming extensive H-bonding array in the framework at saturated humidification. The trend in conductivity as observed in impedance analysis of compound **1** was also supported adsorption profile of compound **1** at 298K. Water adsorption profile of compound **1** indicates step-wise water uptake which in good agreement with sudden increase in conductivity beyond 95% RH (**Figure 5.9.4**).

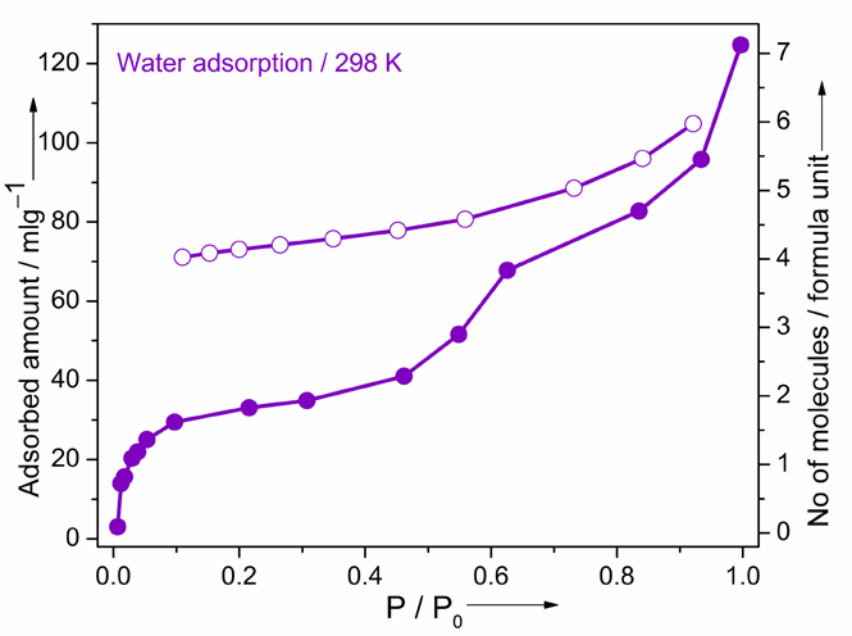

Figure 5.9.4 *Water adsorption profile of the compound at 298K.*

The conductivity of this compound under humid condition is comparatively better than the similar hydrogen bonded compound $[(C_6H_{10}N_2)_2(SO_4)_2.3H_2O]_n$ consisting of phenelyne diamine dication, sulfate anion and water.[13] Moreover, a comparison chart of this sulfate based CP with other related CPs/ MOFs has been given in appendix section (**Appendix 5.5**) .To get the activation energy (E_a) for the proton conduction, temperature dependence conductivity was measured at 95% RH (**Figure. 5.9.4**). The activation energy was measured to be 0.316 eV from the Arrhenius plot (**Figure. 5.9.5**) which is quite low value suggesting that probably Grotthuss mechanism is operating for proton hopping.[2a,14] Impedance analysis of the compound has also been performed under D_2O atmosphere. At 98% RH the conductivity in presence of D_2O became 1.01x 10^{-5} Scm^{-1} which is quite low as compared to H_2O condition (**Figure.5.9.6**). This measurement under D_2O atmosphere further confirmed the water assisted proton conduction in the compound. The protonated melamine behaves as a feasible proton source, which is further hydrogen bonded with the ordered extended H-bonded

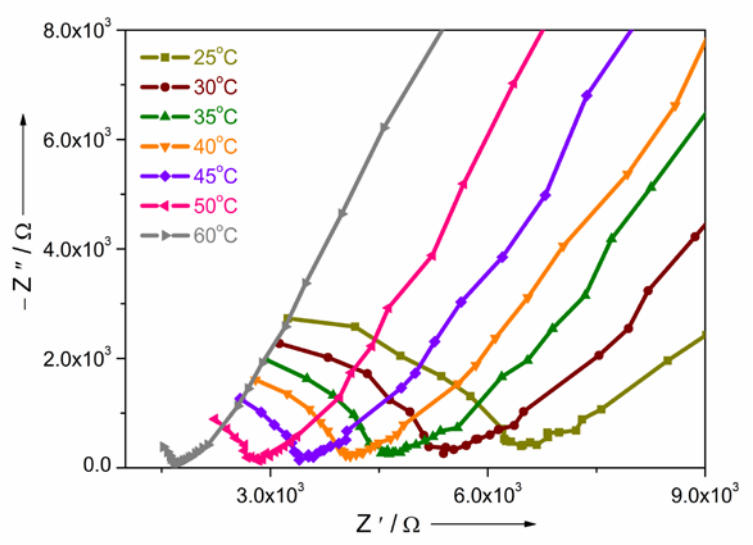

Figure 5.9.4 *Temperature dependent impedance spectra of compound **1** at 95% RH.*

water molecules' chain favoring the proton transport phenomena in this compound. With increase in humidity concentration of carrier molecules increases which results in elevation in conductivity.

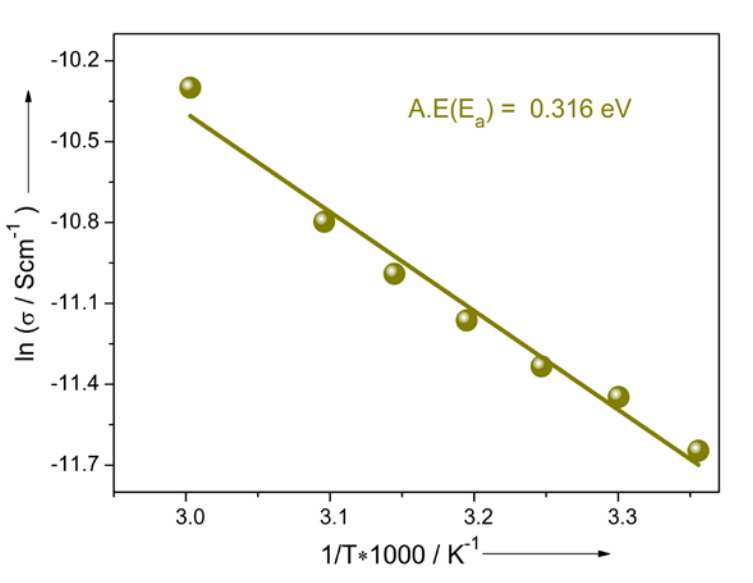

Figure 5.9.5 *Arrhenius plot for temperature dependence of conductivity at 95% RH of compound **1**.*

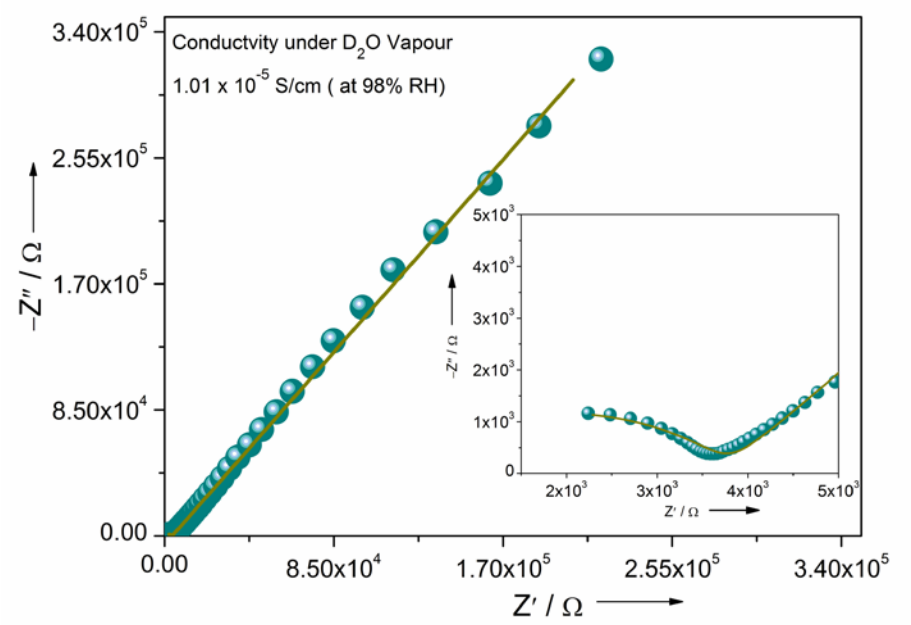

Figure 5.9.6. *Nyquist plot of compound **1** at 98% RH and 30℃ under D_2O atmosphere. Inset showing zoomed high frequency region.*

At saturated humidification, high carrier concentration in the compound may be effective for efficient proton conduction.

5.4. Conclusion:

To conclude, a novel metal- sulfate based coordination polymer has been successfully synthesized forming H-bonded 3D network by rational confinement of nitrogen-rich protonated aromatic cations (protonated melamine) and array of water molecules for solid state proton conduction. The compound shows water mediated proton conduction owing to such extensive H-bonded network of free water molecules, along with aromatic protonated amines present in the compound. Such metal- sulfate based coordination polymers may seek greater attention in the near future towards the further development of solid state electrolytes.

5.5. References:

(1) (a) Zhou, H.-C.; Long, J. R.; Yaghi, O. M. *Chem. Rev*. **2012**, *112*, 673– 674. (b) Horcajada, P.; Gref, R.; Baati, T.; Allan, P. K.; Maurin, G.; Couvreur, P.; Ferey, G.; Morris, R. E.; Serre,

C. *Chem. Rev*. **2012**, *112*, 1232–1268. (c) Stock, N.; Biswas, S. *Chem. Rev*. **2012**, *112*, 933–969. (d) Ahnfeldt, T.; Guillou, N.; Gunzelmann, D.; Margiolaki, I.; Loiseau, T.; Ferey, G.; Senker, J.; Stock, N. *Angew. Chem. Int. Ed.* **2009**, *48*, 5163 –5166. e) Devic, T.; Serre, C. *Chem. Soc. Rev.* **2014**, *43*, 6097-6115. (f) Manna, B.; Chaudhari, A. K.; Joarder, B.; Karmakar, A.; Ghosh, S. K. *Angew. Chem. Int. Ed.* **2013**, *52*, 998 –1002. (g) Manna, B.; Joarder, B.; Desai, A. V.; Karmakar, A.; Ghosh, S. K. *Chem. Eur. J.* **2014**, *20*, 12399 – 12404. (h) Henke , S.; Schneemann , A.; Wütscher, A.; Fischer, R. A. *J. Am. Chem. Soc*. **2012**, *134* , 9464–9474. (i) Bétard, A.; Fischer , R. A. *Chem. Rev.* **2012**, *112* , 1055–1083. (j) Zhang, J.-W.; Zhang, H.-T.; Du, Z.-Y.; Wang, X.; Yu, S.-H.; Jiang, H.-L. *Chem. Commun.***2014**,*50*,1092-1094. (k) Zhang , W.; Hu , Y.; Ge , J.; Jiang H.-L.; Yu, S.-H. *J. Am. Chem. Soc*. **2014**, *136* , 16978–16981. (l) Bloch, W. M.; Burgun, A.; Coghlan, C. J.; Lee, R.; Coote, M. L.; Doonan, C. J.; Sumby, C. J. *Nat.Chem.* **2014**,*6*,906–912.(m) Bloch, W.M.; Sumby, C. J. *Chem. Commun.* **2012**,*48*, 2534-2536. (n)Konidaris, K.F.; Morrison, C. N.; Servetas, J.G.; Haukka, M.; Lan, Y.; Powell, A. K.; Plakatouras, J. C.; Kostakis, G. E. *CrystEngComm*. **2012**,*14*, 1842-1849. (o) Gao, W.-Y.; Chen, Y.; Niu, Y.; Williams, K.; Cash, L.; Perez, P. J.; Wojtas, L.; Cai, J.; Chen, Y.-S.; Ma,S. *Angew. Chem. Int. Ed.* **2014**, *53*, 2615 –2619. (p) Wang, X.-S.; Chrzanowski, M.; Gao, W.-Y.; Wojtas, L.; Chen, Y.-S.; Zaworotko, M. J.; Ma, S. *Chem. Sci*. **2012**, *3*, 2823–2827.

(2) a) Ramaswamy, P.; Wong, N. E.; Shimizu, G. K. H. *Chem. Soc. Rev.* **2014**, *43*, 5913-5932. (b) Yamada, T.; Otsubo, K.; Makiura, R.; Kitagawa, H. *Chem. Soc. Rev.* **2013**, *42*, 6655-6669. (c) Horike, S.; Umeyama, D.; Kitagawa, S. *Acc. Chem. Res.* **2013**, *46*, 2376 – 2384.

(3) (a) Yoon, M.; Suh, K.; Natarajan, S.; Kim, K. *Angew. Chem. Int. Ed.* **2013**, *52*, 2–15. (b) Shimizu, G. K. H.; Taylor, J. M.; Kim, S. *Science*. **2013**, *41*, 354–355. (c) Hurd, J. A.; Vaidhyanathan, R.; Thangadurai, V.; Ratcliffe, C. I.; Moudrakovski, I. L.; Shimizu, G. K. H. *Nat. Chem.* **2009**, *1*, 705 – 710. (d) Sen, S.; Nair, N. N.; Yamada, T.; Kitagawa, H.; Bharadwaj, P. K. *J. Am. Chem. Soc*. **2012**, *134*, 19432−19437. (e) Yamada, T.; Otsubo, K.; Makiura, R.; Kitagawa, H. *Chem. Soc. Rev.* **2013**, *42*, 6655-6669. (f) Shigematsu, A.; Yamada, T.; Kitagawa, H. *J. Am. Chem. Soc.* **2011**, *133*, 2034–2036. (g) Bureekaew, S.; Horike, S.; Higuchi, M.; Mizuno,M.; Kawamura, T.; Tanaka, D.; Yanai, N.; Kitagawa, S. *Nat. Mater.* **2009**, *8*, 831 – 836. (h) Umeyama, D.; Horike, S.; Inukai, M.; Hijikata, Y.;

Kitagawa, S. *Angew. Chem. Int. Ed.* **2011**, *50*, 11706 – 11709. (i) Ponomareva, V. G.; Kovalenko, K. A.; Chupakhin, A. P.; Dybtsev, D. N.; Shutova, E. S.; Fedin, V. P. *J. Am. Chem. Soc.* **2012**, *134*, 15640−15643. (j) Horike, S.; Umeyama, D.; Kitagawa, S. *Acc. Chem. Res.* **2013**, ***46***, 2376 – 2384. (k) Horike, S.; Kamitsubo,Y.; Inukai, M.; Fukushima, T.; Umeyama, D.; Itakura, T.; Kitagawa, S. *J. Am. Chem. Soc.* **2013**, *135*, 4612−4615. (l) García, M. B.; Colodrero, R. M. P.; Papadaki, M.; Garczarek, P.; Zoń, J.; Pastor, P. O.; Losilla, E. R.; Reina, L. L.; Aranda, M. A. G.; Lazarte, D. C.; Demadis, K. D.; Cabeza, A. *J. Am. Chem. Soc.* **2014**, *136*, 5731–5739. (m) Li, S.-L.; Xu, Q.; *Energy Environ. Sci.* 2013, ***6***, 1656 – 1683. (n) Phang, W. J.; Lee, W. R.; Yoo, K.; Ryu, D. W.; Kim, B.; Hong, C. S. *Angew. Chem. Int. Ed*. **2014**, *53*, 8383 –8387. (o) Colodrero, R. M. P.; Papathanasiou, K. E.; Stavgianoudaki, N.; Olivera-Pastor, P.; Losilla, E. R.; Aranda, M. A. G.; Leon-Reina, L.; Sanz, J.; Sobrados, I.; Choquesillo-Lazarte, D.; García-Ruiz, J. M.; Atienzar, P.; Rey, F.; Demadis, K. D.; Cabeza, A. *Chem. Mater*. **2012**, *24*, 3780−3792. (p) Colodrero, R. M. P.; Olivera-Pastor, P.; Losilla, E. R.; Aranda, M. A. G.; Leon-Reina, L.; Papadaki, M.; McKinlay, A. C.; Morris, R. E.; Demadis, K. D.; Cabeza, A. *Dalton Trans*. **2012**, *41*, 4045–4051 . (q) Kim, S. R.; Dawson, K. W.; Gelfand, B. S.; Taylor, J. M.; Shimizu, G. K. H. *J. Am. Chem. Soc.* **2013**, *135*, 963−966. (r) Taylor, J. M.; Mah, R. K.; Moudrakovski, I. L.; Ratcliffe, C. I.; Vaidhyanathan, R.; Shimizu, G. K. H. *J. Am. Chem. Soc.* **2010**, *132*, 14055–14057. (s) Taylor, J. M.; Dawson, K. W.; Shimizu, G. K. H. *J. Am. Chem. Soc.* **2013**, *135*, 1193−1196. (t) Parshamoni, S.; Jena, H. S.; Sanda, S.; Konar, S. *Inorg. Chem. Front.* **2014**,*1*, 611-620. (u) Sen, S.; Yamada, T.; Kitagawa, H.; Bharadwaj, P. K. *Cryst. Growth Des.* **2014**, *14*, 1240−1244. (v) Dybtsev, D. N.; Ponomareva, V. G.; Aliev, S. B.; Chupakhin, A. P.; Gallyamov, M. R.; Moroz, N. K.; Kolesov, B. A.; Kovalenko, K. A.; Shutova, E. S.; Fedin, V. P. *ACS Appl. Mater. Interfaces* . **2014**, *6*, 5161−5167.

(4) (a) Nagarkar, S. S.; Unni, S. M.; Sharma, A.; Kurungot, S.; Ghosh, S. K. *Angew. Chem. Int. Ed.* **2014**, *53*, 2638 –2642. (b) Yamada, T.; Sadakiyo, M.; Kitagawa, H. *J. Am. Chem. Soc.* **2009**, *131***,** 3144–3145. (c) Horike, S.; Chen, W.; Itakura, T.; Inukai, M.; Umeyama, D.; Asakura*e,* H.; Kitagawa, S. *Chem. Commun.* **2014**, *50*, 10241-10243. (d) Inukai, M.; Horike, S.; Chen, W.; Umeyama, D.; Itakurad, T.; Kitagawa, S. *J. Mater. Chem. A.* **2014**, *2*, 10404–10409. (e) Sadakiyo, M.; Yamada, T.; Kitagawa, H. *J. Am. Chem. Soc.* **2009**, *131*, 9906–9907. (f) Sadakiyo, M.; Ōkawa, H.; Shigematsu, A.; Ohba, M.; Yamada, T.,

Kitagawa, H. *J. Am. Chem. Soc.* **2012**, *134*, 5472−5475. (g) Ōkawa, H.; Shigematsu, A.; Sadakiyo,M.; Miyagawa, T.; Yoneda, K.; Ohba, M.; Kitagawa, H. *J. Am. Chem. Soc.* **2009**, *131*, 13516–13522. (h) Horike, S.; Umeyama, D.; Inukai, M.; Itakura, T.; Kitagawa, S. *J. Am. Chem. Soc.* **2012**, *134*, 7612−7615. (i) Umeyama, D.; Horike, S.; Inukai, M.; Kitagawa, S. *J. Am. Chem. Soc.* **2013**, *135*, 11345−11350. (j) Umeyama, D.; Horike, S.; Inukai, M.; Itakura, T.; Kitagawa, S. *J. Am. Chem. Soc*. **2012**, ***134***, 12780−12785.

(5) (a) Kondo, A.; Noguchi, H.; Carlucci, L.; Proserpio, D. M. ; Ciani, G.; Kajiro, H.; Ohba, T.; Kanoh, H.; Kaneko, K. *J. Am. Chem. Soc*. **2007**, *129* , 12362–12363. (b) Kondo, A.; Kajiro, H. ; Noguchi, H. ; Carlucci, L. ; Proserpio, D. M. ; Ciani, G.; Kato, K.; Takata, M. ; Seki, H.; Sakamoto, M. ; Hattori, Y.; Okino, F.; Maeda, K.; Ohba, T.; Kaneko, K.; Kanoh, H. *J. Am. Chem. Soc.* **2011**, *133*, 10512–10522. (c) Biradha, K. ; Fujita, M. *Angew. Chem. Int. Ed.* **2002**, *41*, 3392-3395. (d) Manna, B.; Chaudhari, A. K.; Joarder, B.; Karmakar, A.; Ghosh, S. K. *Angew. Chem. Int. Ed.* **2013**, *52*, 998 –1002. (e) Kotani, R.; Kondo A.; Maeda, K. *Chem. Commun.* **2012**, *48*, 11316–11318.

(6) (a) Yotnoi, B.; Rujiwatra, A.; Reddy, M. L. P.; Sarma, D.; Natarajan, S. *Cryst.Growth Des*.**2011**, *11*, 1347–1356. (b) Doran, M. B.; Norquist, A. J.; O'Hare, D. *Inorg. Chem*. **2003**, *42*, 6989-6995.

(7) (a) Fu, Y.; Xu, Z.; Ren, J.; Wu, H.; Yuan, R. *Inorg. Chem*. **2006**, *45*, 8452-8458. (b) Ramaswamy, P.; Hegde, N. N.; Prabhu, R.; Vidya, V.; Datta, M. A.; Natarajan, S. *Inorg. Chem*. **2009**, *48*, 11697–11711.

(8) *SAINT Plus*, (Version 7.03); Bruker AXS Inc.: Madison, WI, **2004**.

(9) Sheldrick, G. M. *SHELXTL*, *Reference Manual*: version 5.1: Bruker AXS; Madison, WI, **1997**.

(10) Sheldrick, G. M. *Acta Crystallogr. Sect. A* **2008**, *112*.

(11) *WINGX version 1.80.05 Louis Farrugia, University of Glasgow.*

(12) Spek, A. L. PLATON, *A Multipurpose Crystallographic Tool*, Utrecht University, Utrecht, The Netherlands, **2005**.

(13) Xu, H.-R.; Zhang, Q.-C.; Zhao, H.-X.; Long, L.-S.; Huang, R.-B.; Zheng,L.-S.; *Chem. Commun.* **2012**, *48*, 4875–4877.

(14) (a) Marx, D.; Tuckerman, M. E.; Hutter, J.; Parrinello, M. *Nature*. **1999**, *397*, 601-604. (b) van Grotthuss, C. J. T. *Ann. Chim.*, **1806**, *58*, 54–73. (c) Atkins, P.; de Paula**,** J. *Physical Chemistry*, 8th edn, Ch. 21.7, 766 (Oxford Univ. Press, 2006).

Conclusions and Future Outlook

Conclusions and Future Outlook:

In view of the constantly escalating research efforts put together in the exciting regime of new-generation ionic PCP/MOF materials-based research, there is a definite necessity for the development of new design principles as discussed herein. This is essentially aimed at an improved understanding of the underlying rationale, imperative for successful development of the most efficient functional porous materials. Breakthrough discovery in this regime of research can only prosper by a sequential culmination of streamlined explorations, which in fact, is the major drive behind the concentric works presented in this thesis.

Neutral nitrogen rich π-conjugated linkers can render the resultant PCPs luminescent, an exciting attribute which has been decisively exploited to derive intriguing luminescence-based properties. Apart from this, inherently cationic or anionic coordination polymers are fascinating candidates to study ion conduction pathways, such as proton or hydroxide conduction properties (both in anhydrous and humidified conditions) and for enhanced realization of their underlying charge transfer mechanisms. Such property can be well-transcended for addressing a number of pressing environmental concerns involving the selective detection and recognition of potentially harmful toxin species such as, environmental pollutant anions, and metal cations. For superior real-time applicability purposes, water is the ubiquitously preferred medium. Hence, in a way to exhibit the environmentally exigent efficiencies by the ionic PCP materials, hydrolytic stability is a major aspect to be judiciously taken care of. For imparting the desired aqueous stability, the linker prefunctionalization based design principle has proved its worth in the recent years of materials research. Consequently, the current research findings on ionic PCPs might indeed prove crucial stepping stones leading to the development of an array of top-notch, functional ionic MOFs/PCPs, unmatched from the standpoints of their superior efficacies in the frontiers of advanced materials research. In the quest for a better realization of the working principles pertaining to the relatively new regime of ionic CPs (iCPs), the present findings as manifested in the thesis should prove a vital point of reference in future.

Appendix

2.6. Appendix:

Appendix 2.1: *Crystal data and structure refinement for compound **1**.*

Identification code	**Compound1**	
Identification code	Compound**1**	
Empirical formula	C36 H30 Cd Cl2 N12 O8	
Formula weight	942.02	
Temperature	100(2) K	
Wavelength	0.71069 Å	
Crystal system	Trigonal	
Space group	R-3c	
Unit cell dimensions	a = 31.070(5) Å	α= 90.000(5)°.
	b = 31.070(5) Å	β= 90.000(5)°.
	c = 31.862(5) Å	γ = 120.000(5)°.
Volume	26637(7) $Å^3$	
Z	18	
Density (calculated)	1.057 Mg/m^3	
Absorption coefficient	0.504 mm^{-1}	
F(000)	8568	
Crystal size	0.17 x 0.15 x 0.12 mm^3	
Theta range for data collection	1.98 to 28.27°.	
Index ranges	-41<=h<=41, -41<=k<=41, -42<=l<=38	
Reflections collected	158511	
Independent reflections	7342 [R(int) = 0.0453]	
Completeness to theta = 28.27°	99.9 %	
Absorption correction	Semi-empirical from equivalents	
Max. and min. transmission	0.9420 and 0.9192	
Refinement method	Full-matrix least-squares on F2	
Data / restraints / parameters	7342 / 4 / 250	
Goodness-of-fit on F2	1.049	
Final R indices [I>2sigma(I)]	R1 = 0.0622, wR2 = 0.1793	
R indices (all data)	R1 = 0.0664, wR2 = 0.1830	
Extinction coefficient	0.000003(14)	
Largest diff. peak and hole	1.871 and -3.771 $e.Å^{-3}$	

Appendix 2.2: *Crystal data and structure refinement for compound **2.***

Identification code	**Compound2**	
Identification code	Compound**2**	
Empirical formula	C28 H32 Cd Cl2 N8 O11	
Formula weight	839.92	
Temperature	100(2) K	
Wavelength	0.71073 Å	
Crystal system	Monoclinic	
Space group	Cc	
Unit cell dimensions	a = 18.938(8) Å	α= 90°.
	b = 16.008(7) Å	β= 123.948(6)°.
	c = 15.549(11) Å	γ = 90°.
Volume	3910(4) $Å^3$	
Z	4	
Density (calculated)	1.427 Mg/m^3	
Absorption coefficient	0.756 mm^{-1}	
F(000)	1704	
Crystal size	0.17 x 0.14 x 0.11 mm^3	
Theta range for data collection	1.82 to 28.29°.	
Index ranges	-25<=h<=25, -21<=k<=21, -20<=l<=20	
Reflections collected	33545	
Independent reflections	9349 [R(int) = 0.0232]	
Completeness to theta = 28.29°	99.0 %	
Absorption correction	Semi-empirical from equivalents	
Max. and min. transmission	0.9214 and 0.8822	
Refinement method	Full-matrix least-squares on F2	
Data / restraints / parameters	9349 / 14 / 421	
Goodness-of-fit on F2	0.933	
Final R indices [I>2sigma(I)]	R1 = 0.0771, wR2 = 0.2159	
R indices (all data)	R1 = 0.0833, wR2 = 0.2310	
Absolute structure parameter	0.32(4)	

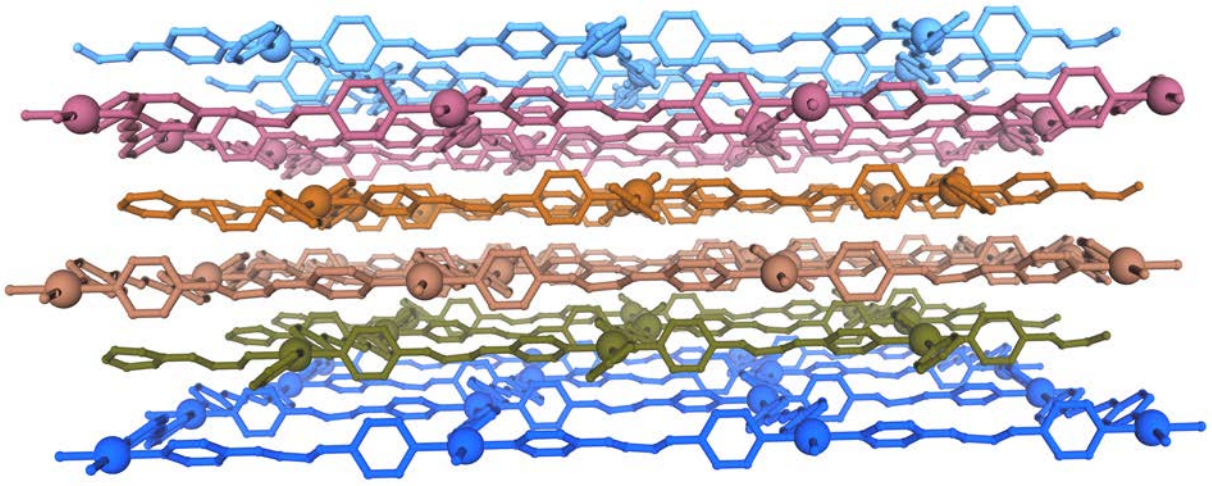

Appendix 2.3: *various 2D sheets of the compound **2**.*

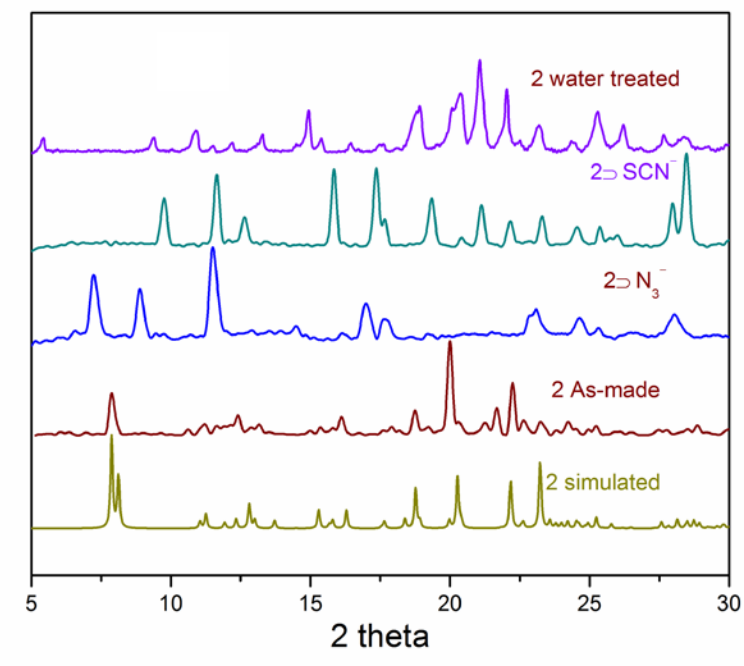

Appendix 2.4: *PXRD patterns of water treated and anion exchange phases of compound **2** indicating structural dynamic nature.*

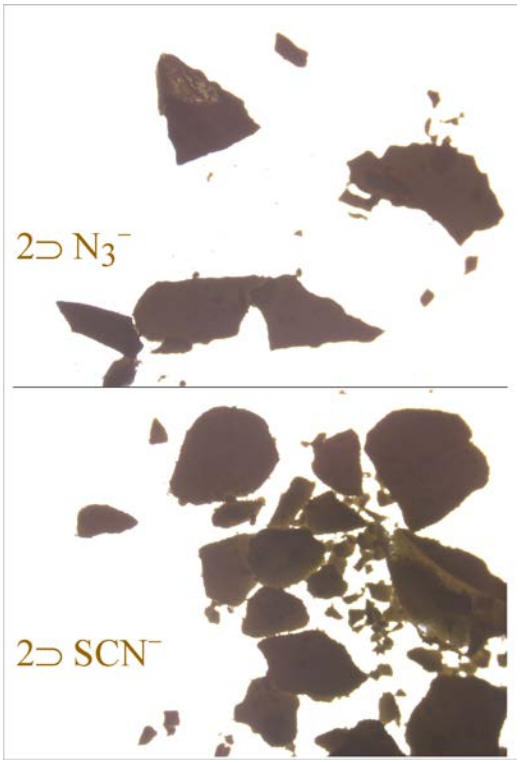

Appendix 2.5: *Microscopic images of polycrystalline phases of anion exchanged compounds.*

3.6. Appendix:

Appendix 3.1: *Crystal data and structure refinement for compound **1a**.*

Identification code	**Compound1a**
Identification code	compound**1a**
Empirical formula	C28 H30 N6 O8 Zn
Formula weight	643.95
Temperature	150(2) K
Wavelength	0.71073 Å
Crystal system	Monoclinic
Space group	C2/c
Unit cell dimensions	a = 17.746(5) Å b = 12.105(4) Å β= 90.244(7)°. c = 15.306(5) Å
Volume	3287.7(19) $Å^3$
Z	4
Density (calculated)	1.301 Mg/m^3
Absorption coefficient	0.800 mm^{-1}
F(000)	1336
Crystal size	0.10 x 0.07 x 0.06 mm^3
Theta range for data collection	2.04 to 27.00°.
Index ranges	-22<=h<=11, -15<=k<=13, -19<=l<=14
Reflections collected	8347
Independent reflections	3451 [R(int) = 0.0178]
Completeness to theta = 27.00°	96.1 %
Absorption correction	Semi-empirical from equivalents
Max. and min. transmission	0.9535 and 0.9242
Refinement method	Full-matrix least-squares on F2
Data / restraints / parameters	3451 / 14 / 205
Goodness-of-fit on F2	1.087
Final R indices [I>2sigma(I)]	R1 = 0.0608, wR2 = 0.1933
R indices (all data)	R1 = 0.0661, wR2 = 0.1991
Largest diff. peak and hole	1.233 and -0.854 $e.Å^{-3}$

Appendix 3.2: *Crystal data and structure refinement for compound **1**.*

Identification code	**Compound1**
Identification code	Compound **1**
Empirical formula	C26 H30 N6 O10 Zn
Formula weight	651.93
Temperature	150(2) K
Wavelength	0.71073 Å
Crystal system	Monoclinic
Space group	P21/n
Unit cell dimensions	a = 15.305(4) Å b = 10.611(3) Å β= 93.120(7)°. c = 18.043(5) Å
Volume	2926.0(14) $Å^3$
Z	4
Density (calculated)	1.480 Mg/m^3
Absorption coefficient	0.905 mm^{-1}
F(000)	1352
Crystal size	0.18 x 0.12 x 0.08 mm^3
Theta range for data collection	2.23 to 28.43°.
Index ranges	-20<=h<=20, -12<=k<=14, -21<=l<=24
Reflections collected	25092
Independent reflections	7324 [R(int) = 0.0418]
Completeness to theta = 28.43°	99.4 %
Absorption correction	Semi-empirical from equivalents
Max. and min. transmission	0.9311 and 0.8540
Refinement method	Full-matrix least-squares on F2
Data / restraints / parameters	7324 / 2 / 413
Goodness-of-fit on F2	1.041
Final R indices [I>2sigma(I)]	R1 = 0.0480, wR2 = 0.1182
R indices (all data)	R1 = 0.0787, wR2 = 0.1384
Largest diff. peak and hole	0.908 and -0.876 $e.Å^{-3}$

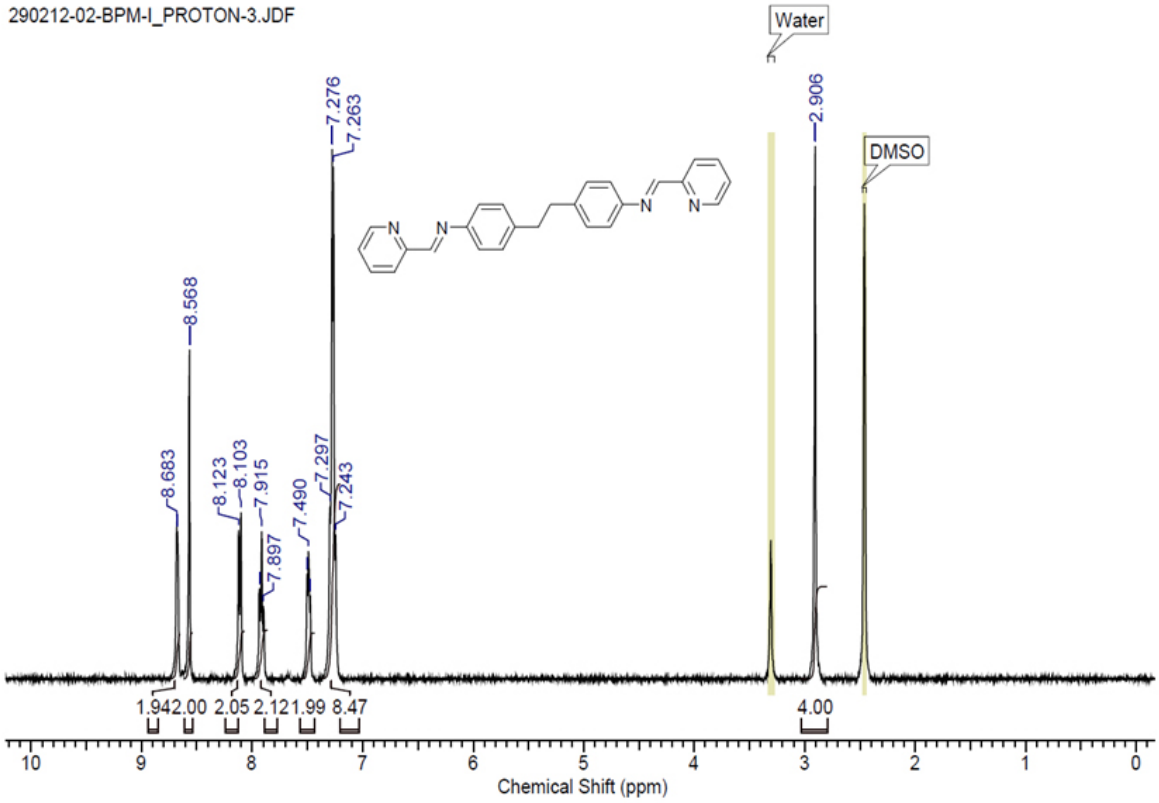

Appendix 3.3: *^{1}H NMR of the corresponding ligand.*

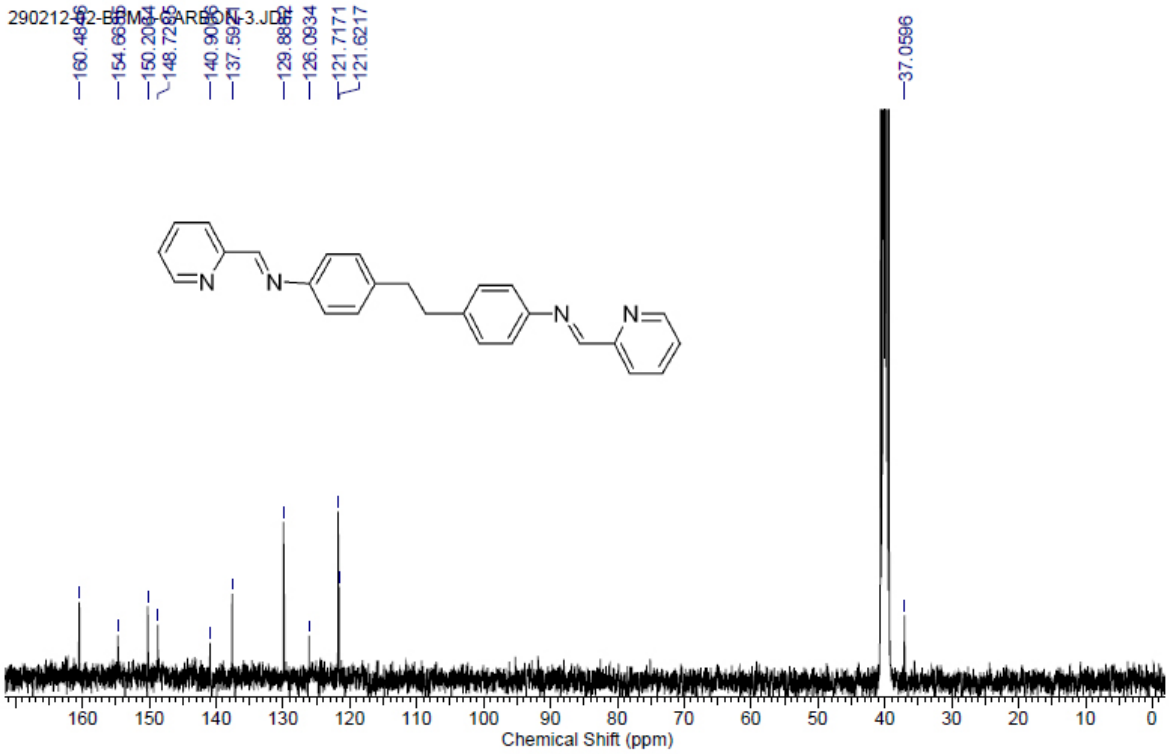

Appendix 3.4: *^{13}C NMR of the corresponding ligand.*

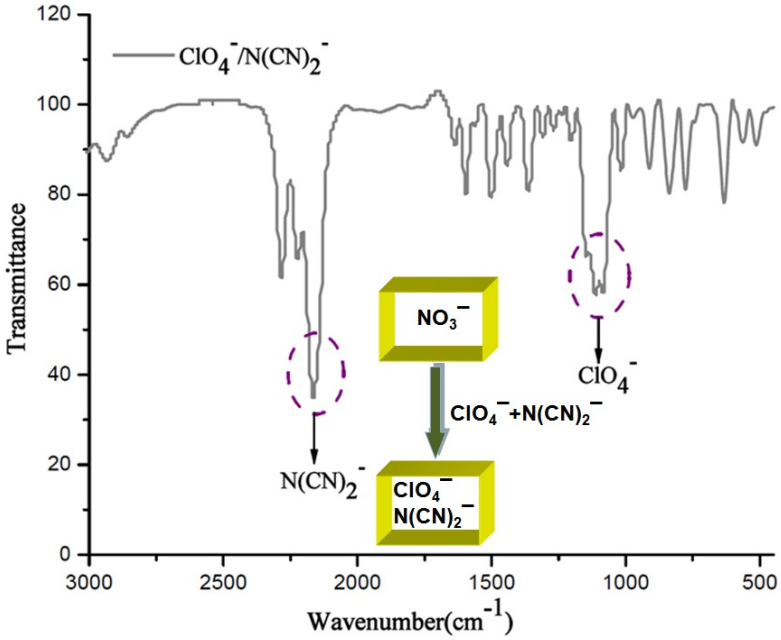

Appendix 3.5: *IR spectra of anion exchange compound (binary combination) at RT showing both ClO4⁻ and N(CN)2⁻ taken by framework **1** from ClO4⁻ / N(CN)2⁻ mixture.*

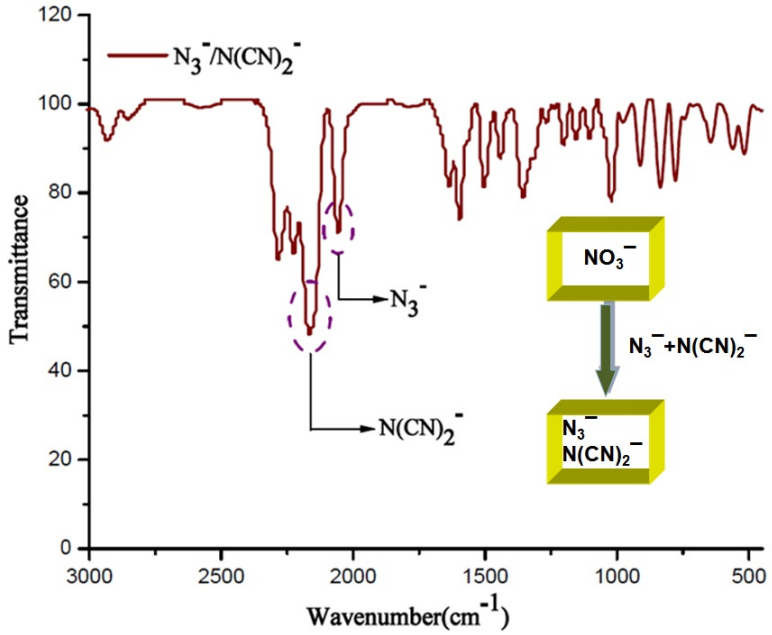

Appendix 3.6: *IR spectra of anion exchange compound (binary combination) at RT showing both N_3^- and N(CN)2⁻ taken by framework **1** from N_3^- / N(CN)2⁻ mixture.*

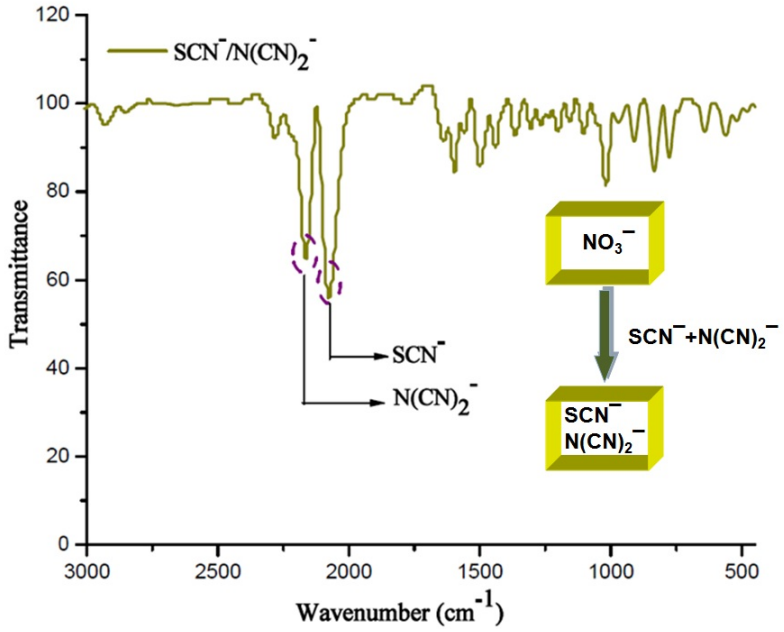

Appendix 3.7: *IR spectra of anion exchange compound (binary combination) at RT showing both SCN^- and $N(CN)2^-$ taken by framework **1** from SCN^- / $N(CN)2^-$ mixture.*

4.6. Appendix:

Appendix 4.1: *Crystal data and structure refinement for compound **1**⊃ NO_3^-.*

Identification code	**Compound1⊃ NO_3^-**	
Identification code	Compound**1**⊃ NO_3^-	
Empirical formula	C29 H31 N6 O10 Zn	
Formula weight	688.97	
Temperature	150(2) K	
Wavelength	0.71073 Å	
Crystal system	Hexagonal	
Space group	P6522	
Unit cell dimensions	a = 10.9848(11) Å	α= 90°.
	b = 10.9848(11) Å	β= 90°.
	c = 44.042(5) Å	γ = 120°.
Volume	4602.4(8) $Å^3$	
Z	6	
Density (calculated)	1.491 Mg/m^3	
Absorption coefficient	0.868 mm^{-1}	
F(000)	2142	
Crystal size	0.17 x 0.15 x 0.12 mm^3	
Theta range for data collection	2.14 to 28.22°.	
Index ranges	-14<=h<=12, -12<=k<=14, -58<=l<=35	
Reflections collected	28513	
Independent reflections	3805 [R(int) = 0.0631]	
Completeness to theta = 28.22°	100.0 %	
Absorption correction	Semi-empirical from equivalents	
Max. and min. transmission	0.9030 and 0.8665	
Refinement method	Full-matrix least-squares on F2	
Data / restraints / parameters	3805 / 0 / 231	
Goodness-of-fit on F2	1.093	
Final R indices [I>2sigma(I)]	R1 = 0.0599, wR2 = 0.1530	
R indices (all data)	R1 = 0.0725, wR2 = 0.1596	
Absolute structure parameter	0.06(3)	
Largest diff. peak and hole	0.824 and -0.361 $e.Å^{-3}$	

Appendix 4.2: *Crystal data and structure refinement for compound* ***1***$\supset ClO_4^-$.

Identification code	**Compound1**$\supset$ **ClO_4^-**
Identification code	Compound**1**$\supset ClO_4^-$
Empirical formula	C26 H30 Cl2 N4 O12 Zn
Formula weight	726.81
Temperature	150(2) K
Wavelength	0.71073 Å
Crystal system	Hexagonal
Space group	P65
Unit cell dimensions	a = 11.1662(11) Å α= 90°. b = 11.1662(11) Å β= 90°. c = 43.103(4) Å γ = 120°.
Volume	4654.3(8) $Å^3$
Z	6
Density (calculated)	1.556 Mg/m^3
Absorption coefficient	1.032 mm^{-1}
F(000)	2244
Crystal size	0.15 x 0.15 x 0.10 mm^3
Theta range for data collection	1.42 to 27.26°.
Index ranges	-14<=h<=14, -13<=k<=14, -55<=l<=37
Reflections collected	26945
Independent reflections	6026 [R(int) = 0.0445]
Completeness to theta = 27.26°	99.7 %
Absorption correction	Semi-empirical from equivalents
Max. and min. transmission	0.9039 and 0.8606
Refinement method	Full-matrix least-squares on F^2
Data / restraints / parameters	6026 / 2 / 424
Goodness-of-fit on F^2	1.087
Final R indices [I>2sigma(I)]	R1 = 0.0367, wR2 = 0.0836
R indices (all data)	R1 = 0.0374, wR2 = 0.0839
Absolute structure parameter	0.496(16)
Extinction coefficient	0.00036(12)
Largest diff. peak and hole	0.381 and -0.410 $e.Å^{-3}$

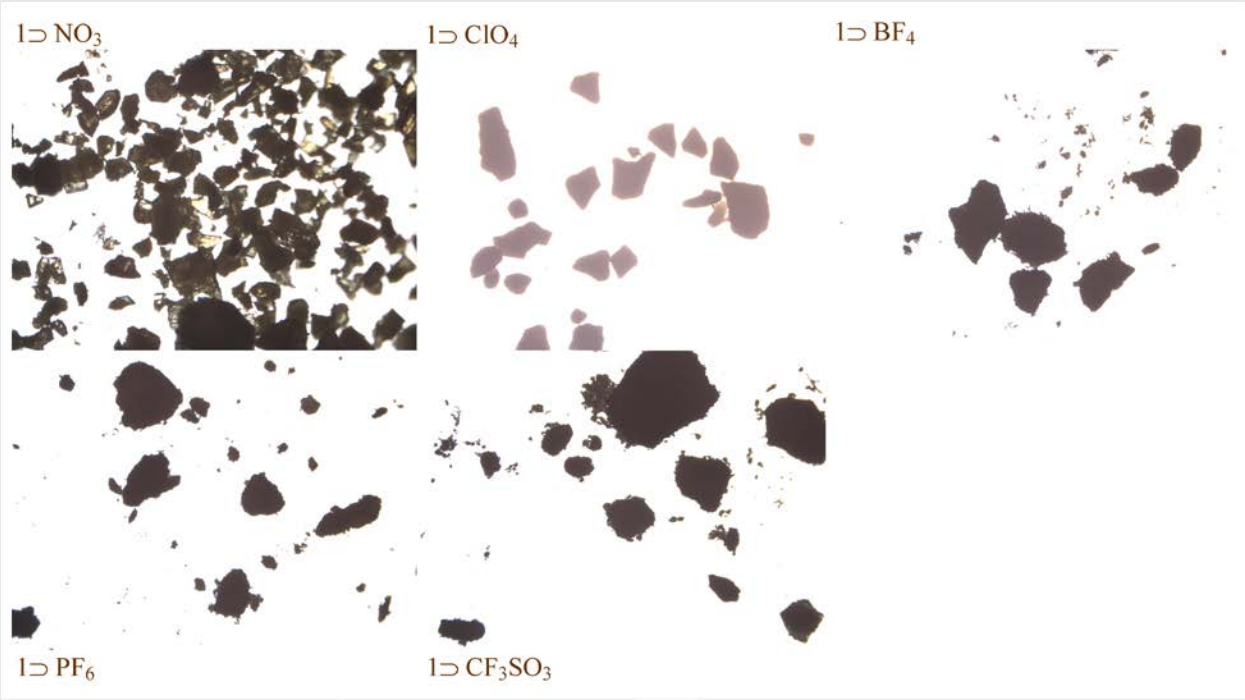

Appendix 4.3: *Microscopic images of single crystalline **1**⊃ NO_3^- and polycrystalline phases of anion exchanged samples for type B anion.*

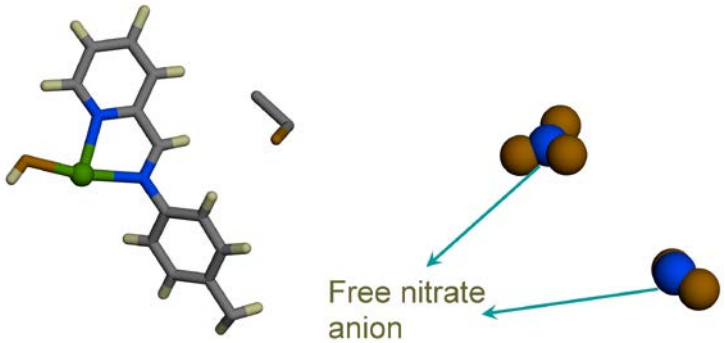

Appendix 4.4: *Asymmetric unit of compound **1**⊃ NO_3^- showing cationic unit and free nitrate anion.*

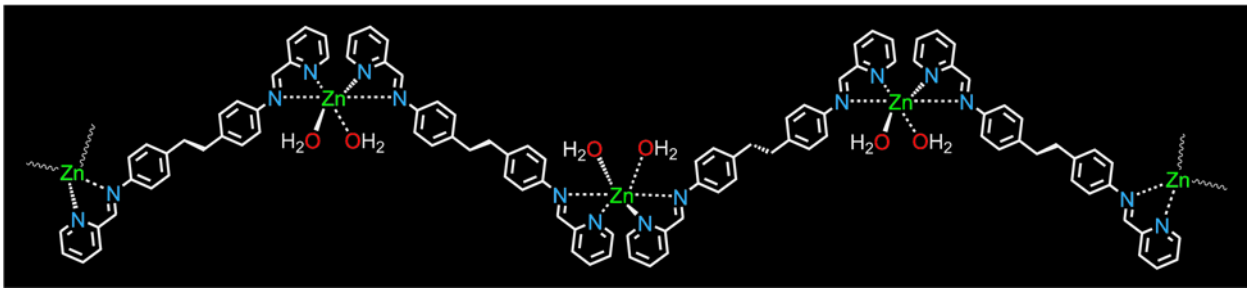

Appendix 4.5: *Chemical diagram of the 1D helical chain showing the ligation of bi-chelating sites at both ends of the ligand.*

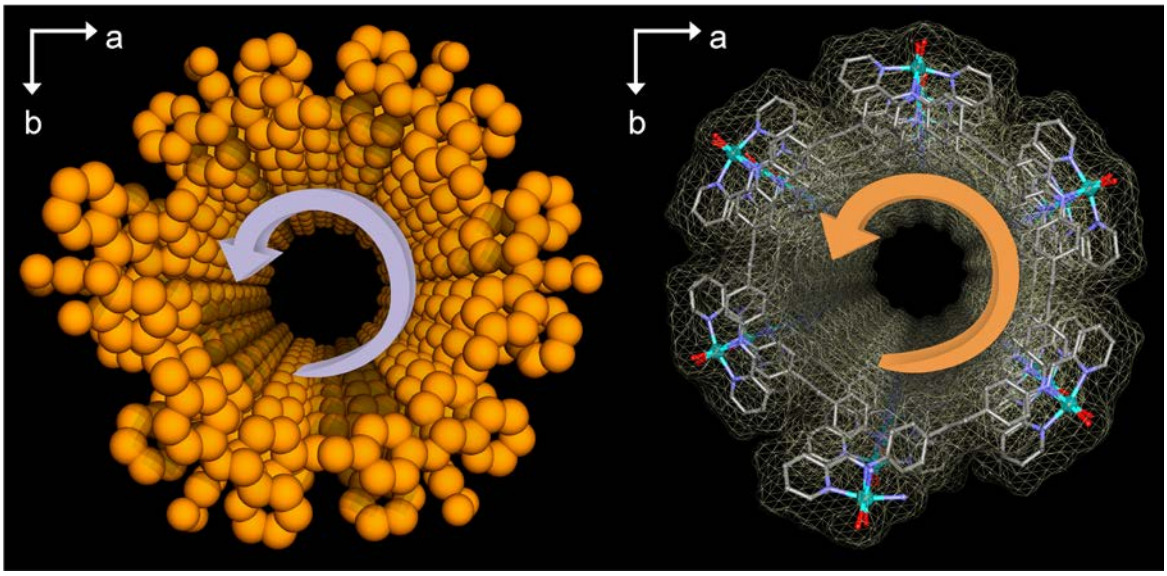

Appendix 4.6: *Perspective view of left handed helix of* ***1***$\supset NO_3^-$ *shown in CPK model (left) and wire mesh view (right).*

.

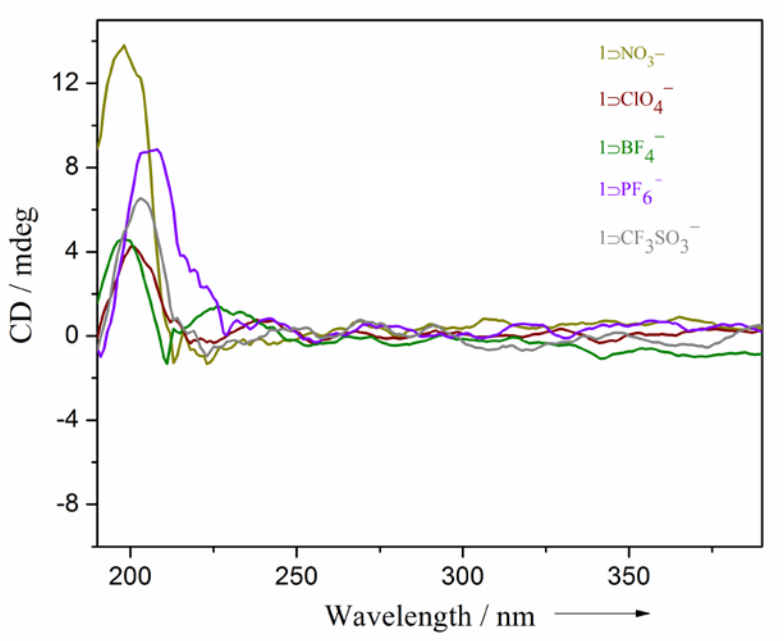

Appendix 4.7: *Solid state CD spectra of* ***1***$\supset NO_3^-$ *and other anion exchange compound in their powder phase showing positive cotton effect.*

5.6. Appendix:

Appendix 5.1: *Crystal data and structure refinement for compound **1**.*

Identification code	**Compound1**
Empirical formula	C12 H30 In2 N24 O22 S4
Formula weight	1220.46
Temperature	100(2) K
Wavelength	0.71073 Å
Crystal system	Monoclinic
Space group	P21/n
Unit cell dimensions	a = 10.8141(17) Å b = 13.092(2) Å β= 90.144(3)°. c = 27.175(4) Å
Volume	3847.4(10) $Å^3$
Z	4
Density (calculated)	2.104 Mg/m^3
Absorption coefficient	1.531 mm^{-1}
F(000)	2424
Crystal size	0.16 x 0.14 x 0.10 mm^3
Theta range for data collection	0.75 to 28.46°.
Index ranges	-14<=h<=14, -16<=k<=17, -36<=l<=34
Reflections collected	58513
Independent reflections	9462 [R(int) = 0.0607]
Completeness to theta = 28.46°	97.3 %
Absorption correction	Semi-empirical from equivalents
Max. and min. transmission	0.8619 and 0.7917
Refinement method	Full-matrix least-squares on F2
Data / restraints / parameters	9462 / 62 / 581
Goodness-of-fit on F2	1.068
Final R indices [I>2sigma(I)]	R1 = 0.0964, wR2 = 0.2504
R indices (all data)	R1 = 0.1180, wR2 = 0.2683

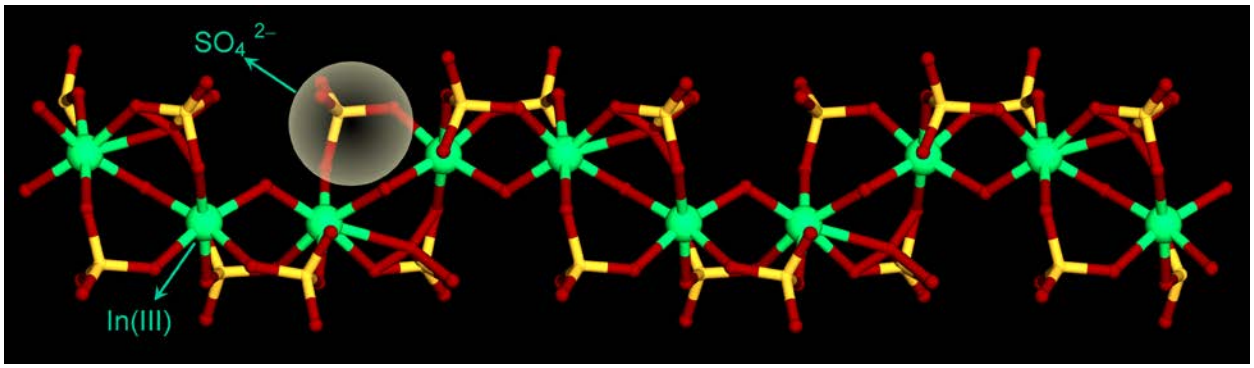

Appendix 5.2: *In-SO_4 1D anionic chain showing In (III) centers and SO_4^{2-} anion.*

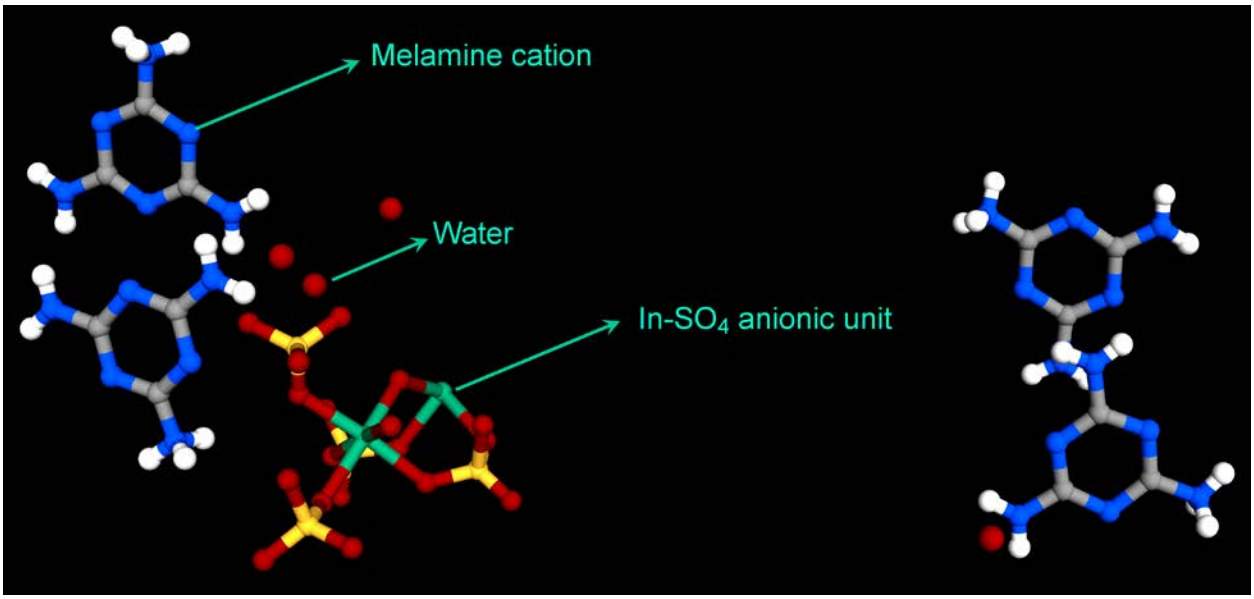

Appendix 5.3: *Asymmetric unit of compound **1** showing anionic unit, free melamine cation and lattice water molecules.*

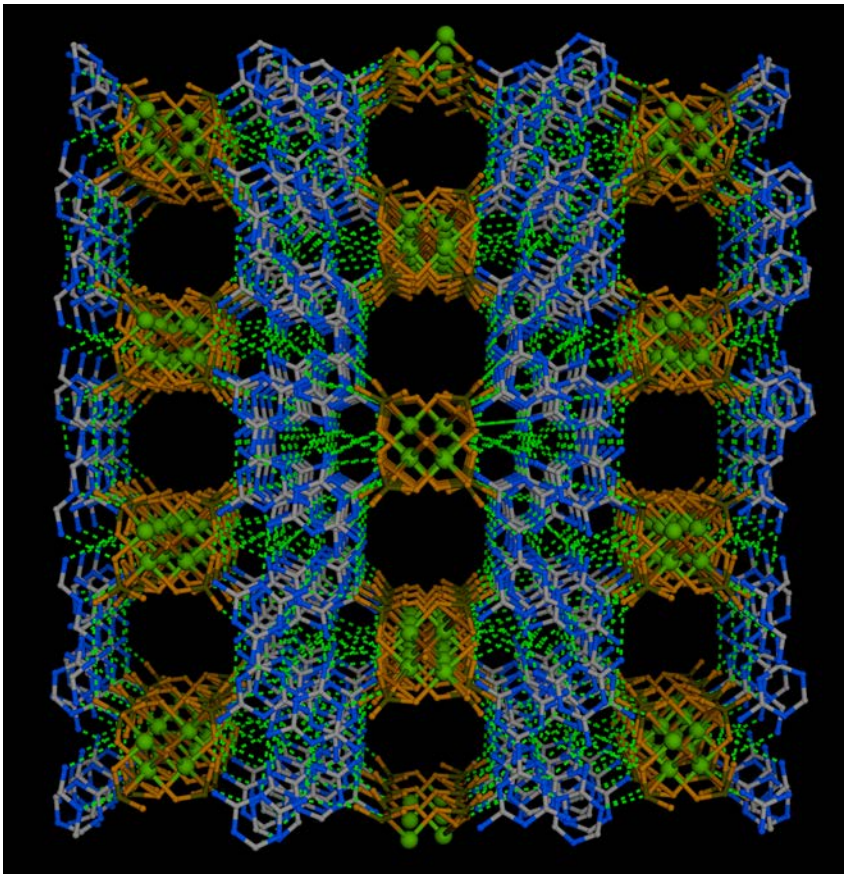

Appendix 5.4: *H-bonded 3D network of compound **1**.*

Appendix 5.5: *A comparison chart of the current sulfate based CP with other related CPs/ MOFs in terms of their proton conduction ability.*

CPs/MOFs	σ / Scm^{-1}	RH / %	T / °C	Reference
$UiO\text{-}66(SO_3H)_2$	8.4×10^{-2}	90	80	1
TfOH@MIL-101	8×10^{-2}	15	60	2
H_2SO_4@MIL-101	6.0×10^{-2}	20	80	3
$\{[Me_2NH_2)_3(SO_4)]_2[Zn_2(ox)_3]\}_n$	4.2×10^{-2}	98	25	4
PCMOF-10	3.55×10^{-2}	95	70	5
$(Zn_3(H_2PO_4)_6)(Hbim)$	1.3×10^{-3}	-	120	6
H^+@Ni-MOF-74(pH-1.8)	2.2×10^{-2}	95	80	7
PCMOF2'/2	2.1×10^{-2}	90	85	8
[Zn(HPO4)(H2PO4)2](ImH2)2	2.6×10^{-4}	-	130	9
$(NH_4)_2(H_2adp)[Zn_2(ox)_3]\cdot 3H_2O$	0.8×10^{-2}	98	25	10
$[Zn(H_2PO_4)_2(HPO_4)]\cdot(H_2dmbim)_2]$	2×10^{-4}	-	190	11
$[\{In_2(\mu\text{-}OH)_2(SO_4)_4\}\cdot\{(LH)_4\}\cdot nH_2O]_n$	4.4×10^{-5}	98	30	12(this work)

References:

1) Phang, W. J.; Jo, H.; Lee, W. R.; Song, J. H.; Yoo, K.; Kim, B.; Hong, C .S. *Angew. Chem. Int. Ed*. **2015**, *54*, 5142-5146.
2) Dybtsev, D. N.; Ponomareva, V. G.; Aliev, S. B.; Chupakhin, A. P.; Gallyamov, M. R.; Moroz, N. K.; Kolesov, B. A.; Kovalenko, K. A.; Shutova, E. S.; Fedin, V. P. *ACS Appl. Mater. Interfaces* . **2014**, *6*, 5161−5167.
3) Ponomareva, V. G.; Kovalenko, K. A.; Chupakhin, A. P.; Dybtsev, D. N.; Shutova, E. S.; Fedin, V. P. *J. Am. Chem. Soc.* **2012**, *134*, 15640−15643.
4) Nagarkar, S. S.; Unni, S. M.; Sharma, A.; Kurungot, S.; Ghosh, S. K. *Angew. Chem. Int. Ed.* **2014**, *53*, 2638 –2642.

5) Ramaswamy,P.; Wong, N. E.; Gelfand B. S.; Shimizu ,G. K. H. *J. Am. Chem.Soc.*, **2015**, *137*, 7640–7643 .
6) Umeyama, D.; Horike, S.; Inukai, M.; Kitagawa, S. *J. Am. Chem. Soc.* **2013**, *135*, 11345-11350.
7) Phang, W. J.; Lee, W. R.; Yoo, K.; Ryu, D. W.; Kim, B.; Hong, C. S. *Angew. Chem. Int. Ed*. **2014**, *53*, 8383 –8387.
8) Kim, S. R.; Dawson, K. W.; Gelfand, B. S.; Taylor, J. M.; Shimizu, G. K. H. *J. Am. Chem. Soc.* **2013**, *135*, 963−966.
9) Horike, S.; Umeyama, D.; Inukai, M.; Itakura, T.; Kitagawa, S. *J. Am. Chem. Soc.* **2012***, 134,* 7612−7615*.*
10) Sadakiyo, M.; Yamada, T.; Kitagawa, H. *J. Am. Chem. Soc*. **2009**, *131*, 9906−9907.
11) Inukai, M.; Horike, S.; Chen, W.; Umeyama, D.; Itakurad, T.; Kitagawa, S. *J. Mater. Chem. A* **2014**, *2*, 10404-10409.
12) Manna, B.; Anothumakkool, B.; Desai, A.V.; Samanta, P.; Kurungot, S.; Ghosh, S.K. *Inorg.Chem*., **2015**, *54*, 5366-5371.